
Wayne State University Dissertations

January 2022

A C0 Finite Element Method For The Biharmonic Problem In A Polygonal Domain

Charuka Dilhara Wickramasinghe
Wayne State University

Follow this and additional works at: https://digitalcommons.wayne.edu/oa_dissertations

 Part of the [Applied Mathematics Commons](#)

Recommended Citation

Wickramasinghe, Charuka Dilhara, "A C0 Finite Element Method For The Biharmonic Problem In A Polygonal Domain" (2022). *Wayne State University Dissertations*. 3704.
https://digitalcommons.wayne.edu/oa_dissertations/3704

This Open Access Dissertation is brought to you for free and open access by DigitalCommons@WayneState. It has been accepted for inclusion in Wayne State University Dissertations by an authorized administrator of DigitalCommons@WayneState.

**A C^0 FINITE ELEMENT METHOD FOR THE BIHARMONIC PROBLEM
IN A POLYGONAL DOMAIN**

by

CHARUKA DILHARA WICKRAMASINGHE

DISSERTATION

Submitted to the Graduate School,

of Wayne State University,

Detroit, Michigan

in partial fulfillment of the requirements

for the degree of

DOCTOR OF PHILOSOPHY

2022

MAJOR: MATHEMATICS

Approved By:

Advisor

Date

© COPYRIGHT BY

CHARUKA DILHARA WICKRAMASINGHE

2022

All Rights Reserved

DEDICATION

This dissertation is dedicated to my beloved parents, wife, sisters, friends, and teachers
for their unconditional love and support.

ACKNOWLEDGEMENTS

I would like to take a moment to thank many people who helped me along the way on this journey.

First, I wish to express my greatest gratitude to my advisor, Prof. Hengguang Li. When he first gave me the problem of solving the biharmonic equation using a mixed finite element method, I never expected I could come this far on this journey. He is always there, providing support and help to me. Every time I feel frustrated, his constant support keeps me going forward. He has brought me to the beautiful world of mathematics and given me much thoughtful advice to follow this academic journey. For me, he is more than just an advisor; he is also a beacon light in my life.

I would like to thank Dr. Peimeng Yin for his continuous support and encouraging me to do different types of numerical examples to check the accuracy of the algorithms.

I would also like to thank my beloved wife, Dr. Nelum Hapuhinna, for her love, encouragement, thought-full ideas, and support for keeping me on task to finish everything on time. I am so thankful for you in my life.

I appreciate Mr. Richard Pineau and Mr. Christopher Leirstein, who have trained me and supported me on teaching and many other educational aspects. I will never forget that all the faculty and staff of the Mathematics Department treated me warmly during my graduate study. I am also grateful to all of my friends in Detroit for making my life here more colorful and joyful.

I would like to thank the Department of Mathematics at Wayne State University for offering me Graduate Teaching Assistantship, Thomas C. Rumble University Graduate Fel-

lowship, and Paul Catlin, Endowed Memorial Scholarship Award. I could not have come this far without these financial supports. I learned a lot from the courses instructed by Prof. Peiyong Wang, Prof. Fatih Celiker, Prof. Zhimin Zhang, and Prof. Boris Mordukhovich. I appreciate all the help provided by Carla Sylvester, Maria Vujic, JoAnne Lewan, Barbara Malicke, and Doris E. King. I also appreciate Pradeep Ranaweera, Priyanka Ahire, Fatemah Alhamede, Qian Zhang, Anuj Bajaj, Nguyen-Truc-Dao Nguyen, Huy NguYen, Nurul Raihen, Lewei Zhao, and Diego Yopez, for the lovely times we have spent together and for the help they have ever provided.

Last but not least, I would like to thank Prof. Peiyong Wang, Prof. Fatih Celiker, Prof. Zhimin Zhang, and Prof. Kamran Avanaki for serving on my dissertation committee.

TABLE OF CONTENTS

Dedication	ii
Acknowledgements	iii
List of Tables	viii
List of Figures	x
Chapter 1 INTRODUCTION	1
1.1 The Finite Element Methods	1
1.2 Definitions	2
1.3 Main Work of the Dissertation	3
1.4 Outline of the Dissertation	4
Chapter 2 THE BIHARMONIC PROBLEM	7
2.1 The Biharmonic Problem	7
2.1.1 The Poisson Equation	11
2.1.2 The Stokes Equation	14
2.2 Well-posedness and Regularity of the Biharmonic Problem	19
2.3 Decoupled Formulations of the Biharmonic Problem	23
2.3.1 The First Decoupled Formulation	23
2.3.2 The Second Decoupled Formulation	32
2.4 Finite Element Algorithms	36
Chapter 3 ERROR ESTIMATE ON QUASI-UNIFORM MESHES	40
3.1 Error Estimates Results for Algorithm 2.17	41
3.2 Error Estimates Results for Algorithm 2.18	46

Chapter 4	ERROR ESTIMATE ON GRADED MESHES	59
4.1	Regularity in Weighted Sobolev Space	59
4.1.1	Weighted Sobolev Space	59
4.1.2	Regularity Results	60
4.2	Graded Meshes	62
4.3	Interpolation Error Estimates on Graded Meshes	64
4.4	Error Estimates Results for Algorithm 2.17	71
4.5	Error Estimates Results for Algorithm 2.18	76
Chapter 5	NUMERICAL ILLUSTRATIONS	88
5.1	Numerical Results For Algorithm 2.17	88
5.1.1	A Comparison with a Reference Solution	88
5.1.2	Convergent Rates on Graded Meshes	91
5.1.3	Re-entrant Corners on the Domain Other Than $3\pi/2$	94
5.1.4	Different Source Terms \mathbf{F} for the Stokes Problem	101
5.1.5	A Complex Source Term in the Biharmonic Problem	102
5.2	Numerical Tests for Algorithm 2.18	105
5.2.1	A Comparison with a Reference Solution	105
5.2.2	Convergent Rates on Graded Meshes	106
5.2.3	Re-entrant Corners on the Domain Other Than $3\pi/2$	108
5.2.4	CPU Time	111
Chapter 6	SUMMARY AND DISCUSSION	113
6.1	General Conclusion	113
6.2	Future Work	114

References	116
Abstract	127
Autobiographical Statement	129

LIST OF TABLES

Table 1	Some numerical values of α_0 and β_0 in terms of different interior angles ω	22
Table 2	The L^∞ error $\ \phi_R - \phi_j\ _{L^\infty(\Omega)}$ in the square domain on quasi-uniform meshes.	89
Table 3	Numerical convergence rates in the square domain with uniform meshes.	90
Table 4	The L^∞ error $\ u_R - \phi_j^h\ _{L^\infty(\Omega)}$ in the L-shaped domain on quasi-uniform meshes.	91
Table 5	Convergence history of finite element approximation of the biharmonic problem in the L-shaped domain.	93
Table 6	Convergence history of the Taylor-Hood element approximations of Stokes problem in the L-shaped domain.	94
Table 7	Convergence history of finite element approximation of the biharmonic problem on a domain with re-entrant corner $7\pi/4$	95
Table 8	Numerical convergence rates of the Stokes equation with Taylor-Hood elements on a domain with two re-entrant corner $7\pi/4$	97
Table 9	Convergence history of finite element approximation of the biharmonic problem in the domain with two re-entrant corners $4\pi/3$	99
Table 10	Numerical convergence rates of the Stokes equation with Taylor-Hood elements on a domain with re-entrant corner $4\pi/3$	100
Table 11	Convergence history of the biharmonic approximations ϕ_j in the L-shaped domain.	102
Table 12	Errors with the reference solution and convergence rates in the L-shaped domain.	102
Table 13	The L^∞ error $\ u_R - \phi_j^h\ _{L^\infty(\Omega)}$ in the square domain on quasi-uniform meshes for $f = \frac{x}{2}(x^2 + y^2)^{-3/4} + \cos(\pi x) + 1$	103
Table 14	The L^∞ error $\ u_R - \phi_j^h\ _{L^\infty(\Omega)}$ in the L-shaped domain on quasi-uniform meshes for $f = \frac{x}{2}(x^2 + y^2)^{-3/4} + \cos(\pi x) + 1$	103

Table 15	Convergence history of finite element approximation of the biharmonic problem in the L-shaped domain for $f = \frac{x}{2}(x^2 + y^2)^{-3/4} + \cos(\pi x) + 1$. .	104
Table 16	Numerical convergence rates of the Stokes equation with Taylor-Hood elements on the L-shaped domain for $f = \frac{x}{2}(x^2 + y^2)^{-3/4} + \cos(\pi x) + 1$.	104
Table 17	The L^∞ error $\ \phi_R - \phi_j\ _{L^\infty(\Omega)}$ in the square domain on quasi-uniform meshes.	106
Table 18	The L^∞ error $\ u_R - \phi_j^h\ _{L^\infty(\Omega)}$ in the L-shaped domain on quasi-uniform meshes.	106
Table 19	Convergence history of finite element approximation of the biharmonic problem in the L-shaped domain.	107
Table 20	Numerical Convergence rates of finite element approximation of the biharmonic problem on a domain with re-entrant corner $7\pi/4$	109
Table 21	Numerical convergence rates of the second the Poisson equation for the methods M1 and M2 with two re-entrant corner $4\pi/3$	110
Table 22	The CPU time (in seconds) of Algorithm 2.17, Aglorithm 2.18, and the Argyris finite element method.	112

LIST OF FIGURES

Figure 1	The Taylor-Hood elements: Velocity \bullet and pressure nodes \circ	17
Figure 2	The Mini element: Velocity \bullet and pressure nodes \circ	18
Figure 3	Domain Ω containing one reentrant corner.	20
Figure 4	(a) α_0, β_0 in terms of ω ; (b) $\alpha_0 - \beta_0$ in terms of ω	21
Figure 5	The new node on an edge AB . (left): $A \neq Q_i$ and $B \neq Q_i$ (midpoint); (right) $A = Q_i$ ($ AD = \kappa_{Q_i} AB $, $\kappa_{Q_i} < 0.5$).	63
Figure 6	Refinement of a triangle $\Delta x_0 x_1 x_2$. First row: (left – right): the initial triangle and the midpoint refinement; second row: two consecutive graded refinements toward $x_0 = Q_i$, ($\kappa_{Q_i} < 0.5$).	63
Figure 7	Mesh layers (left – right): the initial triangle $T_{(0)}$ with a vertex Q_i ; two layers after one refinement; three layers after two refinements.	65
Figure 8	The Square domain: (a) the initial mesh; (b) the solution ϕ_7 ; (c) the difference $ \phi_R - \phi_7 $; (d) the Stokes solution u_1 ; (e) the Stokes solution u_2 ; (f) the pressure.	90
Figure 9	The L-shaped domain: (a) the initial mesh; (b) the solution ϕ_7 ; (c) the difference $ u_R - \phi_7 $; (d) the Stokes solution u_1 ; (e) the Stokes solution u_2 ; (f) the pressure.	91
Figure 10	The L-shaped domain (Example 5.2): (a) the initial mesh; (b), (c) the graded mesh after two and four mesh refinements respectively with $\kappa = 0.2$	92
Figure 11	The domain with re-entrant corner $7\pi/4$: (a) the initial mesh; (b) the mesh after two refinements; (c) the solution ϕ_7 ; (d) the Stokes solution u_1 ; (e) the Stokes solution u_2 ; (f) the pressure	95
Figure 12	Domain with two re-entrant corner $4\pi/3$: (a) the initial mesh; (b) the mesh after four refinements; (c) the solution ϕ_7 (d) the Stokes solution u_1 ; (e) the Stokes solution u_2 ; (f) the pressure.	98

CHAPTER 1 INTRODUCTION

1.1 The Finite Element Methods

In 1943, the finite element method was first introduced in a paper by Courant [41]. The importance of this work was disregarded at that time and, however, in the early fifties the engineers re-invented the finite element method. The earliest references found in the engineering literature are those of [7], [96]. At this point, the method was thought of as a generalization of earlier methods in structural engineering for beams, frames and plates, where the structure was subdivided into small parts, so called finite elements, with known simple behavior.

In the sixties mathematicians, notable Mikhlin [78] started working on the analysis of Galerkin and Ritz methods. They were not aware the contributions of the engineers and the approximate methods which they studies resembled more and more the finite element method. The spread of the method started with the paper by Zlamal [99] which is generally regarded as the first mathematics error analysis of the "general" finite element method as we know it to-day. When the mathematical study of the finite element method started it soon became clear that in fact the method is a general technique for numerical solution of partial differential equations with roots in the variational methods in mathematics introduced in the beginning of the century. During the 60's and 70's the method was developed, by engineers, mathematicians and numerical analysts, into a general method for numerical solution of partial differential equations and integral equations with applications in many areas of science and engineering. Today, finite element methods are used extensively for problems in structural engineering, strength of materials, fluid dynamics,

heat conduction, convection diffusion process and many other areas. A literature survey of some earlier years of FEMs can be found in Babuska's article "Courant element: before and after" in the book [60].

1.2 Definitions

We use the following definition of a finite element introduced by Ciarlet in his 1978 book [37].

Definition 1.1 (The Finite Element). *Let*

- $K \subseteq \mathbb{R}^d$ (for $d = 1, 2, 3, \dots$) be a bounded closed set with nonempty interior and piecewise smooth boundary (the **element domain**),
- \mathcal{P} be a finite dimensional space of functions on K (the space of shape functions) **and**
- $\mathcal{N} = \{N_1, N_2, \dots, N_k\}$ be a basis \mathcal{P}' (the set of nodal variables)

*Then $(K, \mathcal{P}, \mathcal{N})$ is called a **finite element***

The following definitions of nodal basis, local interpolant, and triangulation can be found in the textbook by Brenner and Scott (2008) [25]

Definition 1.2 (Nodal Basis). *Let $(K, \mathcal{P}, \mathcal{N})$ be a finite element. The basis $\{\phi_1, \phi_2, \dots, \phi_k\}$ of \mathcal{P} dual to \mathcal{N} (i.e., $N_i(\phi_j) = \delta_{ij}$) is called the **nodal basis** of \mathcal{P} .*

Definition 1.3 (Local Interpolant). *Given a finite element $(K, \mathcal{P}, \mathcal{N})$, let the set $\{\phi_i : 1 \leq i \leq k\} \subseteq \mathcal{P}$ be a basis dual to \mathcal{N} . If v is a function for which all $N_i \in \mathcal{N}, i = 1, \dots, k$, are defined, then we define the **local interpolant** by $\mathcal{I}_k v := \sum_{i=1}^k N_i(v) \phi_i$*

Definition 1.4 (Triangulation). A *triangulation* of a polygonal domain Ω is a subdivision consisting of triangles having the property that no vertex of any triangle lies in the interior of an edge of another triangle.

Definition 1.5 (Domain). Throughout the dissertation, we use C to denote a generic positive constant which is independent from element size.

Unless otherwise specified, throughout the paper we assume that $\Omega \in \mathbb{R}^d$, $d = 2$ is a bounded Lipschitz domain. A domain $\Omega \in \mathbb{R}^d$ is called a Lipschitz domain if its boundary $\partial\Omega$ is locally a graph of a Lipschitz continuous function, i.e., for all $\mathbf{x} \in \partial\Omega$, there exists a neighborhood $N(\mathbf{x}, r)$ of \mathbf{x} and a Lipschitz continuous function $\phi : \mathbb{R}^{d-1} \rightarrow \mathbb{R}$ such that

$$\partial\Omega \cap N(\mathbf{x}, r) = \{\mathbf{y} = (y_1, y_2, \dots, y_d) : \phi(y_1, y_2, \dots, y_{d-1}) = y_d\}$$

and

$$\Omega \cap N(\mathbf{x}, r) = \{\mathbf{y} = (y_1, y_2, \dots, y_d) : \phi(y_1, y_2, \dots, y_{d-1}) < y_d\}$$

under a proper local coordinate system.

We say a domain has $C^{1,1}$ boundary if $\partial\Omega$ is locally a graph of a Lipschitz continuous function with Lipschitz continuous derivative.

1.3 Main Work of the Dissertation

We propose two mixed finite element algorithms to solve the following two-dimensional biharmonic equation with the Dirichlet boundary condition. Let $\Omega \subset \mathbb{R}^2$ be a polygonal

domain. Consider the biharmonic problem

$$\Delta^2 \phi = f \quad \text{in } \Omega, \quad \phi = 0 \quad \text{and} \quad \partial_{\mathbf{n}} \phi = 0 \quad \text{on } \partial\Omega, \quad (1.1)$$

where \mathbf{n} is the outward normal derivation.

A steady-state Stokes equation and Poisson equations are used to decouple the biharmonic equation. We present H^1 and L^2 error estimates for both algorithms under uniform and graded meshes. Numerical simulations are presented to validate the theoretical results.

1.4 Outline of the Dissertation

The dissertation is organized as follows:

In Chapter 2, first, we introduce our model problem which is the biharmonic problem with Dirichlet boundary condition and discuss the ways it has been solved in the literature. Then, we introduce a Poisson problem and a steady state Stokes problem that we are going to use as parts of our algorithms to solve biharmonic equation. We further discuss wellposedness and regularity of both Poisson and Stokes problems and present their H^1 and L^2 error estimates on a quasi uniform mesh. Next, we present wellposedness and regularity results of the biharmonic equation and its decoupled formulations. The first decoupled formulation is introduced using one Poisson equation and a one steady state Stokes equation. We highlight the fact that the source term of the Stokes equation is not unique based on the first decouple formulation. Then, as a generalization to the first decoupled formulation we introduce the second decoupled formulation using two Poisson equations and one Stokes equation. Moreover, we show that the solutions of the decoupled

formulations are equivalent to the solution of the original biharmonic equation on both convex and non convex domains. Finally, we propose two finite element algorithms based on the two decoupled formulations introduced above to solve the biharmonic equation numerically.

In Chapter 3, we show the error estimate results for both Algorithms (2.17) and (2.18) on a quasi uniform mesh. Here, we present H^1 and L^2 error estimate results. Since the Stokes equation is an intermediate step in each algorithm, we present H^1 and L^2 error estimates for Stokes equation in addition to the error estimate results of the biharmonic equation. During the error estimate of Stokes equation, we discuss the error estimate results for Mini-elements and Taylor-Hood elements for solving Stokes equation.

In Chapter 4, we present H^1 and L^2 error estimates for the both Algorithms (2.17) and (2.18) on a graded mesh. To this end, first we introduce weighted Sobolev space and then we discuss the regularity of the Stokes and Poisson problems in weighted Sobolev space. Then, we present the construction of graded meshes to improve the convergence rates of the numerical approximation from Algorithms (2.17) and (2.18). Moreover, we prove the interpolation error estimate on graded meshes. Finally we present the H^1 and L^2 error estimates of finite element solution to the biharmonic equation and to the Stokes solution in both Algorithms.

In Chapter 5, we present several numerical examples to justify our theoretical finding. First, we compare our numerical solution with a reference solution obtained through Argyris finite elements for convex and non convex domains. Next, we test convergent rates of our solution on non convex domains with re-entrant corner $3\pi/2$ for a sequence of graded meshes including quasi uniform mesh. We further test our method for domains with dif-

ferent re-entrant corners other than $3\pi/2$ including multiple re-entrant corners. The last example is presented with CPU time to show how fast our algorithms.

In Chapter 6, we summarize our work and provide some promising future directions.

CHAPTER 2 THE BIHARMONIC PROBLEM

2.1 The Biharmonic Problem

Let $\Omega \subset \mathbb{R}^2$ be a polygonal domain. Consider the following fourth order elliptic equation called the biharmonic problem

$$\Delta^2 \phi = f \quad \text{in } \Omega, \quad \phi = 0 \quad \text{and} \quad \partial_{\mathbf{n}} \phi = 0 \quad \text{on } \partial\Omega \quad (2.1)$$

where \mathbf{n} is the outward normal derivation and the biharmonic operator

$$\Delta^2 = \nabla^4 = \frac{\partial^4}{\partial x^4} + 2 \frac{\partial^4}{\partial x^2 \partial y^2} + \frac{\partial^4}{\partial y^4}.$$

The homogeneous Dirichlet boundary condition or Clamped boundary conditions [92, 43] used in Equation (2.1) occur for example in fluid mechanics [48, 94, 16] and linear elasticity [37, 16, 82, 53, 61]. In fluid dynamics, Equation (2.1) describes the stream function $\phi(x, y)$ of an incompressible two-dimensional creeping flow (Reynolds number zero). In linear elasticity $\phi(x, y)$ can represent the Airy stress function or as in the theory of thin plates, the vertical displacement due to an external force. There are several approaches to discretize the biharmonic equation in the literature.

If the approximate solution lies in a subspace of the space $H_0^2(\Omega)$ then a conforming finite element method such as the Argyris finite element method [6] can be used. However, this method requires constructing C^1 continuous finite element elements which usually involve large degrees of freedom and hence can be computationally expensive. Therefore, conforming elements are rarely used in scientific and engineering computing since the

1980's.

The non conforming finite elements such as Morley finite element [81, 79] method avoid the difficulty of constructing C^1 elements. However, its convergence depends heavily on the delicate design of the finite element space see [1, 14, 24, 37, 63]. The non conforming finite elements is a popular method to approximate high-order elliptic problems such as the biharmonic problem (2.1). For detail, see [37, 38] and the references therein.

Another way to avoid C^1 elements is by using mixed finite element methods which use continuous Lagrange finite element space. In a mixed method the problem is decomposed into problems involving lower order differential equations.

Ciarlet and Raviart [40], in 1974, proposed a couple system of Poisson problems to solve biharmonic problems choosing u and Δu as unknowns. The error analysis of their method can be found in [87, 86, 11, 49]. The solution u is approximated with the optimal convergence rates. However, approximation to Δu is suboptimal. More precisely, assuming certain L^∞ smoothness assumptions on the derivatives of the solutions, the approximation to Δu converges with rate $h^{k-1/2}$ if piecewise polynomials of degree k are used.

Using linear finite elements Reinhard Scholz [87], in 1978, introduced a mixed finite element method to approximate the solution to biharmonic problem (2.1) and its Laplacian. It is shown that in the case of linear finite elements the mixed method approximations are convergent. Error estimate for L^2 and L^∞ norms are derived in this work. Since the an analogue of the estimate [40] can be shown for finite element spaces of higher degree the error estimates in this case can be improved, especially in the case of quadratic finite elements, provided that the solution is sufficiently smooth.

In 2000, X Cheng, W Han, H Huang [36] proposed some perturbed mixed methods based on a penalty approximation combined with the reduced integration technique to solve the biharmonic problem (2.1). Here they modified the scheme proposed in Malkus and Hughes (1978) [77] and prove the optimal order error estimate without the extra smoothness assumption on the solution made in Johnson and Pitkaranta (1982) [57]. The method studied in their work can be viewed as a version of the wellknown MITC4 element mathematically analyzed in [17, 27, 76] for the Reissner–Mindlin plate model problem.

In 2011, Edvin M Behrenst and Johnny Guzman [18] introduced a new mixed method based on a formulation on where the biharmonic problem is rewritten as a system of four first order equations. Moreover, their method will approximate the second derivatives of u , with optimal order $k+1$, while assuming the correct regularity for the second derivatives of u . Finally, they developed a postprocessing technique that produces a new approximation to u that converges with order $k+3$ for $k \geq 1$.

In 2017, Hailong Guo, Zhimin Zhang, and Qingsong Zou [52] constructed a C^0 linear finite element method for biharmonic equations. In their paper, the post-processing gradient recovery operators are used to calculate approximately the second order partial derivatives of a C^0 linear finite element function. It is shown that the numerical solution of the proposed method converges to the exact one with optimal orders under L^2 norm and discrete H^2 norms, while the recovered numerical gradient converges to the exact one with a superconvergence order.

In 2017, Lothar Banz, Bishnu P. Lamichhane, Ernst P. Stephan [15] considered a three-field (the solution, the gradient and the Lagrange multiplier) formulation of the biharmonic problem. They used the standard Lagrange finite element to discretize the solution

by adding a stabilization term in the discrete setting. The Raviart-Thomas finite elements are used to discretize the gradient. To achieve the optimal error estimate the Lagrange multipliers are constructed.

A quadrature finite element Galerkin scheme for a biharmonic problem on a rectangular polygon is studied by Rakhim Aitbayev [3] in 2008. It is known that, with the Bogner-Fox-Schmit element [39] at least a three-point Gaussian quadrature should be used for approximating the integrals in the finite element Galerkin solution of the biharmonic problem. In this article, they proved that the two-point Gaussian quadrature Galerkin scheme is well-posed and has optimal order error estimates in Sobolev norms. Since fewer function evaluations are required forming the stiffness matrix and the load vector of the quadrature scheme is faster than with the three-point scheme.

There is a rich literature on mixed finite element methods for the biharmonic problem see [45, 85, 40, 56, 44, 4, 69, 80] and references therein. In addition, discontinuous Galerkin methods were also developed for biharmonic problems and nonlinear fourth order partial differential equations (see e.g., [71, 72, 73, 74, 75, 98]).

In this dissertation we discuss a mixed finite element method to discretize the biharmonic equation with Dirichlet boundary conditions. In particular, we propose a method that effectively decouples the fourth-order problem into a system of two Poisson equations and one Stokes equation, or a system of one Stokes equation and one Poisson equation. Thus a deliberate study of the Poisson equation and the steady state Stokes equation is needed to carry out the theoretical and numerical results of this work. In addition, we show the regularity of each decoupled system in both the Sobolev space and a weighted Sobolev space, and we derive the optimal error estimates for the numerical solutions on

both quasi-uniform meshes and graded meshes.

2.1.1 The Poisson Equation

In this subsection, we present the wellposedness and the regularity of a two dimensional Poisson equation with Dirichlet boundary condition. We then present error estimates on quasi uniform meshes and graded meshes. The Poisson equation under considerations is as follows:

Let $\Omega \subset \mathbb{R}^2$ be a polygonal domain. Consider the Poisson problem

$$-\Delta u = f \quad \text{in } \Omega, \quad u = 0 \quad \text{on } \partial\Omega, \quad (2.2)$$

We denote by $H^m(\Omega)$ for an integer $m \geq 0$, the Sobolev space that consists of square integrable functions whose i th weak derivatives are also square integrable for $0 \leq i \leq m$. For $s > 0$ that is not an integer, we denote by $H^s(\Omega)$ the fractional order Sobolev space. For $\tau \geq 0$, $H_0^\tau(\Omega)$ represents the closure in $H^\tau(\Omega)$ of the space of C^∞ functions with compact supports in Ω , and $H^{-\tau}(\Omega)$ represents the dual space of $H_0^\tau(\Omega)$. Let $L^2(\Omega) := H^0(\Omega)$. We shall denote the norm $\|\cdot\|_{L^2(\Omega)}$ by $\|\cdot\|$ when there is no ambiguity about the underlying domain.

By applying Green's formulas, the variational formulation for Poisson problem (2.2) can be written as:

$$a(u, v) := \int_{\Omega} \nabla u \nabla v dx = \int_{\Omega} f \psi dx = (f, v), \quad \forall u \in H_0^1(\Omega). \quad (2.3)$$

The finite element discretized Poisson problem then reads: find the solution $u_n \in V_n^k$ of

the Poisson equation

$$(\nabla u_n, \nabla v) = \langle f, v \rangle \quad \forall v \in V_n^k. \quad (2.4)$$

Wellposedness and Regularity:

For a function $u \in H_0^1(\Omega)$, applying the Poincaré-type inequality [51], it follows

$$a(u, u) = \|\nabla u\|^2 = |u|_{H^1(\Omega)}^2 \geq C \|u\|_{H^1(\Omega)}^2.$$

Theorem 2.1. (*Lax-Milgram lemma*) *Let \mathbf{V} be a Hilbert space, let $a(\cdot, \cdot) : \mathbf{V} \times \mathbf{V} \rightarrow \mathbf{R}$ be a continuous \mathbf{V} elliptic bilinear form, and $f : \mathbf{V} \rightarrow \mathbf{R}$ be a continuous linear form. Then the abstract variational problem: Find u such that*

$$u \in \mathbf{V} \quad \text{and} \quad v \in \mathbf{V} \quad a(u, v) = f(v) \quad (2.5)$$

has one and only one solution.

Thus, for any $f \in H^{-1}(\Omega)$, we have by the Lax-Milgram Theorem that Equation (2.3) admits a unique weak solution $u \in H_0^1(\Omega)$.

The regularity of the solution u depends on the given data f and the domain geometry [2, 21]. We are interested in the case when Ω is concave, and thus the solution of Equation (2.2) possesses corner singularities at vertices of Ω where some of the interior angles are greater than π . Let $\beta = \min_i(\pi/\alpha_i, 1)$ where α_i are interior angles of the polygonal domain Ω . By the regularity theory, the solution u is in $H^{1+\beta}(\Omega)$. Thus the Poisson Equation (2.2) holds the regularity estimate

$$\|u\|_{H^{1+\beta}(\Omega)} \leq C\|f\|_{H^{-1+\beta}(\Omega)}. \quad (2.6)$$

H^1 and L^2 Error Estimate Results:

Suppose that the mesh \mathcal{T}_n consists of quasi-uniform triangles with size h . The interpolation error estimate on \mathcal{T}_n (see e.g., [37]) for any $v \in H^s(\Omega)$, $s > 1$,

$$\|v - v_I\|_{H^l(\Omega)} \leq Ch^{s-l}\|v\|_{H^s(\Omega)}, \quad (2.7)$$

where $l = 0, 1$ and $v_I \in V_n^k$ represents the nodal interpolation of v .

Lemma 2.2. *Let u be the solution of the Poisson problem (2.2), and u_n be the finite element approximation (2.4) on quasi-uniform meshes, then it follows*

$$\|u - u_n\|_{[H^1(\Omega)]} \leq Ch^{\min\{k,\beta\}}, \quad (2.8a)$$

$$\|u - u_n\|_{[L^2(\Omega)]} \leq Ch^{\min\{k+1,\beta+1\}}. \quad (2.8b)$$

By the regularity theory, the solution u is in $H^{1+\beta}(\Omega)$. It is easy to see that when the maximum angle is larger than π , i.e., Ω is concave, $u \notin H^2(\Omega)$, and thus the finite element approximation based on quasi-uniform grids will not produce the optimal convergence rate. Graded meshes near the singular vertices are employed to recovery the optimal convergence rate. Such meshes can be constructed based on a priori estimates [9, 10, 13, 54, 55, 64, 84] or on a posteriori analysis [20, 33, 91]. In this work, we present the

approach used in [13, 64].

To introduce the error estimate results under graded meshes we use the weighted Sobolev space $\mathcal{K}_a^m(\Omega)$. On details of weighted Sobolev spaces used here, we refer readers to [42, 50, 58, 13, 64]. We postpone presenting error estimate results for the Poisson equation under graded mesh as we carry out the same error estimate results in Chapter 5. Until then we refer readers [35].

2.1.2 The Stokes Equation

In this subsection, we present the wellposedness and the regularity of a two dimensional steady state Stokes equation with Dirichlet boundary condition. We then present error H^1 and L^2 error estimates results. Stokes equations under consideration is as follows:

We consider the following Stokes equation

$$\begin{aligned} -\Delta \mathbf{u} + \nabla p &= \mathbf{F} & \text{in } \Omega, \\ \operatorname{div} \mathbf{u} &= 0 & \text{in } \Omega, \\ \mathbf{u} &= 0 & \text{on } \partial\Omega, \end{aligned} \tag{2.9}$$

that describes incompressible flow in which advective inertial forces are negligible compared to viscous forces. $\mathbf{u} = (u_1, u_2)$ is the velocity of the fluid, p the pressure and $\mathbf{F} = (f_1, f_2)$ an external force that drives the motion.

Wellposedness and Regularity:

Assume that the polygonal domain Ω consists of N vertices Q_i , $i = 1, \dots, N$, and the corresponding interior angles are $\omega_i \in (0, 2\pi)$. The largest interior angle $\omega = \max_i \omega_i$ associated with the vertex Q . We set z_j , $j = 1, 2, \dots, n$ the solutions of the following

characteristic equation corresponding to the the Stokes problem (2.9) (see, e.g., [51]),

$$\sin^2(z\omega) = z^2 \sin^2(\omega), \quad (2.10)$$

then there exists a threshold

$$\alpha_0 := \min\{\operatorname{Re}(z_j), j = 1, 2, \dots, n\} \in (1/2, 2], \quad (2.11)$$

such that when $0 \leq \alpha < \alpha_0$.

The weak formulation of the Stokes equations (2.9) is to find $\mathbf{u} \in [H_0^1(\Omega)]^2$ and $p \in L_0^2(\Omega)$ such that

$$\begin{aligned} (\nabla \mathbf{u}, \nabla \mathbf{v}) - (\operatorname{div} \mathbf{v}, p) &= \langle \mathbf{F}, \mathbf{v} \rangle \quad \forall \mathbf{v} \in [H_0^1(\Omega)]^2, \\ -(\operatorname{div} \mathbf{u}, q) &= 0 \quad \forall q \in L_0^2(\Omega), \end{aligned} \quad (2.12)$$

where

$$L_0^2(\Omega) = \{q \in L^2(\Omega), \int_{\Omega} q dx = 0\}.$$

Given that $\mathbf{F} \in [H^{-1}(\Omega)]^2$, then Equation (2.12) admits unique solution $(\mathbf{u}, p) \in [H_0^1(\Omega)]^2 \times L_0^2(\Omega)$ (see, e.g. [62, 95, 47]). For $\mathbf{F} \in [H^{-1+\alpha}(\Omega)]^2$, the Stokes problem holds the regularity estimate [19, 51, 83],

$$\|\mathbf{u}\|_{[H^{1+\alpha}(\Omega)]^2} + \|p\|_{H^\alpha(\Omega)} \leq C \|\mathbf{F}\|_{[H^{-1+\alpha}(\Omega)]^2}. \quad (2.13)$$

H^1 and L^2 Error Estimate Results:

We are interested in solving the Stokes problem numerically using finite elements. Therefore, we choose a regular triangulation \mathcal{T}_n and finite dimensional spaces V_h and Q_h . For this problem we restrict ourselves to the case of conforming elements, i.e. $V_h \subset V = H_0^1(\Omega)$ and $Q_h \subset Q = L_0^2(\Omega)$. The discretized Stokes problem then reads:

Find the solution $\mathbf{u}_n \times p_n \in [V_n^k]^2 \times S_n^{k-1}$ of the Stokes equation

$$\begin{aligned} (\nabla \mathbf{u}_n, \nabla \mathbf{v}) - (p_n, \operatorname{div} \mathbf{v}) &= \langle \mathbf{F}, \mathbf{v} \rangle \quad \forall \mathbf{v} \in [V_n^k]^2, \\ -(\operatorname{div} \mathbf{u}_n, q) &= 0 \quad \forall q \in S_n^{k-1}. \end{aligned} \tag{2.14}$$

It is well known that in order to get working method the spaces V_h and Q_h can not be chosen arbitrarily. The method can be expected to behave well only if the following inf-sup condition is satisfied.

Definition 2.3. (*Inf-sup condition*). *The pair (V_h, Q_h) is said to fulfill the inf-sup condition if there exists $\gamma_1 > 0$ independent of h such that*

$$\sup_{0 \neq \mathbf{v} \in [V_n^k]^2} \frac{(\operatorname{div} \mathbf{v}, q)}{\|\mathbf{v}\|_{[H^1(\Omega)]^2}} \geq \gamma_1 \|q\|, \quad \forall q_n \in S_n^{k-1}, \tag{2.15}$$

where the constant $\gamma_1 > 0$.

General techniques for verifying the inf-sup condition can be found from [22, 89]. In this work we use tow types of finite elements which are known to be stable.

- **The Taylor-Hood Element**

The Taylor-Hood finite element is the standard finite element for simulating incompressible fluid flow, since it gives a good approximation of both velocity and pressure, and since it is not too numerically costly to use. The element consists of

a continuous piecewise quadratic approximation of each velocity component combined with a continuous piecewise linear approximation of the pressure. That is the velocity space is $V_h = \{v \in [C^0(\Omega)]^2 : v|_K \in [P^2(K)]^2\}$ and the pressure space $Q_h = \{v \in C^0(\Omega) : v|_K \in [P^1(K)]^2\}$. Figure 1 shows the position of the velocity and pressure nodes on a triangle element K .

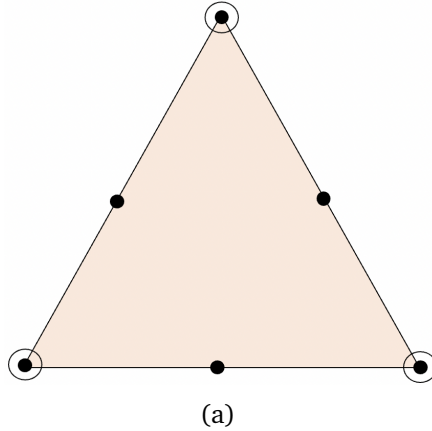


Figure 1: The Taylor-Hood elements: Velocity \bullet and pressure nodes \circ

- **The Mini Element**

The MINI element is the simplest inf-sup stable element. It consists of a continuous piecewise linear approximation for each velocity component as well as for the pressure. However, on each element the velocity space is enriched by cubic bubble functions of the form $\varphi_{bubble} = \varphi_1\varphi_2\varphi_3$, where $\varphi_i, i = 1, 2, 3$ are the usual hat functions. The velocity space is given by $V_h = \{v \in [C^0(\Omega)]^2 : v|_K \in [P^2(K)]^2 \oplus [B(K)]^2\}$ where, $B(K) = \text{span}(\varphi_{bubble})$ is the space of bubble functions on element K . Perhaps needless to say, the bubble function has earned its name from the fact that it has the shape of a bubble. By construction φ_{bubble} vanishes on the boundary ∂K . which is important as it allows all bubble functions to be eliminated from the saddle-point

linear system before attempting to invert it. The MINI element has become popular because it is easy to implement. However, it is also known for giving a poor approximation of the pressure. The velocity and pressure nodes on a triangle element K are shown in figure 2.

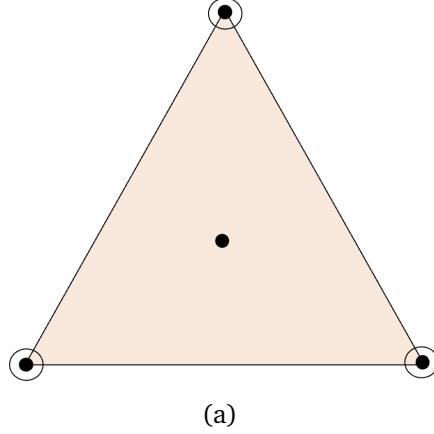


Figure 2: The Mini element: Velocity \bullet and pressure nodes \circ

A common choice of the finite element spaces is the Taylor-Hood pair of order $k \in \mathbb{N}$. Therefore, for the purpose of the error analysis we use Taylor-Hood pair. We refer readers to [48, 90, 24].

Lemma 2.4. *Let (\mathbf{u}, p) be the solution of the Stokes problem (2.12), and (\mathbf{u}_n, p_n) be the Taylor-Hood element solution of Equation (2.14), then it follows the estimate*

$$\|\mathbf{u} - \mathbf{u}_n\|_{[H^1(\Omega)]^2} + \|p - p_n\| \leq C \left(\inf_{\mathbf{v} \in [V_n^k]^2} \|\mathbf{u} - \mathbf{v}\|_{[H^1(\Omega)]^2} + \inf_{q \in S_n^{k-1}} \|p - q\| \right). \quad (2.16)$$

Proof. By Theorem (2.1) and Inf-sup condition (2.15), the proof follows from the technique in [26]. \square

In combination with the approximation result we achieve the following convergence

result.

Lemma 2.5. *Let (\mathbf{u}, p) be the solution of the Stokes problem (2.26), and (\mathbf{u}_n, p_n) be the Mini element solution ($k = 1$) or Taylor-Hood element solution ($k \geq 2$) in Algorithm 2.17 on quasi-uniform meshes, then it follows*

$$\|\mathbf{u} - \mathbf{u}_n\|_{[H^1(\Omega)]^2} + \|p - p_n\| \leq Ch^{\min\{k, \alpha\}}, \quad (2.17a)$$

$$\|\mathbf{u} - \mathbf{u}_n\|_{[L^2(\Omega)]^2} \leq Ch^{\min\{k+1, \alpha+1, 2\alpha\}}. \quad (2.17b)$$

If the largest interior angle $\omega < \pi$, it follows $\min\{\alpha + 1, 2\alpha\} = \alpha + 1$, and if $\omega > \pi$, we have $\min\{\alpha + 1, 2\alpha\} = 2\alpha$.

2.2 Well-posedness and Regularity of the Biharmonic Problem

Denote by $H^m(\Omega)$ for an integer $m \geq 0$, the Sobolev space that consists of square integrable functions whose i th weak derivatives are also square integrable for $0 \leq i \leq m$. For $s > 0$ that is not an integer, we denote by $H^s(\Omega)$ the fractional order Sobolev space. For $\tau \geq 0$, $H_0^\tau(\Omega)$ represents the closure in $H^\tau(\Omega)$ of the space of C^∞ functions with compact supports in Ω , and $H^{-\tau}(\Omega)$ represents the dual space of $H_0^\tau(\Omega)$. Let, $L^2(\Omega) := H^0(\Omega)$. We shall denote the norm $\|\cdot\|_{L^2(\Omega)}$ by $\|\cdot\|$ when there is no ambiguity about the underlying domain. $[\cdot]^2$ represents the vector space. For example, $\mathbf{v} = (v_1, v_2)^T \in [H_0^1(\Omega)]^2$ represents $v_i \in H_0^1(\Omega)$, $i = 1, 2$, where, T is the transposition of a matrix or a vector. For $\mathbf{v} = (v_1, v_2)^T$, we denote $(\text{curl } \mathbf{v}) := \frac{\partial v_2}{\partial x_1} - \frac{\partial v_1}{\partial x_2}$. For a scalar function ψ , we denote $(\text{curl } \psi) := (\psi_{x_2}, -\psi_{x_1})^T$.

By applying Green's formulas, the variational formulation for biharmonic problem (2.1)

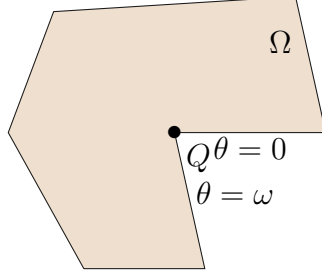


Figure 3: Domain Ω containing one reentrant corner.

can be written as:

$$a(\phi, \psi) := \int_{\Omega} \Delta\phi\Delta\psi dx = \int_{\Omega} f\psi dx = (f, \psi), \quad \forall \psi \in H_0^2(\Omega). \quad (2.18)$$

For a function $\psi \in H_0^2(\Omega)$, applying the Poincaré-type inequality [51] twice, it follows

$$a(\psi, \psi) = \|\Delta\psi\|^2 = |\psi|_{H^2(\Omega)}^2 \geq C\|\psi\|_{H^2(\Omega)}^2.$$

Thus, for any $f \in H^{-2}(\Omega)$, we have by the Lax-Milgram Theorem that (2.18) admits a unique weak solution $\phi \in H_0^2(\Omega)$.

The regularity of the solution ϕ depends on the given data f and the domain geometry [2, 21]. In order to decouple Equation (2.1), we assume that the polygonal domain Ω consists of N vertices Q_i , $i = 1, \dots, N$, and the corresponding interior angles are $\omega_i \in (0, 2\pi)$. The largest interior angle $\omega = \max_i \omega_i \in [\frac{\pi}{3}, 2\pi)$ associated with the vertex Q . A sketch of the domain is given in Figure 3. We set z_j , $j = 1, 2, \dots, n$ the solutions of the following characteristic equation corresponding to the the biharmonic problem (2.1) (see, e.g., [51]),

$$\sin^2(z\omega) = z^2 \sin^2(\omega),$$

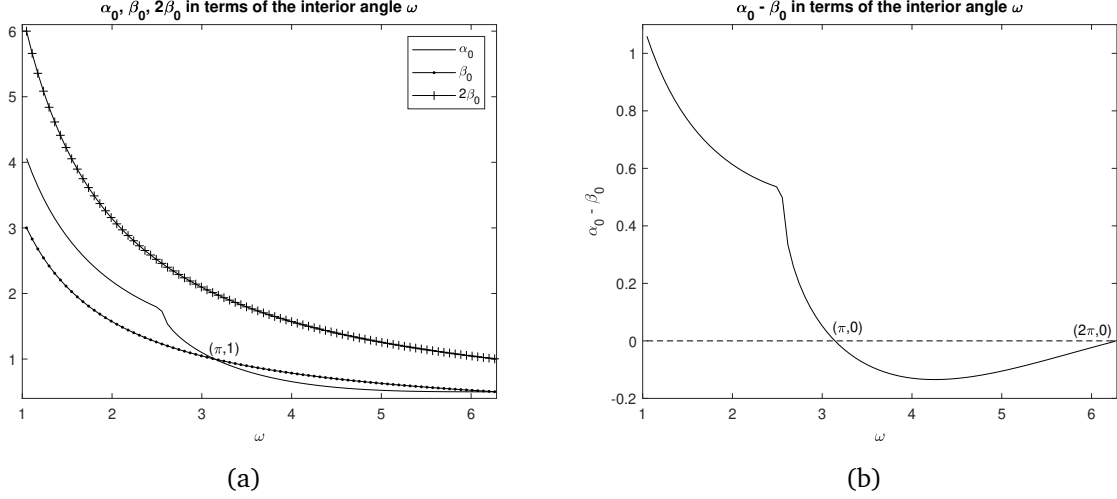


Figure 4: (a) α_0, β_0 in terms of ω ; (b) $\alpha_0 - \beta_0$ in terms of ω .

then there exists a threshold

$$\alpha_0 := \min\{\operatorname{Re}(z_j), j = 1, 2, \dots, n\} > \frac{1}{2}, \quad (2.19)$$

such that when $0 \leq \alpha < \alpha_0$, the biharmonic problem (2.1) holds the regularity estimate [59, 12, 23]

$$\|\phi\|_{H^{2+\alpha}(\Omega)} \leq C\|f\|_{H^{-2+\alpha}(\Omega)}.$$

Sketches of the threshold α_0 in terms of the interior angle ω is shown in Figure 4a. In Figure 4a, as a comparison we also show $\beta_0 = \frac{\pi}{\omega}$, which is threshold of the characteristic equation for the Poisson equation with homogeneous Dirichlet boundary condition in the same polygonal domain. In Figure 4b, we show the difference $\alpha_0 - \beta_0$ in term of the interior angle ω , from which we find $\beta_0 + 1 > \alpha_0$, when the largest interior angle ω satisfies $\frac{\pi}{3} < \omega_0 < \omega < \pi$ for some ω_0 . In Table 1, we present some numerical values of α_0 and β_0 in terms of different interior angles ω .

Table 1: Some numerical values of α_0 and β_0 in terms of different interior angles ω .

	ω	$\alpha_0 \approx$	$\beta_0 \approx$	$\alpha_0 - \beta_0 \approx$
$\omega(< \pi)$	$\pi/6$	8.95500	6.00000	2.95500
	$\pi/4$	5.39100	4.00000	1.39100
	$\pi/3$	4.05933	3.00000	1.05933
	$\pi/2$	2.73959	2.00000	0.73959
	$2\pi/3$	2.09414	1.50000	0.59414
	$3\pi/4$	1.88537	1.33333	0.55204
	$5\pi/6$	1.53386	1.20000	0.33386
	$11\pi/12$	1.20063	1.09090	0.10973
$\omega(> \pi)$	$10\pi/9$	0.81870	0.90000	-0.08130
	$7\pi/6$	0.75197	0.85714	-0.10517
	$6\pi/5$	0.71779	0.83333	-0.11554
	$5\pi/4$	0.67358	0.80000	-0.12642
	$4\pi/3$	0.61573	0.75000	-0.13427
	$3\pi/2$	0.54448	0.66667	-0.12219
	$8\pi/5$	0.52171	0.62500	-0.10329
	$7\pi/4$	0.50501	0.57143	-0.06642

For α_0 and β_0 , we have the following result from [59, Theorem 7.1.1].

Lemma 2.6. *If $\omega \in (0, \pi)$, it follows that α_0 in (2.19) satisfies*

$$\beta_0 < \alpha_0 < 2\beta_0, \quad (2.20)$$

and if $\omega \in (\pi, 2\pi)$, it follows

$$\frac{1}{2} < \alpha_0 < \beta_0, \quad (2.21)$$

where $\beta_0 = \frac{\pi}{\omega}$.

By Lemma 2.6, when $\omega < \pi$, it follows

$$\frac{1}{2} < \frac{\beta_0}{\alpha_0} < 1, \quad (2.22)$$

and when $\omega > \pi$, it follows

$$\frac{\beta_0}{\alpha_0} > 1. \quad (2.23)$$

2.3 Decoupled Formulations of the Biharmonic Problem

2.3.1 The First Decoupled Formulation

It is known that solving high order problems numerically, such as Equation (2.1), is much harder than solving lower order problem. Thus, we decouple Equation (2.1) into one steady-state Stokes problem and one Poisson problem as our first decoupled formulation to solve the biharmonic problem (2.1). We first introduce a steady-state Stokes problem

$$\begin{aligned} -\Delta \mathbf{u} + \nabla p &= \mathbf{F} \quad \text{in } \Omega, \\ \operatorname{div} \mathbf{u} &= 0 \quad \text{in } \Omega, \\ \mathbf{u} &= 0 \quad \text{on } \partial\Omega, \end{aligned} \quad (2.24)$$

where $\mathbf{u} = (u_1, u_2)$ is the velocity field of an incompressible fluid motion, p is the associated pressure, and the source term $\mathbf{F} = (f_1, f_2)$ satisfies

$$\operatorname{curl} \mathbf{F} := \frac{\partial f_2}{\partial x_1} - \frac{\partial f_1}{\partial x_2} = f, \quad (2.25)$$

for f given in Equation (2.1).

The weak formulation of the Stokes equations (2.24) is to find $\mathbf{u} \in [H_0^1(\Omega)]^2$ and $p \in L_0^2(\Omega)$ such that

$$\begin{aligned}
(\nabla \mathbf{u}, \nabla \mathbf{v}) - (\operatorname{div} \mathbf{v}, p) &= \langle \mathbf{F}, \mathbf{v} \rangle \quad \forall \mathbf{v} \in [H_0^1(\Omega)]^2, \\
-(\operatorname{div} \mathbf{u}, q) &= 0 \quad \forall q \in L_0^2(\Omega),
\end{aligned} \tag{2.26}$$

where

$$L_0^2(\Omega) = \left\{ q \in L^2(\Omega), \int_{\Omega} q dx = 0 \right\}.$$

For the bilinear forms in weak formulation (2.26), we have the following Ladyzhenskaya-Babuska-Breezi (LBB) or inf-sup conditions,

$$\begin{aligned}
\inf_{q \in L_0^2(\Omega)} \sup_{\mathbf{v} \in [H_0^1(\Omega)]^2} \frac{-(\operatorname{div} \mathbf{v}, q)}{\|\mathbf{v}\|_{[H_0^1(\Omega)]^2} \|q\|} &\geq \gamma_1 > 0, \\
\inf_{\mathbf{u} \in [H_0^1(\Omega)]^2} \sup_{\mathbf{v} \in [H_0^1(\Omega)]^2} \frac{(\nabla \mathbf{u}, \nabla \mathbf{v})}{\|\mathbf{u}\|_{[H_0^1(\Omega)]^2} \|\mathbf{v}\|_{[H_0^1(\Omega)]^2}} &\geq \gamma_2 > 0,
\end{aligned} \tag{2.27}$$

and the boundedness

$$\begin{aligned}
(\nabla \mathbf{u}, \nabla \mathbf{v}) &\leq C_1 \|\mathbf{u}\|_{[H_0^1(\Omega)]^2} \|\mathbf{v}\|_{[H_0^1(\Omega)]^2}, \\
(\operatorname{div} \mathbf{v}, q) &\leq C_2 \|\mathbf{v}\|_{[H_0^1(\Omega)]^2} \|q\|,
\end{aligned} \tag{2.28}$$

where $\gamma_1, \gamma_2, C_1, C_2$ are constants.

Given that $\mathbf{F} \in [H^{-1}(\Omega)]^2$, under conditions (2.27) and (2.28), the weak formulation (2.26) admits unique solution $(\mathbf{u}, p) \in [H_0^1(\Omega)]^2 \times L_0^2(\Omega)$ (see, e.g. [62, 95, 47]). For $\mathbf{F} \in [H^{-1+\alpha}(\Omega)]^2$, the Stokes problem holds the regularity estimate [19, 51, 83],

$$\|\mathbf{u}\|_{[H^{1+\alpha}(\Omega)]^2} + \|p\|_{H^\alpha(\Omega)} \leq C \|\mathbf{F}\|_{[H^{-1+\alpha}(\Omega)]^2}. \tag{2.29}$$

Since no boundary data is enforced to Equation (2.25), so \mathbf{F} obtained through Equation (2.25) is not unique. Assume that $\mathbf{F}_0 \in [L^2(\Omega)]^2$ is a solution of Equation (2.25), then it

follows that

$$\mathbf{F} = \mathbf{F}_0 + \nabla q, \quad \forall q \in H^1(\Omega),$$

is also a solution of Equation (2.25) in $[L^2(\Omega)]^2$, since for $q \in H^1(\Omega)$, we have $(\text{curl } \nabla q) \equiv 0$.

Now we provide a way to obtain the source term \mathbf{F} of the Stokes equation (2.24).

Lemma 2.7. *Assume that $f \in L^2(\Omega)$.*

(i) *For any fixed x_2 , if $f(\xi, x_2)$ is integrable on $[c_1, x_1]$ for some constant c_1 , then*

$$\mathbf{F} = \left[0, \int_{c_1}^{x_1} f(\xi, x_2) d\xi \right]^T \quad (2.30)$$

satisfies Equation (2.25).

(ii) *Similarly, for any fixed x_1 , if $f(x_1, \zeta)$ is integrable on $[c_2, x_2]$ for some constant c_2 , then*

$$\mathbf{F} = \left[-\int_{c_2}^{x_2} f(x_1, \zeta) d\zeta, 0 \right]^T \quad (2.31)$$

also satisfies Equation (2.25).

(iii) *If both $f(\xi, x_2)$ and $f(x_1, \zeta)$ are integrable, then for any constant η ,*

$$\mathbf{F} = \left[-\eta \int_{c_2}^{x_2} f(x_1, \zeta) d\zeta, (1 - \eta) \int_{c_1}^{x_1} f(\xi, x_2) d\xi \right]^T \quad (2.32)$$

also satisfies Equation (2.25).

Lemma 2.8. *Assume that $\mathbf{F}_l \in [L^2(\Omega)]^2$, $l = 1, 2$ both satisfy Equation (2.25). Let (\mathbf{u}_l, p_l) be*

solutions of Equation (2.24) or Equation (2.26) corresponding to \mathbf{F}_l , then it follows that

$$\begin{aligned} \mathbf{u}_1 = \mathbf{u}_2, \quad & \text{in } [H_0^1(\Omega)]^2 \cap [H^{1+\alpha}(\Omega)]^2, \\ p_1 = p_2 + q, \quad & \text{in } L_0^2(\Omega) \cap H^\alpha(\Omega), \end{aligned} \tag{2.33}$$

where $q \in L_0^2(\Omega) \cap H^1(\Omega)$ satisfies $\nabla q = \mathbf{F}_1 - \mathbf{F}_2$.

Proof. We take $\bar{\mathbf{F}} = \mathbf{F}_1 - \mathbf{F}_2 \in [L^2(\Omega)]^2$, then by Helmholtz decomposition [47], there exist a stream-function ψ and a potential-function $q \in H^1(\Omega)$ uniquely up to a constant such that

$$\bar{\mathbf{F}} = \nabla q + \mathbf{curl} \psi, \tag{2.34}$$

and

$$(\bar{\mathbf{F}} - \nabla q) \cdot \mathbf{n} = (\mathbf{curl} \psi) \cdot \mathbf{n} = 0, \quad \text{in } H^{-\frac{1}{2}}(\partial\Omega). \tag{2.35}$$

From Equation (2.35), we have

$$\frac{\partial \psi}{\partial \tau} = (\mathbf{curl} \psi) \cdot \mathbf{n} = 0 \quad \text{in } H^{-\frac{1}{2}}(\partial\Omega),$$

where τ is the unit tangential vector on $\partial\Omega$, thus we have

$$\psi = C_0 \quad \text{in } H^{\frac{1}{2}}(\partial\Omega), \tag{2.36}$$

where C_0 is a constant. Take \mathbf{curl} on Equation (2.34), we have

$$-\Delta \psi = \mathbf{curl} (\mathbf{curl} \psi) = \mathbf{curl} \bar{\mathbf{F}} = 0, \tag{2.37}$$

where the last equality is based on the fact that $\mathbf{F}_1, \mathbf{F}_2$ satisfy Equation (2.25). By the Lax-Milgram Theorem, the Poisson problem (2.37) and (2.36) admits a unique solution $\psi = C_0$ in $H^1(\Omega)$. Therefore, the decomposition (2.34) is equivalent to

$$\bar{\mathbf{F}} = \nabla q. \quad (2.38)$$

Let $\bar{\mathbf{u}} = \mathbf{u}_1 - \mathbf{u}_2$ and $\bar{p} = p_1 - p_2$, then $(\bar{\mathbf{u}}, \bar{p})$ satisfies

$$\begin{aligned} -\Delta \bar{\mathbf{u}} + \nabla(\bar{p} - q) &= 0 \quad \text{in } \Omega, \\ \operatorname{div} \bar{\mathbf{u}} &= 0 \quad \text{in } \Omega, \\ \bar{\mathbf{u}} &= 0 \quad \text{on } \partial\Omega. \end{aligned} \quad (2.39)$$

By the regularity of the Stokes problem (2.39), the conclusion holds. \square

Lemma 2.9. *Assume that the source term $\mathbf{F} \in [L^2(\Omega)]^2$ of the Stokes problem (2.24) is any vector function determined by $f \in L^2(\Omega)$ satisfying Equation (2.25), then Equation (2.24) admits a unique solution $\mathbf{u} \in [H^{1+\alpha}(\Omega)]^2$ and satisfies*

$$\|\mathbf{u}\|_{[H^{1+\alpha}(\Omega)]^2} \leq C \|f\|_{L^2(\Omega)}. \quad (2.40)$$

Proof. Given $f \in L^2(\Omega)$, we can always find a vector function $\mathbf{F} \in [L^2(\Omega)]^2$ following Lemma 2.7 such that the corresponding Stokes problem (2.24) admits a unique solution $\mathbf{u} \in [H^{1+\alpha}(\Omega)]^2$ satisfying

$$\|\mathbf{u}\|_{[H^{1+\alpha}(\Omega)]^2} \leq C \|\mathbf{F}\|_{[H^{-1+\alpha}(\Omega)]^2} \leq C \|\mathbf{F}\|_{[L^2(\Omega)]^2} \leq C \|f\|_{L^2(\Omega)}. \quad (2.41)$$

For any source term \mathbf{F} also satisfying Lemma 2.7, it follows by Theorem 2.8 that the conclusion holds. \square

Remark 2.10. *By Lemma 2.8, for given the biharmonic source term f , we can obtain a unique \mathbf{u} for the Stokes problem (2.24), but we have infinitely many ways to obtain \mathbf{F} satisfying Equation (2.25). For most of cases, we can solve for \mathbf{F} exactly instead of solving Equation (2.25) or some other equations. In the first decoupled method, we focus on the case that at least one \mathbf{F} can be obtained exactly (e.g., through (2.30), (2.31), or (2.32)).*

To show the connection of the Stokes problem (2.24) with the biharmonic problem (2.1), we introduce the following result from [48, Theorem 3.1].

Lemma 2.11. *A function $\mathbf{v} \in [H^m(\Omega)]^2$ for integer $m \geq 0$ satisfies*

$$\operatorname{div} \mathbf{v} = 0, \quad \langle \mathbf{v} \cdot \mathbf{n}, 1 \rangle_{\partial\Omega} = 0,$$

then there exists a stream function $\psi \in H^{m+1}(\Omega)$ uniquely up to an additive constant satisfying

$$\mathbf{v} = \mathbf{curl} \psi.$$

Since $\mathbf{u} \in [H_0^1(\Omega)]^2 \cap [H^{1+\alpha}(\Omega)]^2$ and $\operatorname{div} \mathbf{u} = 0$, so we have by Lemma 2.11 that there exists $\bar{\phi} \in H^2(\Omega)$ uniquely up to an additive constant satisfying

$$(u_1, u_2)^T = \mathbf{u} = \mathbf{curl} \bar{\phi} = (\bar{\phi}_{x_2}, -\bar{\phi}_{x_1})^T, \tag{2.42}$$

which further implies $|\nabla \bar{\phi}| \in H^{1+\alpha}(\Omega)$, thus we have

$$\bar{\phi} \in H^{2+\alpha}(\Omega). \quad (2.43)$$

Lemma 2.12. *There exists a unique*

$$\bar{\phi} \in H_0^2(\Omega) \cap H^{2+\alpha}(\Omega). \quad (2.44)$$

satisfying Equation (2.42).

Proof. By calculation,

$$\bar{\phi}_\tau = \mathbf{curl} \bar{\phi} \cdot \mathbf{n} = \mathbf{u} \cdot \mathbf{n} = 0,$$

where τ is the unit tangent to $\partial\Omega$, thus it follows

$$\bar{\phi} = \text{constant}, \quad \text{on } \partial\Omega.$$

Without loss of generality, we can take

$$\bar{\phi} = 0, \quad \text{on } \partial\Omega. \quad (2.45)$$

From Equation (2.42), we also have

$$\nabla \bar{\phi} = (\bar{\phi}_{x_1}, \bar{\phi}_{x_2})^T = (-u_2, u_1)^T = \mathbf{0}, \quad \text{on } \partial\Omega. \quad (2.46)$$

Thus, the conclusion of Lemma (2.12) follows from Equations (2.45), (2.46) and (2.43).

□

Instead of solving for $\bar{\phi} \in H_0^2(\Omega) \cap H^{2+\alpha}(\Omega)$ from Equation (2.42) directly, we apply the operator curl on Equation (2.42) to obtain the following Poisson problem

$$-\Delta \bar{\phi} = \operatorname{curl} \mathbf{u} \quad \text{in } \Omega, \quad \bar{\phi} = 0 \quad \text{on } \partial\Omega. \quad (2.47)$$

The weak formulation of Equation (2.47) is to find $\bar{\phi} \in H_0^1(\Omega)$, such that

$$(\nabla \bar{\phi}, \nabla \psi) = (\operatorname{curl} \mathbf{u}, \psi), \quad \forall \psi \in H_0^1(\Omega). \quad (2.48)$$

Since $(\operatorname{curl} \mathbf{u}) \in L^2(\Omega)$, so we have by the Lax-Milgram Theorem that (2.48) admits a unique solution $\bar{\phi} \in H_0^1(\Omega)$.

Lemma 2.13. *The Poisson problem (2.47) admits a unique solution $\bar{\phi} \in H_0^2(\Omega) \cap H^{2+\alpha}(\Omega)$.*

Proof. Since $\bar{\phi} \in H_0^2(\Omega) \cap H^{2+\alpha}(\Omega) \subset H_0^1(\Omega)$ is a solution of Equation (2.42), so it is also a solution of the Poisson problem (2.47). By the uniqueness of the solution of Equation (2.47) in $H_0^1(\Omega)$, the conclusion holds. □

Lemma 2.14. *The solution $\bar{\phi} \in H_0^2(\Omega) \cap H^{2+\alpha}(\Omega)$ obtained through (2.42) or the Poisson problem (2.47) satisfies the biharmonic problem*

$$\Delta^2 \bar{\phi} = \operatorname{curl} \mathbf{F} = f, \quad \text{in } \Omega, \quad \bar{\phi} = 0 \quad \text{and} \quad \partial_{\mathbf{n}} \bar{\phi} = 0 \quad \text{on } \partial\Omega. \quad (2.49)$$

Proof. Following Equation (2.42), we replace \mathbf{u} by $\mathbf{curl} \bar{\phi}$ in Equation (2.24) and obtain

$$-\Delta(\bar{\phi}_{x_2}) + p_{x_1} = f_1, \quad \text{in } \Omega, \quad (2.50a)$$

$$-\Delta(-\bar{\phi}_{x_1}) + p_{x_2} = f_2, \quad \text{in } \Omega. \quad (2.50b)$$

Applying differential operators $-\frac{\partial}{\partial x_2}$ and $\frac{\partial}{\partial x_1}$ to Equation (2.50a) and Equation (2.50b), respectively, and taking the summation lead to the conclusion. \square

From Lemma 2.14, we find that $\bar{\phi}$ in Equation (2.49) satisfies exactly the same problem as ϕ in Equation (2.1) in the following sense,

$$\phi = \bar{\phi}, \quad \text{in } H_0^2(\Omega) \cap H^{2+\alpha}(\Omega). \quad (2.51)$$

Therefore, we will use ϕ to replace the notation $\bar{\phi}$. Thus the Poisson problem (2.47) is equivalent to

$$-\Delta\phi = \mathbf{curl} \mathbf{u} \quad \text{in } \Omega, \quad \phi = 0 \quad \text{on } \partial\Omega. \quad (2.52)$$

The weak formulation (2.48) is equivalent to $\phi \in H_0^1(\Omega)$ satisfying

$$(\nabla\phi, \nabla\psi) = (\mathbf{curl} \mathbf{u}, \psi), \quad \forall \psi \in H_0^1(\Omega). \quad (2.53)$$

By the regularity of the Poisson problem (2.52) and Lemma 2.16, we have that

$$\|\phi\|_{H^{2+\alpha}(\Omega)} \leq C\|\mathbf{curl} \mathbf{u}\|_{H^\alpha(\Omega)} \leq C\|\nabla\mathbf{u}\|_{[H^\alpha(\Omega)]^2} \leq C\|\mathbf{u}\|_{[H^{1+\alpha}(\Omega)]^2} \leq C\|f\|_{L^2(\Omega)}. \quad (2.54)$$

In summary, we can obtain the solution ϕ of the biharmonic problem (2.1) by solving the lower order problems in the following steps,

- (a) Choose an appropriate \mathbf{F} based on Equations (2.30), (2.31), or (2.32);
- (b) Solve \mathbf{u} from the Stokes problem (2.24);
- (c) Solve ϕ from the Poisson problem (2.52).

2.3.2 The Second Decoupled Formulation

In this section we split the Biharmonic equation (2.1) into two Poisson equations and a steady state Stokes equation. In the first decoupled formulation we introduced a way to find \mathbf{F} based on Lemma 2.7 for a given function $f \in L^2(\Omega)$. As a generalization to first decoupled formulation we introduce the second decoupled formulation for a given function $f \in H^{-1}(\Omega)$. To this end, first, we introduce the following Poisson equation for a given f .

$$-\Delta w = f \quad \text{in } \Omega, \quad w = 0 \quad \text{on } \partial\Omega. \quad (2.55)$$

Next, we introduce

$$\mathbf{H}(\text{curl}; \Omega) := \{\mathbf{F} \in [L^2(\Omega)]^2 : \text{curl } \mathbf{F} \in L^2(\Omega)\}.$$

Recall that we use the same Stokes equation (2.24) for the second decoupled formulation and the source term $\mathbf{F} = (f_1, f_2)^T$ satisfies $\text{curl } \mathbf{F} = \frac{\partial f_2}{\partial x_1} - \frac{\partial f_1}{\partial x_2} = f$, for f given in Equation (2.1). Given that $\mathbf{F} \in [H^{-1}(\Omega)]^2$, under conditions (2.27) and (2.28), the

weak formulation (2.26) admits a unique solution $(\mathbf{u}, p) \in [H_0^1(\Omega)]^2 \times L_0^2(\Omega)$. Moreover, if $\mathbf{F} \in [H^{-1+\alpha}(\Omega)]^2$, the Stokes problem holds the regularity estimate (2.29).

Then we have the following results.

Lemma 2.15. *For $f \in H^{-1}(\Omega)$, assume that w is the solution of Equation (2.55), then it follows that*

$$\mathbf{F} = \mathbf{curl} w \in \mathbf{H}(\mathbf{curl}; \Omega) \subset [L^2(\Omega)]^2 \quad (2.56)$$

satisfies Equation (2.25) and

$$\|\mathbf{F}\|_{[L^2(\Omega)]^2} \leq C\|f\|_{H^{-1}(\Omega)}. \quad (2.57)$$

Proof. The Poisson problem (2.55) admits a unique $w \in H_0^1(\Omega)$, which satisfies

$$\|w\|_{H^1(\Omega)} \leq C\|f\|_{H^{-1}(\Omega)}.$$

Note that $\|\mathbf{curl} w\|_{[L^2(\Omega)]^2} = \|w\|_{H^1(\Omega)}$, so we have

$$\|\mathbf{curl} w\|_{[L^2(\Omega)]^2} \leq C\|f\|_{H^{-1}(\Omega)}. \quad (2.58)$$

We also have

$$\mathbf{curl} \mathbf{F} = \mathbf{curl} (\mathbf{curl} w) = -\Delta w = f.$$

Thus, (2.57) holds. In a polygonal domain Ω , if $f \in H^l(\Omega)$ for $l \geq -1$, the regularity

estimate [50, 51] for the Poisson problem (2.55) gives

$$\|w\|_{H^{\min\{1+\beta, l+2\}}(\Omega)} \leq \|f\|_{H^l(\Omega)}, \quad (2.59)$$

where $\alpha < \beta < \beta_0 = \frac{\pi}{\omega}$ with ω being the largest interior angles of Ω . So for \mathbf{F} obtained from (2.56), we have $\mathbf{F} \in [H^{\min\{\beta, l+1\}}(\Omega)]^2$.

□

The conclusion of the Lemma (2.8) still holds for the second decoupled formulation.

Lemma 2.16. *Assume that the source term $\mathbf{F} \in [L^2(\Omega)]^2$ of the Stokes problem (2.24) is any vector function determined by $f \in H^{-1}(\Omega)$ satisfying (2.25), then (2.24) admits a unique solution $\mathbf{u} \in [H^{1+\alpha}(\Omega)]^2$ and satisfies*

$$\|\mathbf{u}\|_{[H^{1+\alpha}(\Omega)]^2} \leq C\|f\|_{H^{-1}(\Omega)}. \quad (2.60)$$

Proof. Given $f \in H^{-1}(\Omega)$, we can always find a vector function $\mathbf{F}_0 \in [L^2(\Omega)]^2$ following Lemma 2.15 such that the corresponding Stokes problem (2.24) admits a unique solution $\mathbf{u}_0 \in [H^{1+\alpha}(\Omega)]^2$ satisfying

$$\|\mathbf{u}_0\|_{[H^{1+\alpha}(\Omega)]^2} \leq C\|\mathbf{F}_0\|_{[H^{-1+\alpha}(\Omega)]^2} \leq C\|\mathbf{F}_0\|_{[L^2(\Omega)]^2} \leq C\|f\|_{H^{-1}(\Omega)}. \quad (2.61)$$

For any source term \mathbf{F} also satisfying Equation (2.56), it follows by Theorem 2.8 that the corresponding solution $\mathbf{u} = \mathbf{u}_0$, so the conclusion holds. □

Since $\mathbf{u} \in [H_0^1(\Omega)]^2 \cap [H^{1+\alpha}(\Omega)]^2$ and $\operatorname{div} \mathbf{u} = 0$, so we have by Lemma 2.11 that there

exists $\bar{\phi} \in H^2(\Omega)$ uniquely up to an additive constant satisfying $(u_1, u_2)^T = \mathbf{u} = \mathbf{curl} \bar{\phi} = (\bar{\phi}_{x_2}, -\bar{\phi}_{x_1})^T$, which further implies by Lemma 2.12 there exists a unique $\bar{\phi} \in H_0^2(\Omega) \cap H^{2+\alpha}(\Omega)$ satisfying $\mathbf{u} = \mathbf{curl} \bar{\phi}$. Instead of solving for $\bar{\phi} \in H_0^2(\Omega) \cap H^{2+\alpha}(\Omega)$ from $\mathbf{u} = \mathbf{curl} \bar{\phi}$ directly, we apply the operator curl on $\mathbf{u} = \mathbf{curl} \bar{\phi}$ to obtain the following Poisson problem

$$-\Delta \bar{\phi} = \mathbf{curl} \mathbf{u} \quad \text{in } \Omega, \quad \bar{\phi} = 0 \quad \text{on } \partial\Omega. \quad (2.62)$$

The weak formulation of Equation (2.62) is to find $\bar{\phi} \in H_0^1(\Omega)$, such that

$$(\nabla \bar{\phi}, \nabla \psi) = (\mathbf{curl} \mathbf{u}, \psi), \quad \forall \psi \in H_0^1(\Omega). \quad (2.63)$$

Since $(\mathbf{curl} \mathbf{u}) \in L^2(\Omega)$, so we have by the Lax-Milgram Theorem that Equation (2.63) admits a unique solution $\bar{\phi} \in H_0^1(\Omega)$. From Lemma 2.13 the Poisson problem 2.62 admits a unique solution $\bar{\phi} \in H_0^2(\Omega) \cap H^{2+\alpha}(\Omega)$.

Now we justify that the solution obtained through the Poisson equations (2.55), (2.62) and the Stokes equation (2.24) solve the biharmonic equation (2.1). Similar to the first decoupled formulation, by the Lemma 2.14, the solution $\bar{\phi} \in H_0^2(\Omega) \cap H^{2+\alpha}(\Omega)$ obtained through $\mathbf{u} = \mathbf{curl} \bar{\phi}$ or the Poisson problem (2.62) satisfies the biharmonic problem

$$\Delta^2 \bar{\phi} = \mathbf{curl} \mathbf{F} = f, \quad \text{in } \Omega, \quad \bar{\phi} = 0 \quad \text{and} \quad \partial_{\mathbf{n}} \bar{\phi} = 0 \quad \text{on } \partial\Omega. \quad (2.64)$$

where, $\mathbf{F} = [f_1, f_2] = \mathbf{curl} w = [w_{x_2}, -w_{x_1}]$.

As in the first decoupled formulation by the Lemma 2.14, we find that $\bar{\phi}$ in Equation (2.64) satisfies exactly the same problem as ϕ in Equation (2.1).

By the regularity of the Poisson problem (2.52) and Lemma 2.16, we have that

$$\|\phi\|_{H^{2+\alpha}(\Omega)} \leq C \|\mathbf{curl} \mathbf{u}\|_{H^\alpha(\Omega)} \leq C \|\nabla \mathbf{u}\|_{[H^\alpha(\Omega)]^2} \leq C \|\mathbf{u}\|_{[H^{1+\alpha}(\Omega)]^2} \leq C \|f\|_{H^{-1}(\Omega)}. \quad (2.65)$$

In summary, we can obtain the solution ϕ of the biharmonic problem (2.1) by solving the lower order problems in the following steps,

- (a) Choose an appropriate \mathbf{F} by Lemma 2.15;
- (b) Solve \mathbf{u} from the Stokes problem (2.24);
- (c) Solve ϕ from the Poisson problem (2.62).

2.4 Finite Element Algorithms

In this section, we propose a linear C^0 finite element method solving the biharmonic problem (2.1) following the two decoupled formulations presented in the Sections 2.3.1 and 2.3.2.

Let \mathcal{T}_n be a triangulation of Ω with shape-regular triangles and let $\mathcal{P}_k(\mathcal{T}_n)$ be the C^0 Lagrange finite element space associated with \mathcal{T}_n ,

$$\mathcal{P}_k(\mathcal{T}_n) := \{v \in C^0(\Omega) : v|_T \in P_k, \forall T \in \mathcal{T}_n\}, \quad (2.66)$$

where P_k is the space of polynomials of degree no more than k . Further, we introduce the

following C^0 Lagrange finite element spaces associated with \mathcal{T}_n ,

$$\begin{aligned} V_n^k &:= \mathcal{P}_k(\mathcal{T}_n) \cap H_0^1(\Omega), \\ S_n^k &:= \mathcal{P}_k(\mathcal{T}_n) \cap L_0^2(\Omega). \end{aligned} \tag{2.67}$$

and the bubble function space

$$B_n^3 := \{v \in C^0(\Omega) : v|_T \in \text{span}\{\lambda_1 \lambda_2 \lambda_3\}, \forall T \in \mathcal{T}_n\},$$

where $\lambda_i, i = 1, 2, 3$ are the barycentric coordinates on T .

Based on the first decoupled formulation to solve biharmonic problem as in the Section 2.3.1 we have the following finite element algorithm to solve the biharmonic equation:

Algorithm 2.17. *We define the finite element solution of the biharmonic problem (2.1) by utilizing the decoupling in Equations (2.26) and (2.48) as follows.*

- *Step 1. For given f , we find an appropriate \mathbf{F} satisfying Equation (2.25). For example, we can choose an appropriate \mathbf{F} based on Equations (2.30), (2.31), or (2.32).*
- *Step 2. For $k = 1$ we find the mini element approximation $u_n \times p_n \in [v_n^1 \oplus B_n^3]^2$ of the Stokes equation.*

$$\begin{aligned} (\nabla \mathbf{u}_n, \nabla \mathbf{v}) - (p_n, \text{div } \mathbf{v}) &= \langle \mathbf{F}, \mathbf{v} \rangle \quad \forall \mathbf{v} \in [v_n^1 \oplus B_n^3]^2, \\ -(\text{div } \mathbf{u}_n, q) &= 0 \quad \forall q \in S_n^{k-1}. \end{aligned} \tag{2.68}$$

For $k \geq 2$, we find the Taylor-Hood element solution $\mathbf{u}_n \times p_n \in [v_n^k]^2 \times S_n^{k-1}$ of the Stokes

equation

$$\begin{aligned} (\nabla \mathbf{u}_n, \nabla \mathbf{v}) - (p_n, \operatorname{div} \mathbf{v}) &= \langle \mathbf{F}, \mathbf{v} \rangle \quad \forall \mathbf{v} \in [V_n^k]^2, \\ -(\operatorname{div} \mathbf{u}_n, q) &= 0 \quad \forall q \in S_n^{k-1}. \end{aligned} \tag{2.69}$$

- *Step 3. Find the finite element solution $\phi_n \in V_n^k$ of the Poisson equation*

$$(\nabla \phi_n, \nabla \psi) = (\operatorname{curl} \mathbf{u}_n, \psi), \quad \forall \psi \in V_n^k, \tag{2.70}$$

Based on the second decoupled formulation to solve biharmonic problem as in the section 2.3.2 we have the following finite element algorithm to solve the biharmonic equation:

Algorithm 2.18. For $f \in H^{-1}(\Omega)$ and $k \geq 1$ we consider the following steps.

- *Step 1. Find $w_n \in V_n^k$ of the Poisson equation.*

$$(\nabla w_n, \nabla \psi) = (f, \psi) \quad \forall \psi \in V_n^k \tag{2.71}$$

then set $\mathbf{F}_n = \operatorname{curl} w_n$.

- *Step 2. For $k = 1$ we find the mini element approximation $u_n \times p_n \in [v_n^1 \oplus B_n^3]^2$ of the Stokes equation.*

$$\begin{aligned} (\nabla \mathbf{u}_n, \nabla \mathbf{v}) - (p_n, \operatorname{div} \mathbf{v}) &= \langle \mathbf{F}, \mathbf{v} \rangle \quad \forall \mathbf{v} \in [v_n^1 \oplus B_n^3]^2, \\ -(\operatorname{div} \mathbf{u}_n, q) &= 0 \quad \forall q \in S_n^{k-1}. \end{aligned} \tag{2.72}$$

For $k \geq 2$, we find the Taylor-Hood element solution $\mathbf{u}_n \times p_n \in [v_n^k]^2 \times S_n^{k-1}$ of the Stokes

equation

$$\begin{aligned}
 (\nabla \mathbf{u}_n, \nabla \mathbf{v}) - (p_n, \operatorname{div} \mathbf{v}) &= \langle \mathbf{F}, \mathbf{v} \rangle \quad \forall \mathbf{v} \in [V_n^k]^2, \\
 -(\operatorname{div} \mathbf{u}_n, q) &= 0 \quad \forall q \in S_n^{k-1}.
 \end{aligned}
 \tag{2.73}$$

- *Step 3. Find the finite element solution $\phi_n \in V_n^k$ of the Poisson equation*

$$(\nabla \phi_n, \nabla \psi) = (\operatorname{curl} \mathbf{u}_n, \psi), \quad \forall \psi \in V_n^k,
 \tag{2.74}$$

CHAPTER 3 ERROR ESTIMATE ON QUASI-UNIFORM MESHES

In this chapter, we propose a linear C^0 finite element method solving the biharmonic problem (2.1) following the finite element Algorithms 2.17 and 2.18. The finite element approximations for the Poisson problems in both Algorithms 2.17 and 2.18 are well defined by the Lax-Milgram Theorem. We take the Mini element method [8] and the Taylor-Hood element method [28, 97] for solving the Stokes problem, other methods could also be used. The Mini element approximations or the Taylor-Hood element approximations are well defined, if i) the bilinear forms in Mini element method satisfy the following LBB condition,

$$\inf_{q \in S_n^1} \sup_{\mathbf{v} \in [V_n^1 \oplus B_n^3]^2} \frac{-(\operatorname{div} \mathbf{v}, q)}{\|\mathbf{v}\|_{[H_0^1(\Omega)]^2} \|q\|} \geq \tilde{\gamma}_1 > 0, \quad (3.1a)$$

$$\inf_{\mathbf{u} \in [V_n^1 \oplus B_n^3]^2} \sup_{\mathbf{v} \in [V_n^1 \oplus B_n^3]^2} \frac{(\nabla \mathbf{u}, \nabla \mathbf{v})}{\|\mathbf{u}\|_{[H_0^1(\Omega)]^2} \|\mathbf{v}\|_{[H_0^1(\Omega)]^2}} \geq \tilde{\gamma}_2 > 0, \quad (3.1b)$$

and these in Taylor-Hood method satisfies the following LBB condition,

$$\inf_{q \in S_n^{k-1}} \sup_{\mathbf{v} \in [V_n^k]^2} \frac{-(\operatorname{div} \mathbf{v}, q)}{\|\mathbf{v}\|_{[H_0^1(\Omega)]^2} \|q\|} \geq \tilde{\gamma}_1 > 0, \quad (3.2a)$$

$$\inf_{\mathbf{u} \in [V_n^k]^2} \sup_{\mathbf{v} \in [V_n^k]^2} \frac{(\nabla \mathbf{u}, \nabla \mathbf{v})}{\|\mathbf{u}\|_{[H_0^1(\Omega)]^2} \|\mathbf{v}\|_{[H_0^1(\Omega)]^2}} \geq \tilde{\gamma}_2 > 0, \quad (3.2b)$$

where $\tilde{\gamma}_1, \tilde{\gamma}_2$ are some constants; ii) the bilinear forms are bounded.

Remark 3.1. *Algorithm 2.18 is similar to method in [29, 30, 46] for fourth order problems in smooth domains or convex polygonal domains. Error estimates were derived in [30] for P_k element approximations in a convex polygonal domain by assuming that the solutions are smooth enough. In [46], error estimates were given for P_1 element approximations based on*

the regularity assumption $|\nabla \mathbf{u}|, |\mathbf{F}|, p, |\nabla \phi| \in H^{s+1}(\Omega)$ for $-1 < s \leq 0$. In this chapter, we carry out the error analysis of Algorithms 2.17 and 2.18 for biharmonic problem (2.1) in convex polygonal domain for P_k polynomials based on the regularity estimates obtained in Chapter 2.

3.1 Error Estimates Results for Algorithm 2.17

Suppose that the mesh \mathcal{T}_n consists of quasi-uniform triangles with size h . The interpolation error estimate on \mathcal{T}_n (see e.g., [37]) for any $v \in H^\sigma(\Omega)$, $\sigma > 1$,

$$\|v - v_I\|_{H^\tau(\Omega)} \leq Ch^{\sigma-\tau} \|v\|_{H^\sigma(\Omega)}, \quad (3.3)$$

where $\tau = 0, 1$ and $v_I \in V_n^k$ represents the nodal interpolation of v .

Corollary 3.2. *Let (\mathbf{u}, p) be the solution of the Stokes problem (2.26), and (\mathbf{u}_n, p_n) be the Taylor-Hood element solution ($k \geq 2$) in Algorithm 2.17 satisfying the LBB condition (3.2), then it follows*

$$\|\mathbf{u} - \mathbf{u}_n\|_{[H^1(\Omega)]^2} + \|p - p_n\| \leq C \left(\inf_{\mathbf{v} \in [V_n^k]^2} \|\mathbf{u} - \mathbf{v}\|_{[H^1(\Omega)]^2} + \inf_{q \in S_n^{k-1}} \|p - q\| \right).$$

For Mini element approximations to the Stokes problem, we have the following error bounds.

Lemma 3.3. *Let (\mathbf{u}, p) be the solution of the Stokes problem (2.26), and (\mathbf{u}_n, p_n) be the Mini element solution ($k = 1$) in Algorithm 2.17 satisfying the LBB condition (3.1), then it follows*

$$\|\mathbf{u} - \mathbf{u}_n\|_{[H^1(\Omega)]^2} + \|p - p_n\| \leq C \left(\inf_{\mathbf{v} \in [V_n^1]^2} \|\mathbf{u} - \mathbf{v}\|_{[H^1(\Omega)]^2} + \inf_{q \in S_n^1} \|p - q\| \right).$$

To make the analysis simple and clear, we assume that $f \in H^{\max\{\alpha_0, \beta_0\}-1}(\Omega) \cap L^2(\Omega)$, where α_0 given in Equation (2.19), and $\beta_0 = \frac{\pi}{\omega}$.

For $f \in H^{\max\{\alpha_0, \beta_0\}-1}(\Omega) \cap L^2(\Omega)$, if \mathbf{F} is given by Lemma 2.7, we have $\mathbf{u} \in [H^{1+\alpha}(\Omega)]^2$, $p \in H^\alpha(\Omega)$. Note that the bilinear forms in the Mini element method ($k = 1$) or Taylor-Hood element method ($k \geq 2$) satisfying the LBB condition (3.1) or (3.2) on quasi-uniform meshes [8, 28, 97], then the standard arguments for error estimate (see e.g., [48, 90, 24]) give the following error estimate.

Lemma 3.4. *Let (\mathbf{u}, p) be the solution of the Stokes problem (2.26), and (\mathbf{u}_n, p_n) be the Mini element solution ($k = 1$) or Taylor-Hood element solution ($k \geq 2$) in Algorithm 2.17 on quasi-uniform meshes, then it follows*

$$\|\mathbf{u} - \mathbf{u}_n\|_{[H^1(\Omega)]^2} + \|p - p_n\| \leq Ch^{\min\{k, \alpha\}}, \quad (3.4a)$$

$$\|\mathbf{u} - \mathbf{u}_n\|_{[L^2(\Omega)]^2} \leq Ch^{\min\{k+1, \alpha+1, 2\alpha\}}, \quad (3.4b)$$

$$\|\mathbf{u} - \mathbf{u}_n\|_{[H^{-1}(\Omega)]^2} \leq Ch^{\min\{2k, k+2, k+\alpha, \alpha+2, 2\alpha\}}. \quad (3.4c)$$

If the largest interior angle $\omega < \pi$, it follows $\min\{\alpha + 1, 2\alpha\} = \alpha + 1$, and if $\omega > \pi$, we have $\min\{\alpha + 1, 2\alpha\} = 2\alpha$.

Theorem 3.5. [68] *Let $\phi_n \in V_n^k$ be the solution of finite element solution of (2.70) from Algorithm 2.17, and ϕ is the solution of the biharmonic problem (2.1), then we have*

$$\|\phi - \phi_n\|_{H^1(\Omega)} \leq Ch^{\min\{k, \alpha+1, 2\alpha\}}; \quad (3.5)$$

Proof. Subtracting Equation (2.70) from Equation (2.53) gives

$$(\nabla(\phi - \phi_n), \nabla\psi) = (\mathbf{curl}(\mathbf{u} - \mathbf{u}_n), \psi), \quad \forall \psi \in V_n^k.$$

Denote by $\phi_I \in V_n^k$ the nodal interpolation of ϕ . Set $\epsilon = \phi_I - \phi$, $e = \phi_I - \phi_n$ and take $\psi = e$, then we have

$$(\nabla e, \nabla e) = (\nabla \epsilon, \nabla e) + (\mathbf{curl}(\mathbf{u} - \mathbf{u}_n), e) = (\nabla \epsilon, \nabla e) + (\mathbf{u} - \mathbf{u}_n, \mathbf{curl} e),$$

which gives

$$\begin{aligned} \|e\|_{H^1(\Omega)}^2 &\leq \|\epsilon\|_{H^1(\Omega)} \|e\|_{H^1(\Omega)} + \|\mathbf{u} - \mathbf{u}_n\|_{[L^2(\Omega)]^2} \|\mathbf{curl} e\|_{[L^2(\Omega)]^2} \\ &\leq C(\|\epsilon\|_{H^1(\Omega)} + \|\mathbf{u} - \mathbf{u}_n\|_{[L^2(\Omega)]^2}) \|e\|_{H^1(\Omega)}, \end{aligned} \quad (3.6)$$

By the triangle inequality, we have

$$\|\phi - \phi_n\|_{H^1(\Omega)} \leq \|\epsilon\|_{H^1(\Omega)} + \|e\|_{H^1(\Omega)} \leq C(\|\epsilon\|_{H^1(\Omega)} + \|\mathbf{u} - \mathbf{u}_n\|_{[L^2(\Omega)]^2}) \quad (3.7)$$

Recall that $\phi \in H^{2+\alpha}(\Omega)$, so it follows

$$\|\epsilon\|_{H^1(\Omega)} \leq Ch^{\min\{k, 1+\alpha\}},$$

which together with Equation (3.4) leads to the conclusion. \square

Theorem 3.6. [68] Let ϕ_n be the solution of finite element solution of Equation (2.70) from

Algorithm 2.17, and ϕ be the solution of the biharmonic problem (2.1), then we have

$$\|\phi - \phi_n\| \leq Ch^{\min\{k+1, \alpha+2, 2\alpha\}}; \quad (3.8)$$

Proof. Consider the Poisson problem

$$-\Delta v = \phi - \phi_n \text{ in } \Omega, \quad v = 0 \text{ on } \partial\Omega. \quad (3.9)$$

Then we have

$$\|\phi - \phi_n\|^2 = (\nabla(\phi - \phi_n), \nabla v). \quad (3.10)$$

By Subtracting Equation (2.70) from Equation (2.53), it follows

$$(\nabla(\phi - \phi_n), \nabla\psi) = (\mathbf{curl}(\mathbf{u} - \mathbf{u}_n), \psi), \quad \forall \psi \in V_n^k. \quad (3.11)$$

Set $\psi = v_I \in V_n^k$ the nodal interpolation of v and subtract Equation (3.11) from Equation (3.10), we have

$$\begin{aligned} \|\phi - \phi_n\|^2 &= (\nabla(\phi - \phi_n), \nabla(v - v_I)) + (\mathbf{curl}(\mathbf{u} - \mathbf{u}_n), v_I), \\ &= (\nabla(\phi - \phi_n), \nabla(v - v_I)) + (\mathbf{curl}(\mathbf{u} - \mathbf{u}_n), v_I - v) + (\mathbf{curl}(\mathbf{u} - \mathbf{u}_n), v), \\ &= (\nabla(\phi - \phi_n), \nabla(v - v_I)) + (\mathbf{u} - \mathbf{u}_n, \mathbf{curl}(v_I - v)) + (\mathbf{u} - \mathbf{u}_n, \mathbf{curl} v), \\ &\leq \|\phi - \phi_n\|_{H^1(\Omega)} \|v - v_I\|_{H^1(\Omega)} + \|\mathbf{u} - \mathbf{u}_n\|_{[L^2(\Omega)]^2} \|v - v_I\|_{H^1(\Omega)} \\ &\quad + \|\mathbf{u} - \mathbf{u}_n\|_{[H^{-\min\{\lfloor \beta \rfloor, 1\}}(\Omega)]^2} \|\mathbf{curl} v\|_{H^{\min\{\lfloor \beta \rfloor, 1\}}(\Omega)}, \end{aligned}$$

where $\lfloor \cdot \rfloor$ represents the floor function. The regularity result [50, 51] of the Poisson prob-

lem (3.41) gives

$$\|v\|_{H^{\min\{1+\beta,2\}}(\Omega)} \leq C\|\phi - \phi_n\|_{H^{\min\{\beta-1,0\}}(\Omega)} \leq C\|\phi - \phi_n\|, \quad (3.12)$$

where $\beta < \frac{\pi}{\omega}$. From Equation (3.3), we have

$$\|v - v_I\|_{H^1(\Omega)} \leq Ch^{\min\{\beta,1\}}\|v\|_{H^{\min\{1+\beta,2\}}(\Omega)}.$$

Then, we have the following result by Equation (3.4). Since $\beta < \frac{\pi}{\omega}$, so if $\omega > \pi$ we have $[\beta] = 0$, and

$$\|\mathbf{u} - \mathbf{u}_n\|_{[H^{-\min\{[\beta],1\}}(\Omega)]^2} = \|\mathbf{u} - \mathbf{u}_n\|_{[L^2(\Omega)]^2} \leq Ch^{2\alpha}. \quad (3.13)$$

and if $\omega < \pi$, we have $[\beta] = 1$, and

$$\|\mathbf{u} - \mathbf{u}_n\|_{[H^{-\min\{[\beta],1\}}(\Omega)]^2} \leq Ch^{\min\{2k,k+2,k+\alpha,\alpha+2,2\alpha\}}. \quad (3.14)$$

For $\omega \in (0, 2\pi) \setminus \{\pi\}$, Equations (3.13) and (3.14) imply that

$$\|\mathbf{u} - \mathbf{u}_n\|_{[H^{-\min\{[\beta],1\}}(\Omega)]^2} \leq Ch^{\min\{2k,k+2,k+\alpha,\alpha+2,2\alpha\}}. \quad (3.15)$$

Thus, we have by Equations (3.5), (3.4), and (3.15),

$$\begin{aligned} \|\phi - \phi_n\|^2 &\leq Ch^{\min\{k+1,\alpha+2,k+\beta,2\alpha+\beta\}}\|v\|_{H^{\min\{1+\beta,2\}}(\Omega)} + Ch^{\min\{2k,k+2,k+\alpha,\alpha+2,2\alpha\}}\|v\|_{H^{\min\{1+\beta,2\}}(\Omega)} \\ &\leq Ch^{\min\{k+1,\alpha+2,2\alpha\}}\|v\|_{H^{\min\{1+\beta,2\}}(\Omega)}. \end{aligned} \quad (3.16)$$

By Equations (3.12) and (3.16), the estimate (3.8) holds. \square

Remark 3.7. *The error estimate Theorems 3.5, and 3.6 show that Algorithm 2.17 produces numerical solutions that converge to the solution of the biharmonic problem (2.1) no matter the polygonal domain is convex or non-convex. We note that if the domain is non-convex, the convergence rate on quasi-uniform meshes is suboptimal.*

3.2 Error Estimates Results for Algorithm 2.18

In this section we present the error estimate results for Algorithm 2.18 which involve two Poisson equations and a steady state Stokes equation. If \mathbf{F} is given by Lemma 2.15, then for the Poisson equation (2.55) in a polygonal domain with $f \in H^{\max\{\alpha_0, \beta_0\}-1}(\Omega) \cap L^2(\Omega)$, the regularity estimate gives $v \in H^{1+\beta}(\Omega)$ for $\beta < \beta_0 = \frac{\pi}{\omega}$ (see e.g., [50, 51]), it implies that

$$\mathbf{F} = \mathbf{curl} w \in [H^\beta(\Omega)]^2 \subset [H^{\alpha-1}(\Omega)]^2 \cap [H^\beta(\Omega)]^2,$$

where $\alpha < \alpha_0$. Therefore, we also have $\mathbf{u} \in [H^{\alpha+1}(\Omega)]^2 \cap [H^{\beta+2}(\Omega)]^2$, $p \in H^\alpha(\Omega) \cap H^{\beta+1}(\Omega)$, and $\phi \in H^{\alpha+2}(\Omega) \cap H^{\beta+3}(\Omega)$. For the finite element approximations w_n in Equation (2.71), the standard error estimate [37] yields

$$\|w - w_n\|_{H^1(\Omega)} \leq Ch^{\min\{k, \beta\}}, \quad \|w - w_n\| \leq Ch^{\min\{k+1, \beta+1, 2\beta\}}, \quad (3.17)$$

which implies that

$$\begin{aligned} \|\mathbf{F} - \mathbf{F}_n\|_{[L^2(\Omega)]^2} &= \|\mathbf{curl} w - \mathbf{curl} w_n\|_{[L^2(\Omega)]^2} \leq \|w - w_n\|_{H^1(\Omega)} \leq Ch^{\min\{k, \beta\}}, \\ \|\mathbf{F} - \mathbf{F}_n\|_{[H^{-1}(\Omega)]^2} &= \|\mathbf{curl} w - \mathbf{curl} w_n\|_{[H^{-1}(\Omega)]^2} \leq C\|w - w_n\| \leq Ch^{\min\{k+1, \beta+1, 2\beta\}}. \end{aligned} \quad (3.18)$$

For \mathbf{F}_n in Algorithm 2.18, we further have the following result.

Lemma 3.8. [68] *If \mathbf{F}_n is given by $\mathbf{F}_n = \mathbf{curl} w_n$ in Step 1 of Algorithm 2.18, and $\mathbf{F} = \mathbf{curl} w$ is given in Equation (2.56), then it follows*

$$\langle \mathbf{F} - \mathbf{F}_n, \mathbf{curl} \psi \rangle = 0, \quad \forall \psi \in V_n^k. \quad (3.19)$$

Proof. Subtract Equation (2.71) from the weak formulation of Equation (2.55), then we have the Galerkin orthogonality,

$$(\nabla(w - w_n), \nabla \psi) = (w - w_n)_{x_1} \psi_{x_1} + (w - w_n)_{x_2} \psi_{x_2} = 0, \quad \forall \psi \in V_n^k, \quad (3.20)$$

which implies that

$$\langle \mathbf{F} - \mathbf{F}_n, \mathbf{curl} \psi \rangle = \langle \mathbf{curl} (w - w_n), \mathbf{curl} \psi \rangle = (w - w_n)_{x_x} \psi_{x_2} + (w - w_n)_{x_1} \psi_{x_1} = 0. \quad (3.21)$$

□

Next, we consider the error estimates of Taylor-Hood element approximations. Subtract Equation (2.73) from Equation (2.26), we have the following equality,

$$(\nabla(\mathbf{u} - \mathbf{u}_n), \nabla \mathbf{v}) - (\operatorname{div} \mathbf{v}, p - p_n) = \langle \mathbf{F} - \mathbf{F}_n, \mathbf{v} \rangle \quad \forall \mathbf{v} \in [V_n^k]^2, \quad (3.22a)$$

$$-(\operatorname{div}(\mathbf{u} - \mathbf{u}_n), q) = 0 \quad \forall q \in S_n^{k-1}. \quad (3.22b)$$

We introduce the adjoint problem of the the Stokes equations (2.24),

$$\begin{aligned}
-\Delta \mathbf{r} + \nabla s &= \mathbf{g} \quad \text{in } \Omega, \\
\operatorname{div} \mathbf{r} &= 0 \quad \text{in } \Omega, \\
\mathbf{r} &= 0 \quad \text{on } \partial\Omega,
\end{aligned} \tag{3.23}$$

where $\mathbf{g} \in [H_0^l(\Omega)]^2$ for some $l = 0, 1$. Here, the notation $H_0^0(\Omega) := H^0(\Omega) = L^2(\Omega)$. The weak formulation of Equation (3.23) is to find $\mathbf{r} \in [H_0^1(\Omega)]^2$ and $s \in L_0^2(\Omega)$ such that

$$\begin{aligned}
(\nabla \mathbf{r}, \nabla \mathbf{v}) - (\operatorname{div} \mathbf{v}, s) &= \langle \mathbf{g}, \mathbf{v} \rangle \quad \forall \mathbf{v} \in [H_0^1(\Omega)]^2, \\
-(\operatorname{div} \mathbf{r}, q) &= 0 \quad \forall q \in L_0^2(\Omega).
\end{aligned} \tag{3.24}$$

We have the following regularity result,

$$\|\mathbf{r}\|_{[H^{1+\min\{\alpha, l+1\}}(\Omega)]^2} + \|s\|_{H^{\min\{\alpha, l+1\}}(\Omega)} \leq C \|\mathbf{g}\|_{[H^{\min\{\alpha, l+1\}-1}(\Omega)]^2} \leq C \|\mathbf{g}\|_{[H^l(\Omega)]^2}, \tag{3.25}$$

where $\alpha < \alpha_0$.

Note that $\mathbf{r} \in [H^{1+\min\{\alpha, l+1\}}(\Omega)]^2$ satisfying Equations (3.25) and (3.23), we have by Lemma 2.11 that there exists $\psi \in H^{2+\min\{\alpha, l+1\}}(\Omega) \cap H_0^1(\Omega)$ such that

$$\mathbf{r} = \operatorname{curl} \psi. \tag{3.26}$$

We also have that $\|\psi\|_{H^{2+\min\{\alpha, l+1\}}(\Omega)} \leq C \|\mathbf{r}\|_{[H^{1+\min\{\alpha, l+1\}}(\Omega)]^2}$.

Next, we present error bounds of finite element approximation to the Stokes equation.

In particular prove the error bound of the Taylor-Hood approximations to the Stokes prob-

lem, the error bound of the the Mini element approximations can be proved similarly. First, we introduce the following operators.

$$\begin{aligned}\mathcal{B} &= -\operatorname{div} : [H_0^1(\Omega)]^2 \rightarrow (L_0^2(\Omega))' = L_0^2(\Omega), \quad \langle \mathcal{B}\mathbf{v}, q \rangle = -(\operatorname{div} \mathbf{v}, q), \\ \mathcal{B}' &= \nabla : L_0^2(\Omega) \rightarrow [H^{-1}(\Omega)]^2, \quad \langle \mathbf{v}, \mathcal{B}'q \rangle = -(\operatorname{div} \mathbf{v}, q).\end{aligned}\tag{3.27}$$

We denote $\mathcal{B}_n : [V_n^k]^2 \rightarrow (S_n^{k-1})'$ be the discrete counterpart of the operator \mathcal{B} and it satisfies

$$\langle \mathcal{B}_n \mathbf{v}, q \rangle = \langle \mathcal{B}\mathbf{v}, q \rangle = -(\operatorname{div} \mathbf{v}, q), \quad \forall (\mathbf{v}, q) \in [V_n^k]^2 \times S_n^{k-1}.$$

The nullspace of \mathcal{B}_n is given by

$$\ker(\mathcal{B}_n) = \{\mathbf{v} \in [V_n^k]^2 \mid \forall q \in S_n^{k-1}, (\operatorname{div} \mathbf{v}, q) = 0\}.\tag{3.28}$$

Lemma 3.9. [68] *Let (\mathbf{u}, p) be the solution of the Stokes problem (2.26), and (\mathbf{u}_n, p_n) be the Taylor-Hood element solution ($k \geq 2$) of Equation (2.73) satisfying the LBB condition (3.2), then it follows*

$$\|\mathbf{u} - \mathbf{u}_n\|_{[H^1(\Omega)]^2} + \|p - p_n\| \leq C \left(\inf_{\mathbf{v} \in [V_n^k]^2} \|\mathbf{u} - \mathbf{v}\|_{[H^1(\Omega)]^2} + \inf_{q \in S_n^{k-1}} \|p - q\| + \|\mathbf{F} - \mathbf{F}_n\|_{[H^{-1}(\Omega)]^2} \right).$$

Proof. By the LBB condition (3.2a), we have that the operator B_n is surjective. Thus, for given $\mathbf{v} \in [V_n^k]^2$, there exists $\tilde{\mathbf{v}} \in [V_n^k]^2$ such that

$$\mathcal{B}_n \tilde{\mathbf{v}} = \mathcal{B}_n(\mathbf{u}_n - \mathbf{v})\tag{3.29}$$

and

$$\tilde{\gamma}_1 \|\tilde{\mathbf{v}}\|_{[H^1(\Omega)]^2} \leq \sup_{q \in S_n^{k-1}} \frac{-(\operatorname{div}(\mathbf{u}_n - \mathbf{v}), q)}{\|q\|} = \sup_{q \in S_n^{k-1}} \frac{-(\operatorname{div}(\mathbf{u} - \mathbf{v}), q)}{\|q\|} \leq C_1 \|\mathbf{u} - \mathbf{v}\|_{[H^1(\Omega)]^2}, \quad (3.30)$$

where we have used Equation (3.22b).

Set $\mathbf{w} = \mathbf{v} + \tilde{\mathbf{v}} \in [V_n^k]^2$, then it follows by Equation (3.29),

$$\mathcal{B}_n(\mathbf{u}_n - \mathbf{w}) = \mathcal{B}_n(\mathbf{u}_n - \mathbf{v} - \tilde{\mathbf{v}}) = 0,$$

which implies that $\mathbf{u}_n - \mathbf{w} \in \ker(\mathcal{B}_n)$.

By Equation (3.2b), we have

$$\begin{aligned} \tilde{\gamma}_2 \|\mathbf{u}_n - \mathbf{w}\|_{[H^1(\Omega)]^2} &\leq \frac{(\nabla(\mathbf{u}_n - \mathbf{w}), \nabla(\mathbf{u}_n - \mathbf{w}))}{\|\mathbf{u}_n - \mathbf{w}\|_{[H^1(\Omega)]^2}} \leq \sup_{\tilde{\mathbf{w}} \in \ker(\mathcal{B}_n)} \frac{(\nabla(\mathbf{u}_n - \mathbf{w}), \nabla \tilde{\mathbf{w}})}{\|\tilde{\mathbf{w}}\|_{[H^1(\Omega)]^2}} \\ &= \sup_{\tilde{\mathbf{w}} \in \ker(\mathcal{B}_n)} \frac{(\nabla(\mathbf{u}_n - \mathbf{u}), \nabla \tilde{\mathbf{w}}) + (\nabla(\mathbf{u} - \mathbf{w}), \nabla \tilde{\mathbf{w}})}{\|\tilde{\mathbf{w}}\|_{[H^1(\Omega)]^2}} \\ &= \sup_{\tilde{\mathbf{w}} \in \ker(\mathcal{B}_n)} \frac{-(\operatorname{div} \tilde{\mathbf{w}}, p - p_n) - \langle \mathbf{F} - \mathbf{F}_n, \tilde{\mathbf{w}} \rangle + (\nabla(\mathbf{u} - \mathbf{w}), \nabla \tilde{\mathbf{w}})}{\|\tilde{\mathbf{w}}\|_{[H^1(\Omega)]^2}} \\ &= \sup_{\tilde{\mathbf{w}} \in \ker(\mathcal{B}_n)} \frac{-(\operatorname{div} \tilde{\mathbf{w}}, p - p_n) + (\nabla(\mathbf{u} - \mathbf{w}), \nabla \tilde{\mathbf{w}})}{\|\tilde{\mathbf{w}}\|_{[H^1(\Omega)]^2}} + \sup_{\tilde{\mathbf{w}} \in \ker(\mathcal{B}_n)} \frac{-\langle \mathbf{F} - \mathbf{F}_n, \tilde{\mathbf{w}} \rangle}{\|\tilde{\mathbf{w}}\|_{[H^1(\Omega)]^2}}, \end{aligned}$$

where we have used Equation (3.22a). For any $q \in S_n^{k-1}$, we have by Equation (3.28) with

$\tilde{\mathbf{w}} \in \ker(\mathcal{B}_n)$,

$$-(\operatorname{div} \tilde{\mathbf{w}}, p_n - q) = 0.$$

Therefore, it follows

$$\begin{aligned} \tilde{\gamma}_2 \|\mathbf{u}_n - \mathbf{w}\|_{[H^1(\Omega)]^2} &\leq \sup_{\tilde{\mathbf{w}} \in \ker(\mathcal{B}_n)} \frac{-(\operatorname{div} \tilde{\mathbf{w}}, p - q) - \langle \mathbf{F} - \mathbf{F}_n, \tilde{\mathbf{w}} \rangle + (\nabla(\mathbf{u} - \mathbf{w}), \nabla \tilde{\mathbf{w}})}{\|\tilde{\mathbf{w}}\|_{[H^1(\Omega)]^2}} \\ &\leq C_1 \|p - q\| + C_2 \|\mathbf{u} - \mathbf{w}\|_{[H^1(\Omega)]^2} + \|\mathbf{F} - \mathbf{F}_n\|_{[H^{-1}(\Omega)]^2}, \end{aligned} \quad (3.31)$$

Note that using triangle inequality and Equation (3.30) yields

$$\|\mathbf{u} - \mathbf{w}\|_{[H^1(\Omega)]^2} \leq \|\mathbf{u} - \mathbf{v}\|_{[H^1(\Omega)]^2} + \|\tilde{\mathbf{v}}\|_{[H^1(\Omega)]^2} \leq \left(1 + \frac{C_1}{\tilde{\gamma}_1}\right) \|\mathbf{u} - \mathbf{v}\|_{[H^1(\Omega)]^2}. \quad (3.32)$$

Thus, we have by the triangle inequality and Equation (3.32)

$$\begin{aligned} \|\mathbf{u} - \mathbf{u}_n\|_{[H^1(\Omega)]^2} &\leq \left(1 + \frac{C_2}{\tilde{\gamma}_2}\right) \|\mathbf{u} - \mathbf{w}\|_{[H^1(\Omega)]^2} + \frac{C_2}{\tilde{\gamma}_2} \|p - q\| + \frac{1}{\tilde{\gamma}_2} \|\mathbf{F} - \mathbf{F}_n\|_{[H^{-1}(\Omega)]^2} \\ &\leq C_3 \|\mathbf{u} - \mathbf{v}\|_{[H^1(\Omega)]^2} + \frac{C_2}{\tilde{\gamma}_2} \|p - q\| + \frac{1}{\tilde{\gamma}_2} \|\mathbf{F} - \mathbf{F}_n\|_{[H^{-1}(\Omega)]^2}, \end{aligned} \quad (3.33)$$

where $C_3 = \left(1 + \frac{C_1}{\tilde{\gamma}_1}\right) \left(1 + \frac{C_2}{\tilde{\gamma}_2}\right)$.

Next, we need to obtain the estimate for $\|p - p_n\|$. From Equation (3.22a), we have

$$-(\operatorname{div} \mathbf{v}, q - p_n) = -(\nabla(\mathbf{u} - \mathbf{u}_n), \nabla \mathbf{v}) + \langle \mathbf{F} - \mathbf{F}_n, \mathbf{v} \rangle - (\operatorname{div} \mathbf{v}, q - p).$$

By the LBB condition (3.2a) and the boundedness of the bilinear forms, we have

$$\tilde{\gamma}_1 \|q - p_n\| \leq C_2 \|\mathbf{u} - \mathbf{u}_n\|_{[H^1(\Omega)]^2} + \|\mathbf{F} - \mathbf{F}_n\|_{[H^{-1}(\Omega)]^2} + C_1 \|p - q\|.$$

Thus, we have

$$\|p - p_n\| \leq \left(1 + \frac{C_1}{\tilde{\gamma}_1}\right) \|p - q\| + \frac{C_2}{\tilde{\gamma}_1} \|\mathbf{u} - \mathbf{u}_n\|_{[H^1(\Omega)]^2} + \frac{1}{\tilde{\gamma}_1} \|\mathbf{F} - \mathbf{F}_n\|_{[H^{-1}(\Omega)]^2}. \quad (3.34)$$

The conclusion follows from Equations (3.33) and (3.34). \square

If \mathbf{F}_n is the L^2 projection of \mathbf{F} , i.e., $\langle \mathbf{F} - \mathbf{F}_n, \mathbf{v} \rangle = 0$ for $\forall \mathbf{v} \in [V_n^k]^2$, then Equation (3.22) becomes the Galerkin orthogonality of a general Taylor-Hood method, and the result in Lemma 3.9 degenerates to the well known estimate bound in [26].

For Mini element approximations to the Stokes problem, we have the following error bounds.

Lemma 3.10. *Let (\mathbf{u}, p) be the solution of the Stokes problem (2.26), and (\mathbf{u}_n, p_n) be the Mini element solution ($k = 1$) in Algorithm 2.18 satisfying the LBB condition (3.1), then it follows*

$$\|\mathbf{u} - \mathbf{u}_n\|_{[H^1(\Omega)]^2} + \|p - p_n\| \leq C \left(\inf_{\mathbf{v} \in [V_n^1]^2} \|\mathbf{u} - \mathbf{v}\|_{[H^1(\Omega)]^2} + \inf_{q \in S_n^1} \|p - q\| + \|\mathbf{F} - \mathbf{F}_n\|_{[H^{-1}(\Omega)]^2} \right).$$

Lemma 3.11. [68] *Let (\mathbf{u}, p) be the solution of the Stokes problem (2.26), and (\mathbf{u}_n, p_n) be the Mini element solution ($k = 1$) or Taylor-Hood element solution ($k \geq 2$) in Algorithm 2.18 on quasi-uniform meshes, then it follows the error estimates*

$$\|\mathbf{u} - \mathbf{u}_n\|_{[H^1(\Omega)]^2} + \|p - p_n\| \leq Ch^{\min\{k, \alpha, \beta + 1\}}, \quad (3.35a)$$

$$\|\mathbf{u} - \mathbf{u}_n\|_{[L^2(\Omega)]^2} \leq Ch^{\min\{k+1, \alpha+1, \beta+2, 2\alpha\}}, \quad (3.35b)$$

$$\|\mathbf{u} - \mathbf{u}_n\|_{[H^{-1}(\Omega)]^2} \leq Ch^{\min\{2k, k+2, k+\beta, \alpha+2, \beta+3, 2\alpha\}}. \quad (3.35c)$$

Proof. We will only present the proof of error estimates of the Taylor-Hood element approximations, the error estimates of the Mini element approximations can be proved similarly.

By Lemma 3.9, we have

$$\begin{aligned} \|\mathbf{u} - \mathbf{u}_n\|_{[H^1(\Omega)]^2} + \|p - p_n\| &\leq C \left(\inf_{\mathbf{v} \in [V_n^k]^2} \|\mathbf{u} - \mathbf{v}\|_{[H^1(\Omega)]^2} + \inf_{q \in S_n^{k-1}} \|p - q\| + \|\mathbf{F} - \mathbf{F}_n\|_{[H^{-1}(\Omega)]^2} \right) \\ &\leq Ch^{\min\{k, \alpha, \beta+1\}} + Ch^{\min\{k+1, \beta+1, 2\beta\}} \leq Ch^{\min\{k, \alpha, \beta+1\}}. \end{aligned}$$

We take $\mathbf{v} = \mathbf{u} - \mathbf{u}_n$, $q = p - p_n$ in Equation (3.24), then we have

$$\|\mathbf{u} - \mathbf{u}_n\|_{[H^{-l}(\Omega)]^2} = \sup_{\mathbf{g} \in [H_0^l(\Omega)]^2} \frac{\langle \mathbf{g}, \mathbf{u} - \mathbf{u}_n \rangle}{\|\mathbf{g}\|_{[H^l(\Omega)]^2}},$$

where $l = 0, 1$. Let (\mathbf{r}_n, s_n) be the Taylor-Hood solution of Equation (3.23), then it follows

$$\begin{aligned} \langle \mathbf{g}, \mathbf{u} - \mathbf{u}_n \rangle &= (\nabla \mathbf{r}, \nabla \mathbf{u}) - (\nabla \mathbf{r}_n, \nabla \mathbf{u}_n) - (\operatorname{div} \mathbf{u}, s) + (\operatorname{div} \mathbf{u}_n, s_n) = (\nabla(\mathbf{u} - \mathbf{u}_n), \nabla(\mathbf{r} - \mathbf{r}_n)) \\ &\quad + (\operatorname{div} \mathbf{r} - \mathbf{r}_n, p - p_n) - (\operatorname{div}(\mathbf{u} - \mathbf{u}_n), s - s_n) + \langle \mathbf{F} - \mathbf{F}_n, \mathbf{r}_n \rangle \\ &:= T_1 + T_2 + T_3 + T_4. \end{aligned}$$

For \mathbf{r}_n and s_n , we have the following estimate

$$\begin{aligned} \|\mathbf{r} - \mathbf{r}_n\|_{[H^1(\Omega)]^2} + \|s - s_n\| &\leq C \left(\inf_{\mathbf{r}_I \in [V_n^k(\Omega)]^2} \|\mathbf{r} - \mathbf{r}_I\|_{[H^1(\Omega)]^2} + \inf_{s_I \in S_n^{k-1}} \|s - s_I\| \right) \\ &\leq Ch^{\min\{k, \alpha, l+1\}} (\|\mathbf{r}\|_{[H^{\min\{k+1, \alpha+1, l+2\}}(\Omega)]^2} + \|s\|_{H^{\min\{k, \alpha, l+1\}}(\Omega)}). \end{aligned} \tag{3.36}$$

We have the following estimate for each term.

$$\begin{aligned} |T_1| &\leq |\mathbf{u} - \mathbf{u}_n|_{[H^1(\Omega)]^2} |\mathbf{r} - \mathbf{r}_n|_{[H^1(\Omega)]^2} \leq Ch^{\min\{k, \alpha, \beta+1\} + \min\{k, \alpha, l+1\}} \|\mathbf{r}\|_{[H^{1+\min\{k, \alpha, l+1\}}(\Omega)]^2} \\ &= Ch^{\min\{2k, k+l+1, k+\alpha, \alpha+l+1, k+\beta+1, \alpha+\beta+1, \beta+l+2, 2\alpha\}} \|\mathbf{r}\|_{[H^{1+\min\{k, \alpha, l+1\}}(\Omega)]^2}. \end{aligned}$$

$$|T_2| \leq \|p - p_n\| \|\mathbf{r} - \mathbf{r}_n\|_{[H^1(\Omega)]^2} \leq Ch^{\min\{2k, k+l+1, k+\alpha, \alpha+l+1, k+\beta+1, \alpha+\beta+1, \beta+l+2, 2\alpha\}} \|\mathbf{r}\|_{[H^{1+\min\{k, \alpha, l+1\}}(\Omega)]^2}.$$

$$|T_3| \leq |\mathbf{u} - \mathbf{u}_n|_{[H^1(\Omega)]^2} \|s - s_n\| \leq Ch^{\min\{2k, k+l+1, k+\alpha, \alpha+l+1, k+\beta+1, \alpha+\beta+1, \beta+l+2, 2\alpha\}} \|s\|_{H^{\min\{k, \alpha, l+1\}}(\Omega)}.$$

For T_4 , we have

$$T_4 = \langle \mathbf{F} - \mathbf{F}_n, \mathbf{r}_n - \mathbf{r} \rangle + \langle \mathbf{F} - \mathbf{F}_n, \mathbf{r} \rangle := T_{41} + T_{42}.$$

$$\begin{aligned} |T_{41}| &\leq \|\mathbf{F} - \mathbf{F}_n\|_{[H^{-1}(\Omega)]^2} \|\mathbf{r} - \mathbf{r}_n\|_{[H^1(\Omega)]^2} \leq Ch^{\min\{k+1, \beta+1, 2\beta\} + \min\{k, \alpha, l+1\}} \|\mathbf{r}\|_{[H^{1+\min\{\alpha, l+1\}}(\Omega)]^2} \\ &= Ch^{\min\{2k+1, k+l+2, k+\beta+1, \beta+l+2, \alpha+\beta+1, 2\beta+\alpha\}} \|\mathbf{r}\|_{[H^{1+\min\{\alpha, l+1\}}(\Omega)]^2}. \end{aligned}$$

By Equation (3.26) and Lemma 3.8, we have

$$\begin{aligned} |T_{42}| &= |\langle \mathbf{F} - \mathbf{F}_n, \mathbf{curl} \psi \rangle| = |\langle \mathbf{F} - \mathbf{F}_n, \mathbf{curl} (\psi - \psi_I) \rangle| \leq \|\mathbf{F} - \mathbf{F}_n\|_{[L^2(\Omega)]^2} \|\mathbf{curl} (\psi - \psi_I)\|_{[L^2(\Omega)]^2} \\ &\leq \|\mathbf{F} - \mathbf{F}_n\|_{[L^2(\Omega)]^2} \|\psi - \psi_I\|_{H^1(\Omega)} \leq Ch^{\min\{k, \beta\} + \min\{k, \alpha+1, l+2\}} \|\mathbf{r}\|_{[H^{1+\min\{\alpha, l+1\}}(\Omega)]^2} \\ &\leq Ch^{\min\{2k, k+l+2, k+\beta, \beta+l+2, \alpha+\beta+1\}} \|\mathbf{r}\|_{[H^{1+\min\{\alpha, l+1\}}(\Omega)]^2}. \end{aligned}$$

where ψ_I is the nodal interpolation of ψ . It can be verified that

$$|T_4| \leq |T_{41}| + |T_{42}| \leq Ch^{\min\{2k, k+l+2, k+\beta, \beta+l+2, \alpha+\beta+1, \alpha+2\beta\}} \|\mathbf{r}\|_{[H^{1+\min\{\alpha, l+1\}}(\Omega)]^2}.$$

By the regularity in Equation (3.25) and the summation of estimates $|T_i|$, $i = 1, \dots, 4$,

the error estimate $\|\mathbf{u} - \mathbf{u}_n\|_{[H^{-l}(\Omega)]^2}$ holds.

□

Theorem 3.12. [68] Let $\phi_n \in V_n^k$ be the solution of finite element solution of (2.74) from Algorithm 2.18, and ϕ is the solution of the biharmonic problem (2.1), then we have

$$\|\phi - \phi_n\|_{H^1(\Omega)} \leq Ch^{\min\{k, \beta+2, \alpha+1, 2\alpha\}}. \quad (3.37)$$

Proof. Subtracting Equation (2.74) from Equation (2.53) gives

$$(\nabla(\phi - \phi_n), \nabla\psi) = (\mathbf{curl}(\mathbf{u} - \mathbf{u}_n), \psi), \quad \forall \psi \in V_n^k.$$

Denote by $\phi_I \in V_n^k$ the nodal interpolation of ϕ . Set $\epsilon = \phi_I - \phi$, $e = \phi_I - \phi_n$ and take $\psi = e$, then we have

$$(\nabla e, \nabla e) = (\nabla \epsilon, \nabla e) + (\mathbf{curl}(\mathbf{u} - \mathbf{u}_n), e) = (\nabla \epsilon, \nabla e) + (\mathbf{u} - \mathbf{u}_n, \mathbf{curl} e),$$

which gives

$$\begin{aligned} \|e\|_{H^1(\Omega)}^2 &\leq \|\epsilon\|_{H^1(\Omega)} \|e\|_{H^1(\Omega)} + \|\mathbf{u} - \mathbf{u}_n\|_{[L^2(\Omega)]^2} \|\mathbf{curl} e\|_{[L^2(\Omega)]^2} \\ &\leq C(\|\epsilon\|_{H^1(\Omega)} + \|\mathbf{u} - \mathbf{u}_n\|_{[L^2(\Omega)]^2}) \|e\|_{H^1(\Omega)}, \end{aligned} \quad (3.38)$$

By the triangle inequality, we have

$$\|\phi - \phi_n\|_{H^1(\Omega)} \leq \|\epsilon\|_{H^1(\Omega)} + \|e\|_{H^1(\Omega)} \leq C(\|\epsilon\|_{H^1(\Omega)} + \|\mathbf{u} - \mathbf{u}_n\|_{[L^2(\Omega)]^2}) \quad (3.39)$$

Recall that $\phi \in H^{2+\alpha}(\Omega)$, so it follows

$$\|\epsilon\|_{H^1(\Omega)} \leq Ch^{\min\{k, 1+\alpha\}},$$

which together with Equation (3.11) leads to the conclusion. \square

Theorem 3.13. [68] *Let ϕ_n be the solution of finite element solution of Equation (2.74) from Algorithm 2.18, and ϕ be the solution of the biharmonic problem (2.1), then we have*

$$\|\phi - \phi_n\| \leq Ch^{\min\{k+1, \alpha+2, \beta+3, 2\alpha\}}. \quad (3.40)$$

Proof. Consider the Poisson problem

$$-\Delta v = \phi - \phi_n \text{ in } \Omega, \quad v = 0 \text{ on } \partial\Omega. \quad (3.41)$$

Then we have

$$\|\phi - \phi_n\|^2 = (\nabla(\phi - \phi_n), \nabla v). \quad (3.42)$$

By Subtracting Equation (2.74) from Equation (2.53), it follows

$$(\nabla(\phi - \phi_n), \nabla\psi) = (\text{curl}(\mathbf{u} - \mathbf{u}_n), \psi), \quad \forall \psi \in V_n^k. \quad (3.43)$$

Set $\psi = v_I \in V_n^k$ the nodal interpolation of v and subtract Equation (3.43) from Equation

(3.41), we have

$$\begin{aligned}
\|\phi - \phi_n\|^2 &= (\nabla(\phi - \phi_n), \nabla(v - v_I)) + (\mathbf{curl}(\mathbf{u} - \mathbf{u}_n), v_I), \\
&= (\nabla(\phi - \phi_n), \nabla(v - v_I)) + (\mathbf{curl}(\mathbf{u} - \mathbf{u}_n), v_I - v) + (\mathbf{curl}(\mathbf{u} - \mathbf{u}_n), v), \\
&= (\nabla(\phi - \phi_n), \nabla(v - v_I)) + (\mathbf{u} - \mathbf{u}_n, \mathbf{curl}(v_I - v)) + (\mathbf{u} - \mathbf{u}_n, \mathbf{curl} v), \\
&\leq \|\phi - \phi_n\|_{H^1(\Omega)} \|v - v_I\|_{H^1(\Omega)} + \|\mathbf{u} - \mathbf{u}_n\|_{[L^2(\Omega)]^2} \|v - v_I\|_{H^1(\Omega)} \\
&\quad + \|\mathbf{u} - \mathbf{u}_n\|_{[H^{-\min\{\lfloor\beta\rfloor, 1\}}(\Omega)]^2} \|\mathbf{curl} v\|_{H^{\min\{\lfloor\beta\rfloor, 1\}}(\Omega)},
\end{aligned}$$

where $\lfloor \cdot \rfloor$ represents the floor function. The regularity result [50, 51] of the Poisson problem (3.41) gives

$$\|v\|_{H^{\min\{1+\beta, 2\}}(\Omega)} \leq C \|\phi - \phi_n\|_{H^{\min\{\beta-1, 0\}}(\Omega)} \leq C \|\phi - \phi_n\|_{\cdot}, \quad (3.44)$$

where $\beta < \frac{\pi}{\omega}$. From Equation (3.3), we have

$$\|v - v_I\|_{H^1(\Omega)} \leq Ch^{\min\{\beta, 1\}} \|v\|_{H^{\min\{1+\beta, 2\}}(\Omega)}.$$

Then, we have the following result by Equation (3.4). Since $\beta < \frac{\pi}{\omega}$, so if $\omega > \pi$ we have $\lfloor \beta \rfloor = 0$, and

$$\|\mathbf{u} - \mathbf{u}_n\|_{[H^{-\min\{\lfloor\beta\rfloor, 1\}}(\Omega)]^2} = \|\mathbf{u} - \mathbf{u}_n\|_{[L^2(\Omega)]^2} \leq Ch^{2\alpha}. \quad (3.45)$$

and if $\omega < \pi$, we have $\lfloor \beta \rfloor = 1$, and

$$\|\mathbf{u} - \mathbf{u}_n\|_{[H^{-\min\{\lfloor\beta\rfloor, 1\}}(\Omega)]^2} \leq Ch^{\min\{2k, k+2, k+\alpha, \alpha+2, 2\alpha\}}. \quad (3.46)$$

For $\omega \in (0, 2\pi) \setminus \{\pi\}$, (3.45) and (3.46) imply that

$$\|\mathbf{u} - \mathbf{u}_n\|_{[H^{-\min\{\lfloor \beta \rfloor, 1\}}(\Omega)]^2} \leq Ch^{\min\{2k, k+2, k+\alpha, \alpha+2, 2\alpha\}}. \quad (3.47)$$

Then we have

$$\begin{aligned} \|\phi - \phi_n\|^2 &\leq Ch^{\min\{k+1, \alpha+2, \beta+3, k+\beta, 2\alpha+\beta\}} \|v\|_{H^{\min\{1+\beta, 2\}}(\Omega)} \\ &\quad + Ch^{\min\{2k, k+2, k+\beta, \alpha+2, \beta+3, \alpha+\beta+1, 2\alpha\}} \|v\|_{H^{\min\{1+\beta, 2\}}(\Omega)} \\ &\leq Ch^{\min\{k+1, \alpha+2, \beta+3, 2\alpha\}} \|v\|_{H^{\min\{1+\beta, 2\}}(\Omega)}. \end{aligned} \quad (3.48)$$

By (3.44) and (3.48), the estimate (3.40) holds. \square

CHAPTER 4 ERROR ESTIMATE ON GRADED MESHES

In this chapter, we shall introduce the weighted Sobolev space $\mathcal{K}_{\mathbf{a}}^m(G)$ and provide preliminary results in order to carry out analysis on graded meshes. On details of weighted Sobolev spaces used here, we refer readers to [13, 58, 64]. Then we use the graded mesh algorithm to improve the convergence rates. To this end, we start with the regularity in weighted Sobolev space.

4.1 Regularity in Weighted Sobolev Space

4.1.1 Weighted Sobolev Space

Recall that $Q_i, i = 1, \dots, N$ are the vertices of domain Ω . Let $r_i = r_i(x, Q_i)$ be the distance from x to Q_i and let

$$\rho(x) = \prod_{1 \leq i \leq N} r_i(x, Q_i). \quad (4.1)$$

Let $\mathbf{a} = (a_1, \dots, a_i, \dots, a_N)$ be a vector with i th component associated with Q_i . We denote $t + \mathbf{a} = (t + a_1, \dots, t + a_N)$, so we have

$$\rho(x)^{(t+\mathbf{a})} = \prod_{1 \leq i \leq N} r_i^{(t+\mathbf{a})}(x, Q_i) = \prod_{1 \leq i \leq N} r_i^t(x, Q_i) \prod_{1 \leq i \leq N} r_i^{\mathbf{a}}(x, Q_i) = \rho(x)^t \rho(x)^{\mathbf{a}}.$$

Then, we introduce the Kondratiev-type weighted Sobolev spaces for the analysis of the Stokes problem (2.26) and the Poisson problem (2.52).

Definition 4.1. (*Weighted Sobolev spaces*) For $a \in \mathbb{R}$, $m \geq 0$, and $G \subset \Omega$, we define the

weighted Sobolev space

$$\mathcal{K}_{\mathbf{a}}^m(G) := \{v \mid \rho^{|\nu|-\mathbf{a}} \partial^\nu v \in L^2(G), \forall |\nu| \leq m\},$$

where the multi-index $\nu = (\nu_1, \nu_2) \in \mathbb{Z}_{\geq 0}^2$, $|\nu| = \nu_1 + \nu_2$, and $\partial^\nu = \partial_x^{\nu_1} \partial_y^{\nu_2}$. The $\mathcal{K}_{\mathbf{a}}^m(G)$ norm for v is defined by

$$\|v\|_{\mathcal{K}_{\mathbf{a}}^m(G)} = \left(\sum_{|\nu| \leq m} \iint_G |\rho^{|\nu|-\mathbf{a}} \partial^\nu v|^2 dx dy \right)^{\frac{1}{2}}.$$

Remark 4.2. According to Definition 4.1, in the region that is away from the corners, the weighted space $\mathcal{K}_{\mathbf{a}}^m$ is equivalent to the Sobolev space H^m . In the neighborhood of Q_i , the space $\mathcal{K}_{\mathbf{a}}^m(B_i)$ is the equivalent to the Kondratiev space [42, 50, 58],

$$\mathcal{K}_{a_i}^m(B_i) := \{v \mid r_i^{|\nu|-a_i} \partial^\nu v \in L^2(B_i), \forall |\nu| \leq m\},$$

where $B_i \subset \Omega$ represents the neighborhood of Q_i satisfying $B_i \cap B_j = \emptyset$ for $i \neq j$.

4.1.2 Regularity Results

Let α_0^i the solution of Equation (2.19) with ω being replaced by the interior angle ω_i at Q_i . We denote the vector $\alpha_0 = (\alpha_0^1, \dots, \alpha_0^i, \dots, \alpha_0^N)$. By Lemma 2.15, for $f \in H^{-1}(\Omega)$, there exists $\mathbf{F} \in [\mathcal{K}_{\mathbf{a}-1}^0(\Omega)]^2$ with $a_i < \min_i \{\alpha_0^i\}$ satisfying Equation (2.25) and

$$\|\mathbf{F}\|_{[\mathcal{K}_{\mathbf{a}-1}^0(\Omega)]^2} \leq C \|f\|_{H^{-1}(\Omega)}. \quad (4.2)$$

If $f \in \mathcal{K}_{\mathbf{a}-2}^{m-2}(\Omega) \cap H^{-1}(\Omega)$ with $m \geq 1$ and $0 \leq \mathbf{a} < \alpha_0$, then we can find $\mathbf{F} \in [\mathcal{K}_{\mathbf{a}-1}^{m-1}(\Omega)]^2$ satisfying Equation (2.25) and

$$\|\mathbf{F}\|_{[\mathcal{K}_{\mathbf{a}-1}^{m-1}(\Omega)]^2} \leq C \|f\|_{\mathcal{K}_{\mathbf{a}-2}^{m-2}(\Omega)}. \quad (4.3)$$

For the Stokes problem (2.24), we have the following regularity estimate in weighted Sobolev space [19].

Lemma 4.3. *Let $(\mathbf{u}, p) \in [H_0^1(\Omega)]^2 \times L_0^2(\Omega)$ be the solution of the Stokes problem (2.24). For $m \geq 1$ and $0 \leq \mathbf{a} \leq \alpha_0$, if $\mathbf{F} \in [\mathcal{K}_{\mathbf{a}-1}^{m-1}(\Omega)]^2$, then it follows*

$$\|\mathbf{u}\|_{[\mathcal{K}_{\mathbf{a}+1}^{m+1}(\Omega)]^2} + \|p\|_{\mathcal{K}_{\mathbf{a}}^m(\Omega)} \leq C \|\mathbf{F}\|_{[\mathcal{K}_{\mathbf{a}-1}^{m-1}(\Omega)]^2}. \quad (4.4)$$

We then have the following result.

Lemma 4.4. *Given $f \in \mathcal{K}_{\mathbf{a}-2}^{m-2}(\Omega) \cap H^{-1}(\Omega)$ for $0 \leq \mathbf{a} < \alpha_0$ and $m \geq 1$, let $\phi \in H_0^2(\Omega)$ be the solution of the Poisson problem (2.52), then it follows*

$$\|\phi\|_{\mathcal{K}_{\mathbf{a}+2}^{m+2}(\Omega)} \leq C \|f\|_{\mathcal{K}_{\mathbf{a}-2}^{m-2}(\Omega)}. \quad (4.5)$$

Proof. By Lemma 4.3, we have $\mathbf{u} \in [\mathcal{K}_{\mathbf{a}+1}^{m+1}(\Omega)]^2 \cap [H_0^1(\Omega)]^2$, thus we have $(\operatorname{curl} \mathbf{u}) \in \mathcal{K}_{\mathbf{a}}^m(\Omega)$ and

$$\|\operatorname{curl} \mathbf{u}\|_{\mathcal{K}_{\mathbf{a}}^m(\Omega)} \leq C \|\nabla \mathbf{u}\|_{[\mathcal{K}_{\mathbf{a}}^m(\Omega)]^2} \leq C \|\mathbf{u}\|_{[\mathcal{K}_{\mathbf{a}+1}^{m+1}(\Omega)]^2} \leq C \|\mathbf{F}\|_{[\mathcal{K}_{\mathbf{a}-1}^{m-1}(\Omega)]^2}. \quad (4.6)$$

By the regularity estimate [50, 64] for the Poisson problem (2.52), we have

$$\|\phi\|_{\mathcal{K}_{\mathbf{a}+2}^{m+2}(\Omega)} \leq \|\mathbf{curl} \mathbf{u}\|_{\mathcal{K}_{\mathbf{a}}^m(\Omega)}. \quad (4.7)$$

The conclusion holds by combining Equations (4.3), (4.6) and (4.7). \square

4.2 Graded Meshes

We now present the construction of graded meshes to improve the convergence rate of the numerical approximation from Algorithm 2.17.

Algorithm 4.5. (*Graded refinements*) Let \mathcal{T} be a triangulation of Ω with shape-regular triangles. Recall that $Q_i, i = 1, \dots, N$ are the vertices of Ω . Let AB be an edge in the triangulation \mathcal{T} with A and B as the endpoints. Then, in a graded refinement, a new node D on AB is produced according to the following conditions:

1. (Neither A or B coincides with Q_i .) We choose D as the midpoint ($|AD| = |BD|$).
2. (A coincides with Q_i .) We choose r such that $|AD| = \kappa_{Q_i}|AB|$, where $\kappa_{Q_i} \in (0, 0.5)$ is a parameter that will be specified later. See Figure 5 for example.

Then, the graded refinement, denoted by $\kappa(\mathcal{T})$, proceeds as follows. For each triangle $T \in \mathcal{T}$, a new node is generated on each edge of T as described above. Then, T is decomposed into four small triangles by connecting these new nodes (Figure 6). Given an initial mesh \mathcal{T}_0 satisfying the condition above, the associated family of graded meshes $\{\mathcal{T}_n, n \geq 0\}$ is defined recursively $\mathcal{T}_{n+1} = \kappa(\mathcal{T}_n)$.

Given a grading parameter κ_{Q_i} , Algorithm 4.5 produces smaller elements near Q_i for better approximation of singular solution. It is an explicit construction of graded meshes



Figure 5: The new node on an edge AB . (left): $A \neq Q_i$ and $B \neq Q_i$ (midpoint); (right) $A = Q_i$ ($|AD| = \kappa_{Q_i}|AB|$, $\kappa_{Q_i} < 0.5$).

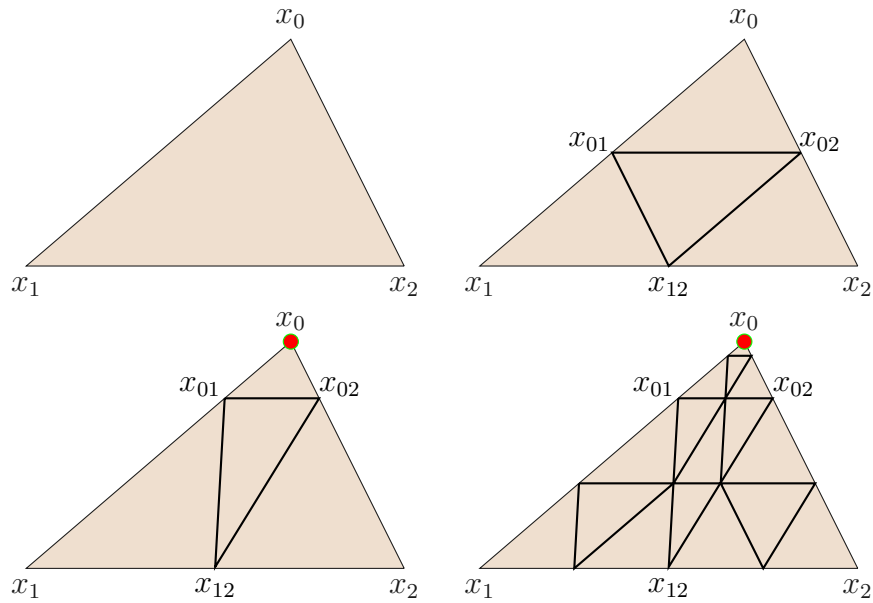


Figure 6: Refinement of a triangle $\triangle x_0 x_1 x_2$. First row: (left – right): the initial triangle and the midpoint refinement; second row: two consecutive graded refinements toward $x_0 = Q_i$, ($\kappa_{Q_i} < 0.5$).

based on recursive refinements. See also [5, 13, 64, 66] and references therein for more discussions on the graded mesh.

Note that after n refinements, the number of triangles in the mesh \mathcal{T}_n is $O(4^n)$, so we denote the “mesh size” of \mathcal{T}_n by

$$h = 2^{-n}. \quad (4.8)$$

In Algorithm 4.5, we choose the parameter κ_{Q_i} for each vertex Q_i as follows. Recall that α_0^i is the solution of (2.19) with ω being replaced by the interior angle ω_i at Q_i . Given the degree of polynomials k in Algorithm 2.17, we choose

$$\kappa_{Q_i} = 2^{-\frac{\theta}{a_i}} \left(\leq \frac{1}{2} \right), \quad (4.9)$$

where $a_i > 0$ and θ could be any possible constants satisfying

$$a_i \leq \theta \leq \min\{k, m\}. \quad (4.10)$$

In (4.10), if we take $a_i = \theta$, the grading parameter $\kappa_{Q_i} = \frac{1}{2}$.

4.3 Interpolation Error Estimates on Graded Meshes

Lemma 4.6. *Let $T_{(0)} \in \mathcal{T}_0$ be an initial triangle of the triangulation \mathcal{T}_n in Algorithm 4.5 with grading parameters κ_{Q_i} given by Equation (4.9). For $m \geq 1, k \geq 1$, we denote $v_I \in V_n^k$ (resp. $q_I \in S_n^{k-1}$) the nodal interpolation of $v \in \mathcal{K}_{\mathbf{a}+1}^{m+1}(\Omega)$ (resp. $q \in \mathcal{K}_{\mathbf{a}}^m(\Omega)$). If $\bar{T}_{(0)}$ does not contain any vertices $Q_i, i = 1, \dots, N$, then*

$$\|v - v_I\|_{H^1(T_{(0)})} \leq Ch^{\min\{k, m\}}, \quad \|q - q_I\|_{L^2(T_{(0)})} \leq Ch^{\min\{k, m\}},$$

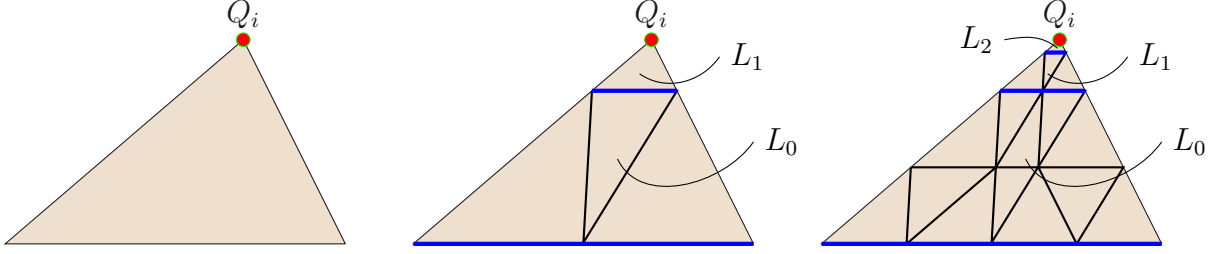


Figure 7: Mesh layers (left – right): the initial triangle $T_{(0)}$ with a vertex Q_i ; two layers after one refinement; three layers after two refinements.

where $h = 2^{-n}$.

Proof. If \bar{T}_0 does not contain any vertices Q_i of the domain Ω , we have $v \in \mathcal{K}_{\mathbf{a}+1}^{m+1}(\Omega) \subset H^{m+1}(T_{(0)})$ (see Remark 4.2) and the mesh on $T_{(0)}$ is quasi-uniform (Algorithm 4.5) with size $O(2^{-n})$. Therefore, based on the standard interpolation error estimate, we have

$$\|v - v_I\|_{H^1(T_{(0)})} \leq Ch^{\min\{k,m\}} \|v\|_{H^{m+1}(T_{(0)})}. \quad (4.11)$$

Note that $q \in \mathcal{K}_{\mathbf{a}}^m(\Omega) \subset H^m(\Omega)$, we can similar obtain the estimate for $\|q - q_I\|$. \square

We now study the interpolation error in the neighborhood Q_i , $i = 1, \dots, N$. In the rest of this subsection, we assume $T_{(0)} \in \mathcal{T}_0$ is an initial triangle such that the i th vertex Q_i is a vertex of $T_{(0)}$. We first define mesh layers on $T_{(0)}$ which are collections of triangles in \mathcal{T}_n .

Definition 4.7. (*Mesh layers*) Let $T_{(t)} \subset T_{(0)}$ be the triangle in \mathcal{T}_t , $0 \leq t \leq n$, that is attached to the singular vertex Q_i of $T_{(0)}$. For $0 \leq t < n$, we define the t th mesh layer of \mathcal{T}_n on $T_{(0)}$ to be the region $L_t := T_{(t)} \setminus T_{(t+1)}$; and for $t = n$, the n th layer is $L_n := T_{(n)}$. See Figure 7 for example.

Remark 4.8. The triangles in \mathcal{T}_n constitute n mesh layers on $T_{(0)}$. According to Algorithm 4.5 and the choice of grading parameters κ_{Q_i} given by Equation (4.9), the mesh size in the t th

layer L_t is

$$O(\kappa_{Q_i}^t 2^{t-n}). \quad (4.12)$$

Meanwhile, the weight function ρ in Equation (4.1) satisfies

$$\rho = O(\kappa_{Q_i}^t) \quad \text{in } L_t \quad (0 \leq t < n) \quad \text{and} \quad \rho \leq C\kappa_{Q_i}^n \quad \text{in } L_n. \quad (4.13)$$

Although the mesh size varies in different layers, the triangles in \mathcal{T}_n are shape regular.

In addition, using the local Cartesian coordinates such that Q is the origin, the mapping

$$\mathbf{B}_t = \begin{pmatrix} \kappa_{Q_i}^{-t} & 0 \\ 0 & \kappa_{Q_i}^{-t} \end{pmatrix}, \quad 0 \leq t \leq n \quad (4.14)$$

is a bijection between L_t and L_0 for $0 \leq t < n$ and a bijection between L_n and $T_{(0)}$. We call L_0 (resp. $T_{(0)}$) the reference region associated to L_t for $0 \leq t < n$ (resp. L_n).

With the mapping (4.14), we have that for any point $(x, y) \in L_t$, $0 \leq t \leq n$, the image point $(\hat{x}, \hat{y}) := \mathbf{B}_t(x, y)$ is in its reference region. We introduce the following dilation result.

Lemma 4.9. *For $0 \leq t \leq n$, given a function $v(x, y) \in \mathcal{K}_a^l(L_t)$, the function $\hat{v}(\hat{x}, \hat{y}) := v(x, y)$ belongs to $\mathcal{K}_a^l(\hat{L})$, where $(\hat{x}, \hat{y}) := \mathbf{B}_t(x, y)$, $\hat{L} = L_0$ for $0 \leq t < n$, and $\hat{L} = T_{(0)}$ for $t = n$.*

Then, it follows

$$\|\hat{v}(\hat{x}, \hat{y})\|_{\mathcal{K}_a^l(\hat{L})} = \kappa_{Q_i}^{t(a-1)} \|v(x, y)\|_{\mathcal{K}_a^l(L_t)}.$$

Proof. The proof can be found in [67, Lemma 4.5]. □

We then derive the interpolation error estimate in each layer.

Lemma 4.10. *For $k \geq 1, m \geq 1$, set κ_{Q_i} in Equation (4.9) with θ satisfying (4.10) for the*

graded mesh on $T_{(0)}$. Let $h := 2^{-n}$, then in the t th layer L_t on $T_{(0)}$, $0 \leq t < n$,

(i) if $v_I \in V_n^k$ be the nodal interpolation of $v \in \mathcal{K}_{\mathbf{a}+1}^{m+1}(\Omega)$, it follows

$$|v - v_I|_{H^1(L_t)} \leq Ch^\theta \|v\|_{\mathcal{K}_{\mathbf{a}+1}^{m+1}(L_t)}; \quad (4.15)$$

(ii) if $q_I \in V_n^{k-1}$ be the nodal interpolation of $q \in \mathcal{K}_{\mathbf{a}}^m(\Omega)$, it follows

$$\|q - q_I\|_{L^2(L_t)} \leq Ch^\theta \|q\|_{\mathcal{K}_{\mathbf{a}}^m(L_t)}. \quad (4.16)$$

Proof. For L_t associated with Q_i , $0 \leq t < n$, the space $\mathcal{K}_{\mathbf{a}+1}^{m+1}(L_t)$ (resp. $\mathcal{K}_{\mathbf{a}}^m(L_t)$) is equivalent to $H^{m+1}(L_t)$ (resp. $H^m(L_t)$). Therefore, v (resp. q) is a continuous function in L_t . For any point $(x, y) \in L_t$, let $(\hat{x}, \hat{y}) = \mathbf{B}_t(x, y) \in L_0$. For $v(x, y)$ (resp. $q(x, y)$) in L_t , we define $\hat{v}(\hat{x}, \hat{y}) := v(x, y)$ (resp. $\hat{q}(\hat{x}, \hat{y}) := q(x, y)$) in L_0 .

(i). Using the standard interpolation error estimate, the scaling argument, the estimate in (4.12), and the mapping in (4.14), we have

$$|v - v_I|_{H^1(L_t)} = |\hat{v} - \hat{v}_I|_{H^1(L_0)} \leq C2^{(t-n)\mu} \|\hat{v}\|_{\mathcal{K}_{\mathbf{a}+1}^{m+1}(L_0)} \leq C2^{(t-n)\mu} \kappa_{Q_i}^{a_i t} \|v\|_{\mathcal{K}_{\mathbf{a}+1}^{m+1}(L_t)},$$

where we have used Lemma 4.9 in the last inequality. Since $\kappa_{Q_i} = 2^{-\frac{\theta}{a_i}}$, so we have $\kappa_{Q_i}^{a_i t} = 2^{-\theta t}$. Set $\mu = \min\{k, m\}$, by $\theta \leq \mu$ from (4.10) and $t < n$, we have $2^{(n-t)(\theta-\mu)} < 2^0 = 1$.

Therefore, we have the estimate

$$\begin{aligned} |v - v_I|_{H^1(L_t)} &\leq C2^{(t-n)\mu-\theta t} \|v\|_{\mathcal{K}_{\mathbf{a}+1}^{m+1}(L_t)} = C2^{-n\theta} 2^{(n-t)(\theta-\mu)} \|v\|_{\mathcal{K}_{\mathbf{a}+1}^{m+1}(L_t)} \\ &\leq C2^{-n\theta} \|v\|_{\mathcal{K}_{\mathbf{a}+1}^{m+1}(L_t)} \leq Ch^\theta \|v\|_{\mathcal{K}_{\mathbf{a}+1}^{m+1}(L_t)}. \end{aligned}$$

(ii). We can show that

$$\|q - q_I\|_{L^2(L_t)} = \kappa_{Q_i}^t \|\hat{q} - \hat{q}_I\|_{L^2(L_0)} \leq C \kappa_{Q_i}^t 2^{(t-n)\mu} \|\hat{q}\|_{\mathcal{K}_{a_i}^m(L_0)} \leq C 2^{(t-n)\mu} \kappa_{Q_i}^{a_i t} \|q\|_{\mathcal{K}_{a_i}^m(L_t)},$$

where again we used Lemma 4.9 in the last inequality. Using the similar argument as in (i), the estimate (4.16) holds. \square

Before deriving the interpolation error estimate in the last layer L_n on $T_{(0)}$, we first introduce the following results.

Lemma 4.11. *For $\forall v \in \mathcal{K}_a^l(L_n)$, if $0 \leq l' \leq l$ and $a' \leq a$, then it follows*

$$\|v\|_{\mathcal{K}_{a'}^{l'}(L_n)} \leq C \kappa_{Q_i}^{n(a-a')} \|v\|_{\mathcal{K}_a^l(L_n)}. \quad (4.17)$$

Proof. This is a direct application of [66, Lemma 2.6] under condition (4.13) on L_n . \square

Lemma 4.12. *For $\forall v \in \mathcal{K}_a^l(L_n)$, if $a \geq l$, then it follows that*

$$\|v\|_{H^l(L_n)} \leq C \kappa_{Q_i}^{n(a-l)} \|v\|_{\mathcal{K}_a^l(L_n)}. \quad (4.18)$$

Proof. This is a direct application of [66, Lemma 2.8] under condition (4.13) on L_n . \square

Lemma 4.13. *For $k \geq 1, m \geq 1$, set κ_{Q_i} in (4.9) with θ satisfying (4.10) for the graded mesh on $T_{(0)}$. Let $h := 2^{-n}$, then in the n th layer L_n on $T_{(0)}$ for n sufficiently large,*

(i) *if $v_I \in V_n^k$ be the nodal interpolation of $v \in \mathcal{K}_{a+1}^{m+1}(\Omega)$, it follows*

$$|v - v_I|_{H^1(L_n)} \leq Ch^\theta \|v\|_{\mathcal{K}_{a+1}^{m+1}(L_n)}; \quad (4.19)$$

(ii) if $q_I \in V_n^{k-1}$ be the nodal interpolation of $q \in \mathcal{K}_a^m(\Omega)$, it follows

$$\|q - q_I\|_{L^2(L_n)} \leq Ch^\theta \|q\|_{\mathcal{K}_{a_i}^m(L_n)}. \quad (4.20)$$

Proof. Recall the mapping \mathbf{B}_n in (4.14). For any point $(x, y) \in L_n$, let $(\hat{x}, \hat{y}) = \mathbf{B}_n(x, y) \in T_{(0)}$.

(i). Let $\eta : T_{(0)} \rightarrow [0, 1]$ be a smooth function that is equal to 0 in a neighborhood of Q_i , but is equal to 1 at all the other nodal points in \mathcal{T}_0 . For a function $v(x, y)$ in L_n , we define $\hat{v}(\hat{x}, \hat{y}) := v(x, y)$ in $T_{(0)}$. We take $w = \eta\hat{v}$ in $T_{(0)}$. Consequently, we have for $l \geq 0$

$$\|w\|_{\mathcal{K}_1^l(T_{(0)})}^2 = \|\eta\hat{v}\|_{\mathcal{K}_1^l(T_{(0)})}^2 \leq C\|\hat{v}\|_{\mathcal{K}_1^l(T_{(0)})}^2, \quad (4.21)$$

where C depends on l and the smooth function η . Moreover, the condition $\hat{v} \in \mathcal{K}_{a_i+1}^{m+1}(T_{(0)})$ with and $m \geq 2$ implies $\hat{v}(Q) = 0$ (see, e.g., [66, Lemma 4.7]). Let $w_{\hat{I}}$ be the nodal interpolation of w associated with the mesh \mathcal{T}_0 on $T_{(0)}$. Therefore, by the definition of w , we have

$$w_{\hat{I}} = \hat{v}_{\hat{I}} = \hat{v}_I \quad \text{in } T_{(0)}. \quad (4.22)$$

Note that the \mathcal{K}_1^l norm and the H^l norm are equivalent for w on $T_{(0)}$, since $w = 0$ in the neighborhood of the vertex Q_i . Let r be the distance from (x, y) to Q_i , and \hat{r} be the distance from (\hat{x}, \hat{y}) to Q_i . Then, by the definition of the weighted space, the scaling

argument, Equations (4.21), (4.22), and (4.13), we have

$$\begin{aligned}
|v - v_I|_{H^1(L_n)}^2 &\leq C \|v - v_I\|_{\mathcal{K}_1^1(L_n)}^2 \leq C \sum_{|\nu| \leq 1} \|r(x, y)^{|\nu|-1} \partial^\nu (v - v_I)\|_{L^2(L_n)}^2 \\
&\leq C \sum_{|\nu| \leq 1} \|\hat{r}(\hat{x}, \hat{y})^{|\nu|-1} \partial^\nu (\hat{v} - \hat{v}_I)\|_{L^2(T_{(0)})}^2 \leq C \|\hat{v} - w + w - \hat{v}_I\|_{\mathcal{K}_1^1(T_{(0)})}^2 \\
&\leq C (\|\hat{v} - w\|_{\mathcal{K}_1^1(T_{(0)})}^2 + \|w - \hat{v}_I\|_{\mathcal{K}_1^1(T_{(0)})}^2) = C (\|\hat{v} - w\|_{\mathcal{K}_1^1(T_{(0)})}^2 + \|w - w_I\|_{\mathcal{K}_1^1(T_{(0)})}^2) \\
&\leq C (\|\hat{v}\|_{\mathcal{K}_1^1(T_{(0)})}^2 + \|w\|_{\mathcal{K}_1^{m+1}(T_{(0)})}^2) \leq C (\|\hat{v}\|_{\mathcal{K}_1^1(T_{(0)})}^2 + \|\hat{v}\|_{\mathcal{K}_1^{m+1}(T_{(0)})}^2) \\
&= C (\|v\|_{\mathcal{K}_1^1(L_n)}^2 + \|v\|_{\mathcal{K}_1^{m+1}(L_n)}^2) \leq C \kappa_{Q_i}^{2na_i} \|v\|_{\mathcal{K}_{a_i+1}^{m+1}(L_n)}^2 \\
&\leq C 2^{-2n\theta} \|v\|_{\mathcal{K}_{a_i+1}^{m+1}(L_n)}^2 \leq Ch^{2\theta} \|v\|_{\mathcal{K}_{a_i+1}^{m+1}(L_n)}^2,
\end{aligned}$$

where the ninth and tenth relationships are based on Lemma 4.9 and Lemma 4.11, respectively. This completes the proof of (4.15).

(ii). Since $q \in L^2(\Omega)$, we have that the interpolation operator is L^2 stable

$$\|q_I\|_{L^2(L_n)} \leq C \|q\|_{L^2(L_n)}. \quad (4.23)$$

Thus, by Equations (4.23) and (4.18), we have

$$\|q - q_I\|_{L^2(L_n)} \leq C \|q\|_{L^2(L_n)} \leq C \kappa_{Q_i}^{na_i} \|q\|_{\mathcal{K}_{a_i}^m(L_n)} \leq C 2^{-n\theta} \|q\|_{\mathcal{K}_{a_i}^m(L_n)} \leq Ch^\theta \|q\|_{\mathcal{K}_{a_i}^m(L_n)}.$$

□

Theorem 4.14. [68] *Let \mathcal{T}_0 be an initial triangle of the triangulation \mathcal{T}_n in Algorithm 4.5 with grading parameters κ_{Q_i} in (4.9). For $k \geq 1, m \geq 1$, if $v_I \in V_n^k$ (resp. $q_I \in V_n^{k-1}$) be the nodal interpolation of $v \in \mathcal{K}_{\mathbf{a}+1}^{m+1}(\Omega)$ (resp. $q \in \mathcal{K}_{\mathbf{a}}^m(\Omega)$). Then, it follows the following*

interpolation error

$$\|v - v_I\|_{H^1(\Omega)} \leq Ch^\theta \|v\|_{\mathcal{K}_{\mathbf{a}+1}^{m+1}(\Omega)}, \quad \|q - q_I\| \leq Ch^\theta \|q\|_{\mathcal{K}_{\mathbf{a}}^m(\Omega)}, \quad (4.24)$$

where $h := 2^{-n}$, and θ satisfying (4.10).

Proof. By summing the estimates in Lemmas 4.6, 4.10, and 4.13, we have

$$\begin{aligned} \|v - v_I\|_{H^1(\Omega)}^2 &= \sum_{T_{(0)} \in \mathcal{T}_0} \|v - v_I\|_{H^1(T_{(0)})}^2 \leq Ch^{2\theta} \|v\|_{\mathcal{K}_{\mathbf{a}+1}^{m+1}(\Omega)}^2, \\ \|q - q_I\|^2 &= \sum_{T_{(0)} \in \mathcal{T}_0} \|v - v_I\|_{L^2(T_{(0)})}^2 \leq Ch^{2\theta} \|q\|_{\mathcal{K}_{\mathbf{a}}^m(\Omega)}^2. \end{aligned}$$

□

4.4 Error Estimates Results for Algorithm 2.17

To better observe threshold of grading parameter κ_{Q_i} in obtaining the optimal convergence rates, we always assume $1 \leq k \leq m$ in the following discussions, otherwise we just replace k by $\min\{k, m\}$. In this section, we assume that $f \in \mathcal{K}_{\mathbf{a}-1}^{m-1}(\Omega) \cap \mathcal{K}_{\mathbf{b}-1}^{m-1}(\Omega)$ with $0 < \mathbf{a} < \alpha_0$, and $0 < \mathbf{b} < \beta_0$, where $\beta_0 = (\frac{\pi}{\omega_1}, \dots, \frac{\pi}{\omega_N})$. For \mathbf{F} given by Lemma 2.7, we have $\mathbf{F} \in [\mathcal{K}_{\mathbf{a}-1}^{m-1}(\Omega)]^2$, and the regularities in Lemma 4.3 and Lemma 4.4 hold. Now we have the following error estimate of the Mini element approximation ($k = 1$) or Taylor-Hood method ($k \geq 2$) in Algorithm 2.17 on graded meshes for the Stokes problem (2.24).

Lemma 4.15. *The bilinear forms in both Mini element method and the Taylor-Hood method on graded meshes satisfies the LBB or inf-sup condition (3.1) or (3.2).*

Proof. For given $\kappa = \min_i \{\kappa_{Q_i}\}$, Algorithm 4.5 implies that there exists a constant $\sigma(\kappa) > 0$

such that

$$h_T \leq \sigma(\kappa)\rho_T, \quad \forall T \in \mathcal{T}_n, \quad (4.25)$$

where h_T is the diameter of T , and ρ_T is the maximum diameter of all circles contained in T . Under condition (4.25) of the graded mesh, the conclusion follows from [89, Theorem 3.1]. \square

Theorem 4.16. [68] *Set the grading parameters $\kappa_{Q_i} = 2^{-\frac{\theta}{a_i}}$ with $0 < a_i < \alpha_0^i$ and θ being any constants satisfying $a_i \leq \theta \leq k$. Let (\mathbf{u}, p) be the solution of the Stokes problem (2.26), and (\mathbf{u}_n, p_n) be the Mini element solution ($k = 1$) or Taylor-Hood element solution ($k \geq 2$) on graded meshes \mathcal{T}_n . If (\mathbf{u}_n, p_n) is the solution of in Algorithm 2.17, then it follows*

$$\|\mathbf{u} - \mathbf{u}_n\|_{[H^1(\Omega)]^2} + \|p - p_n\| \leq Ch^\theta. \quad (4.26)$$

Proof. By Corollary 3.2 and the interpolation error estimates in Lemma 4.14 under the regularity result in Lemma 4.3, the estimate (4.26) holds.

We also have the following result.

Theorem 4.17. [68] *Set the grading parameters $\kappa_{Q_i} = 2^{-\frac{\theta}{a_i}}$ with $0 < a_i < \alpha_0^i$ and θ being any constants satisfying $a_i \leq \theta \leq k$. Let (\mathbf{u}, p) be the solution of the Stokes problem (2.26), and (\mathbf{u}_n, p_n) be the Mini element solution ($k = 1$) or Taylor-Hood element solution ($k \geq 2$) in Algorithm 2.17 on graded meshes \mathcal{T}_n . Then it follows*

$$\begin{aligned} \|\mathbf{u} - \mathbf{u}_n\|_{[L^2(\Omega)]^2} &\leq Ch^{\min\{2\theta, \theta+1\}}, \\ \|\mathbf{u} - \mathbf{u}_n\|_{[(\mathcal{K}_b^1(\Omega))^*]^2} &\leq Ch^{\min\{2\theta, \theta+2\}}; \end{aligned} \quad (4.27)$$

Here, $(\cdot)^*$ represents the dual space.

Remark 4.18. By Theorem 4.22 and Theorem 4.23, we can find that if we take

$$\theta = k \tag{4.28}$$

in the grading parameter κ_{Q_i} , then we can obtain the optimal convergence rate for the Stokes approximations in Algorithm 2.17 [68],

$$\|\mathbf{u} - \mathbf{u}_n\|_{[H^1(\Omega)]^2} + \|p - p_n\| \leq Ch^k, \tag{4.29a}$$

$$\|\mathbf{u} - \mathbf{u}_n\|_{[L^2(\Omega)]^2} \leq Ch^{k+1}. \tag{4.29b}$$

However, to obtain the optimal convergence rate for the biharmonic approximation, the convergence rates of Mini element or Taylor-Hood element approximations don't have to be optimal. Therefore, we shall figure out the admissible parameters θ such that the convergence rate of the biharmonic approximation is optimal.

Theorem 4.19. [68] Set the grading parameters $\kappa_{Q_i} = 2^{-\frac{\theta}{a_i}}$ with $0 < a_i < \alpha_0^i$ and

$$\theta = \max\{k - 1, a'_i\}, \tag{4.30}$$

where $a'_i = \min\{\alpha_0, a_i\} \leq \alpha_0$ for α_0 given by (2.19). Let $\phi_n \in V_n^k$ be the solution of finite element solution of (2.70), and ϕ is the solution of the biharmonic problem (2.1). If ϕ_n is the solution in Algorithm 2.17, then it follows

$$\|\phi - \phi_n\|_{H^1(\Omega)} \leq Ch^k. \tag{4.31}$$

Proof. Denote by $\phi_I \in V_n^k$ the nodal interpolation of ϕ . Similar to Theorem 3.5, we have

$$\|\phi - \phi_n\|_{H^1(\Omega)} \leq C (\|\phi - \phi_I\|_{H^1(\Omega)} + \|\mathbf{u} - \mathbf{u}_n\|_{[L^2(\Omega)]^2}) \quad (4.32)$$

Recall that $\phi \in \mathcal{K}_{\mathbf{a}+2}^{m+2}(\Omega) = \mathcal{K}_{(\mathbf{a}+1)+1}^{(m+1)+1}(\Omega)$ with $m \geq k$, so by Lemma 4.14 with grading parameter $\kappa_{Q_i} = 2^{-\frac{\theta_1}{1+a_i}} (= 2^{-\frac{\theta}{a_i}})$ with θ given in (4.60) and $\theta_1 = \frac{1+a_i}{a_i}\theta = \theta + \frac{1}{a_i}\theta \geq \theta + 1 \geq k$, we have

$$\|\phi - \phi_I\|_{H^1(\Omega)} \leq Ch^{\min\{k, \theta_1\}} = Ch^k. \quad (4.33)$$

For θ given in (4.30), Theorem 4.17 indicates for Algorithm 2.17,

$$\|\mathbf{u} - \mathbf{u}_n\|_{[L^2(\Omega)]^2} \leq Ch^{\min\{\max\{2\alpha_0, 2(k-1)\}, \max\{\alpha_0+1, k\}\}}. \quad (4.34)$$

Plugging (4.33) and (4.34) into (4.32), the estimate (4.31) holds. □

Theorem 4.20. [68] *Set the grading parameters $\kappa_{Q_i} = 2^{-\frac{\theta}{a_i}}$ with $0 < a_i < \alpha_0^i$ and θ given by*

$$\theta = \max \left\{ k - 1, \frac{k + 1}{2}, a'_i \right\}, \quad (4.35)$$

where $a'_i = \min\{\alpha_0, a_i\} \leq \alpha_0$ for α_0 given by Equation (2.19). Let ϕ_n be the solution of finite element solution of Equation (2.70), and ϕ be the solution of the biharmonic problem (2.1). If ϕ_n is the solution in Algorithm 2.17, then it follows

$$\|\phi - \phi_n\| \leq Ch^{k+1}. \quad (4.36)$$

Proof. Set $\psi = v_I \in V_n^k$ the nodal interpolation of v of the Poisson problem (3.42). Similar to Theorem 3.6, we have

$$\begin{aligned} \|\phi - \phi_n\|^2 &\leq \|\phi - \phi_n\|_{H^1(\Omega)} \|v - v_I\|_{H^1(\Omega)} + \|\mathbf{u} - \mathbf{u}_n\|_{[L^2(\Omega)]^2} \|v - v_I\|_{H^1(\Omega)} \\ &+ \|\mathbf{u} - \mathbf{u}_n\|_{[(\mathcal{K}_b^1(\Omega))^*]^2} \|\mathbf{curl} v\|_{[\mathcal{K}_b^1(\Omega)]^2} := T_1 + T_2 + T_3. \end{aligned} \quad (4.37)$$

Based on the results in [13], the solution $v \in \mathcal{K}_{\mathbf{b}'_{+1}}^2(\Omega)$ satisfies the regularity estimate

$$\|v\|_{\mathcal{K}_{\mathbf{b}'_{+1}}^2(\Omega)} \leq C \|\phi - \phi_n\|, \quad (4.38)$$

where the i th entry of \mathbf{b}' is given by $b'_i = \min\{b_i, 1\}$ with $b_i < \frac{\pi}{\omega_i}$. If $\omega > \pi$, we have

$$\theta' \geq \theta \geq \frac{k+1}{2} \geq 1,$$

so it follows the interpolation error

$$\|v - v_I\|_{H^1(\Omega)} \leq Ch^{\min\{\theta', 1\}} \|v\|_{\mathcal{K}_{\mathbf{b}'_{+1}}^2(\Omega)} = Ch \|v\|_{\mathcal{K}_{\mathbf{b}'_{+1}}^2(\Omega)}. \quad (4.39)$$

If $\omega < \pi$, the interpolation error (4.39) is obvious since $v \in H^2(\Omega)$.

For Algorithm 2.17, we have the following estimate for each T_i , $i = 1, 2, 3$. By Theorem 4.19 and Equation (4.39), it follows

$$T_1 = \|\phi - \phi_n\|_{H^1(\Omega)} \|v - v_I\|_{H^1(\Omega)} \leq Ch^{k+1} \|v\|_{\mathcal{K}_{\mathbf{b}'_{+1}}^2(\Omega)}.$$

By Theorem 4.23 and (4.39), it follows

$$T_2 = \|\mathbf{u} - \mathbf{u}_n\|_{[L^2(\Omega)]^2} \|v - v_I\|_{H^1(\Omega)} \leq Ch^{k+2} \|v\|_{K_{\mathbf{b}'+1}^2(\Omega)}.$$

Again, by Theorem 4.23, it follows

$$T_3 \leq C \|\mathbf{u} - \mathbf{u}_n\|_{[(K_{\mathbf{b}'}^1(\Omega))^*]^2} \|v\|_{K_{\mathbf{b}'+1}^2(\Omega)} \leq Ch^{k+1} \|v\|_{K_{\mathbf{b}'+1}^2(\Omega)}.$$

Thus, the regularity estimate (4.68) and the summation of T_i , $i = 1, 2, 3$ give the estimate (4.36).

□

4.5 Error Estimates Results for Algorithm 2.18

Recall that the threshold of grading parameter κ_{Q_i} in obtaining the optimal convergence rates, we always assume $1 \leq k \leq m$ in the following discussions, otherwise we just replace k by $\min\{k, m\}$. In this section, we assume that $f \in \mathcal{K}_{\mathbf{a}-1}^{m-1}(\Omega) \cap \mathcal{K}_{\mathbf{b}-1}^{m-1}(\Omega)$ with $0 < \mathbf{a} < \boldsymbol{\alpha}_0$, and $0 < \mathbf{b} < \boldsymbol{\beta}_0$, where $\boldsymbol{\beta}_0 = (\frac{\pi}{\omega_1}, \dots, \frac{\pi}{\omega_N})$. For \mathbf{F} given by Lemma 2.15, by the regularity estimate [13] for the Poisson problem (2.55) on weighted Sobolev space, it follows that

$$\|w\|_{\mathcal{K}_{\mathbf{b}'+1}^{m+1}(\Omega)} \leq C \|f\|_{\mathcal{K}_{\mathbf{b}-1}^{m-1}(\Omega)}, \quad (4.40)$$

which implies $\mathbf{F} = \mathbf{curl} w \in [\mathcal{K}_{\mathbf{b}}^m(\Omega)]^2 \subset [\mathcal{K}_{\mathbf{b}}^{m-1}(\Omega)]^2$. Then the solution of the Stokes problem (2.24) satisfies

$$\|\mathbf{u}\|_{[\mathcal{K}_{\mathbf{c}+1}^{m+1}(\Omega)]^2} + \|p\|_{\mathcal{K}_{\mathbf{c}}^m(\Omega)} \leq C\|\mathbf{F}\|_{[\mathcal{K}_{\mathbf{c}-1}^{m-1}(\Omega)]^2} \leq C\|\mathbf{F}\|_{[\mathcal{K}_{\mathbf{b}-1}^{m-1}(\Omega)]^2}, \quad (4.41)$$

where $\mathbf{c} = (c_1, \dots, c_N)$ with $c_i = \min\{b_i + 1, a_i\}$. Thus, the solution of the Poisson problem (2.52) satisfies $\phi \in \mathcal{K}_{\mathbf{c}+2}^{m+2}(\Omega)$.

Since the bilinear functional in (2.71) is coercive and continuous on V_n^k , so we have by Céa's Theorem,

$$\|w - w_n\|_{H^1(\Omega)} \leq C \inf_{v \in V_n^k} \|w - v\|_{H^1(\Omega)}. \quad (4.42)$$

Recall that $\alpha_0 = \min_i\{\alpha_0^i\}$ given by Equation (2.19), and $\beta_0 = \min_i\{\beta_0^i\} = \frac{\pi}{\omega}$ are the thresholds corresponding to the largest interior angle ω , then we have the following result.

Lemma 4.21. [68] *Set the grading parameters $\kappa_{Q_i} = 2^{-\frac{\theta}{a_i}}$ ($= 2^{-\frac{\theta'}{b_i}}$) with $0 < a_i < \alpha_0^i$, $0 < b_i < \beta_0^i$, θ being any constant satisfying $a_i \leq \theta \leq k$, and $\theta' = \min\left\{\frac{\beta_0}{\alpha_0} \max\{\theta, \alpha_0\}, k\right\}$ satisfying $b_i \leq \theta' \leq k$. Let $w_n \in V_n^k$ be the solution of finite element solution of Equation (2.71), and w is the solution of the Poisson problem (2.55), then it follows*

$$\|w - w_n\|_{H^1(\Omega)} \leq Ch^{\theta'}, \quad \|w - w_n\| \leq Ch^{\min\{2\theta', \theta' + 1\}}, \quad (4.43)$$

where $h := 2^{-n}$.

Proof. By Equation (4.42) and the interpolation error estimates in Lemma 4.14 under the

regularity result in Equation (4.40) and $\kappa_{Q_i} = 2^{-\frac{\theta}{a_i}} = 2^{-\frac{\theta'}{b_i}}$, we have the estimate

$$\|w - w_n\|_{H^1(\Omega)} \leq C\|w - w_I\|_{H^1(\Omega)} \leq Ch^{\theta'}.$$

Consider the Poisson problem

$$-\Delta v = w - w_n \text{ in } \Omega, \quad v = 0 \text{ on } \partial\Omega. \quad (4.44)$$

Then we have

$$\|w - w_n\|^2 = (\nabla(w - w_n), \nabla v). \quad (4.45)$$

Subtract Equation (2.71) from weak formulation of Equation (2.55), we have the Galerkin orthogonality,

$$(\nabla(w - w_n), \nabla\psi) = 0, \quad \forall \psi \in V_n^k. \quad (4.46)$$

Setting $\psi = v_I \in V_n^k$ the nodal interpolation of v and subtract Equation (4.46) from Equation (4.45), we have

$$\|w - w_n\|^2 = (\nabla(w - w_n), \nabla(v - v_I)) \leq \|w - w_n\|_{H^1(\Omega)} \|v - v_I\|_{H^1(\Omega)}. \quad (4.47)$$

Similarly, the solution $v \in \mathcal{K}_{\mathbf{b}'+1}^2(\Omega)$ satisfies the regularity estimate

$$\|v\|_{K_{\mathbf{b}'+1}^2(\Omega)} \leq C\|w - w_n\|_{K_{\mathbf{b}'-1}^0(\Omega)} \leq C\|w - w_n\|, \quad (4.48)$$

where the i th entry of \mathbf{b}' satisfying $b'_i = \min\{b_i, 1\}$. By Lemma 4.14 with grading parameter

$\kappa_{Q_i} = 2^{-\frac{\theta'}{b_i}} (= 2^{-\frac{\theta}{a_i}})$ again, we have the interpolation error

$$\|v - v_I\|_{H^1(\Omega)} \leq Ch^{\min\{\theta', 1\}} \|v\|_{K_{\mathbf{b}'+1}^2(\Omega)}. \quad (4.49)$$

The L^2 error estimate in Equation (4.43) can be obtained by combining Equations (4.47), (4.48), and (4.49). \square

Thus, we have the following result,

$$\begin{aligned} \|\mathbf{F} - \mathbf{F}_n\|_{[L^2(\Omega)]^2} &= \|\mathbf{curl} v - \mathbf{curl} v_n\|_{[L^2(\Omega)]^2} \leq \|w - w_n\|_{H^1(\Omega)} \leq Ch^{\theta'}, \\ \|\mathbf{F} - \mathbf{F}_n\|_{[H^{-1}(\Omega)]^2} &= \|\mathbf{curl} w - \mathbf{curl} w_n\|_{[H^{-1}(\Omega)]^2} \leq C\|w - w_n\| \leq Ch^{\min\{\theta'+1, 2\theta'\}}. \end{aligned} \quad (4.50)$$

Now we have the following error estimate of the Mini element approximation ($k = 1$) or Taylor-Hood method ($k \geq 2$) in Algorithm 2.18 on graded meshes for the Stokes problem (2.24).

Theorem 4.22. [68] *Set the grading parameters $\kappa_{Q_i} = 2^{-\frac{\theta}{a_i}}$ with $0 < a_i < \alpha_0^i$ and θ being any constants satisfying $a_i \leq \theta \leq k$. Let (\mathbf{u}, p) be the solution of the Stokes problem (2.26), and (\mathbf{u}_n, p_n) be the Mini element solution ($k = 1$) or Taylor-Hood element solution ($k \geq 2$) on graded meshes \mathcal{T}_n . If (\mathbf{u}_n, p_n) is the solution of in Algorithm 2.18, then it follows*

$$\|\mathbf{u} - \mathbf{u}_n\|_{[H^1(\Omega)]^2} + \|p - p_n\| \leq Ch^{\min\{\theta, \theta'+1\}}, \quad (4.51)$$

where θ' is given in Lemma 4.21.

Proof. For Algorithm 2.18, by Lemma 3.9 with the estimate (4.50) and the interpolation

error estimates in Theorem 4.14 under the regularity result (4.41), it follows

$$\|\mathbf{u} - \mathbf{u}_n\|_{[H^1(\Omega)]^2} + \|p - p_n\| \leq Ch^\theta + Ch^{\min\{\theta'+1, 2\theta'\}} \leq Ch^{\min\{\theta, \theta'+1\}}.$$

Here, we have used the fact that if $\omega > \pi$, $\theta \leq \theta' < 2\theta'$. Note that $\theta' = \min\left\{\frac{\beta_0}{\alpha_0} \max\{\theta, \alpha_0\}, k\right\}$,

so if $\theta' = k$, then $\theta \leq k = \theta'$; otherwise

$$\theta' = \frac{\beta_0}{\alpha_0} \max\{\alpha_0, \theta\} \geq \frac{\beta_0}{\alpha_0} \theta > \theta,$$

where we have used (2.23).

If $\omega < \pi$, by taking $1 < b_i = \frac{\beta_0}{\alpha_0} a_i < \beta_0 \leq \beta_0^i$, it follows $\theta' = \frac{b_i}{a_i} \theta \geq b_i > 1$, so that $\theta' + 1 < 2\theta'$. Thus, the estimate (4.51) hold. \square

In weighted Sobolev space, the regularity result for (3.25) with $l = 0, 1$ has the form

$$\|\mathbf{r}\|_{[\mathcal{K}_{\mathbf{a}'+1}^{l+2}(\Omega)]^2} + \|s\|_{\mathcal{K}_{\mathbf{a}'}^{l+1}(\Omega)} \leq C\|\mathbf{g}\|_{[\mathcal{K}_{\mathbf{a}'-1}^l(\Omega)]^2} \leq C\|\mathbf{g}\|_{[\mathcal{K}_{\mathbf{b}}^l(\Omega)]^2}, \quad (4.52)$$

where $0 < \mathbf{a}' = \min\{\mathbf{a}, l + 1\}$ with $0 < \mathbf{a} < \alpha_0$ and $0 < \mathbf{b} < \beta_0$. Then we have the following result.

Theorem 4.23. [68] *Set the grading parameters $\kappa_{Q_i} = 2^{-\frac{\theta}{a_i}}$ with $0 < a_i < \alpha_0^i$ and θ being any constants satisfying $a_i \leq \theta \leq k$. Let (\mathbf{u}, p) be the solution of the Stokes problem (2.26), and (\mathbf{u}_n, p_n) be the Mini element solution ($k = 1$) or Taylor-Hood element solution ($k \geq 2$) in Algorithm 2.18 on graded meshes \mathcal{T}_n . Then it follows*

$$\|\mathbf{u} - \mathbf{u}_n\|_{[L^2(\Omega)]^2} \leq Ch^{\min\{2\theta, \theta+1, \theta'+2\}}, \quad (4.53)$$

$$\|\mathbf{u} - \mathbf{u}_n\|_{[(\mathcal{K}_b^1(\Omega))^*]^2} \leq Ch^{\min\{2\theta, \theta+2, k+\theta', \theta+\theta'+1, \theta'+3\}}.$$

Here, $(\cdot)^*$ represents the dual space.

Proof. We prove Equation (4.53) for Taylor-Hood method, all other cases can be proved similarly. Similar to Lemma 3.11, we take $\mathbf{v} = \mathbf{u} - \mathbf{u}_n$, $q = p - p_n$ in Equation (3.24), then we have

$$\|\mathbf{u} - \mathbf{u}_n\|_{[(\mathcal{K}_b^l(\Omega))^*]^2} = \sup_{g \in (\mathcal{K}_b^l(\Omega))^2} \frac{\langle \mathbf{g}, \mathbf{u} - \mathbf{u}_n \rangle}{\|\mathbf{g}\|_{[(\mathcal{K}_b^l(\Omega))^2]}}$$

where $l = 0, 1$. Let (\mathbf{r}_n, s_n) be the Taylor-Hood solution of (3.23), then it follows

$$\langle \mathbf{g}, \mathbf{u} - \mathbf{u}_n \rangle = T_1 + T_2 + T_3 + T_4,$$

where T_i , $i = 1, \dots, 4$ have the same expressions as those in Lemma 3.11. For \mathbf{r}_n and s_n , we have the following estimate in the weighted Sobolev space

$$\begin{aligned} \|\mathbf{r} - \mathbf{r}_n\|_{[H^1(\Omega)]^2} + \|s - s_n\| &\leq C \left(\inf_{\mathbf{r}_I \in [V_n^k(\Omega)]^2} \|\mathbf{r} - \mathbf{r}_I\|_{[H^1(\Omega)]^2} + \inf_{s_I \in S_n^{k-1}} \|s - s_I\| \right) \\ &\leq Ch^{\min\{\theta, l+1\}} (\|\mathbf{r}\|_{[\mathcal{K}_{\mathbf{a}'+1}^{l+2}(\Omega)]^2} + \|s\|_{\mathcal{K}_{\mathbf{a}'}^{l+1}(\Omega)}). \end{aligned} \quad (4.54)$$

Here we have

$$\begin{aligned} |T_j| &\leq Ch^{\min\{\theta, \theta'+1\} + \min\{\theta, l+1\}} (\|\mathbf{r}\|_{[\mathcal{K}_{\mathbf{a}'+1}^{l+2}(\Omega)]^2} + \|s\|_{\mathcal{K}_{\mathbf{a}'}^{l+1}(\Omega)}) \\ &= Ch^{\min\{2\theta, \theta+l+1, \theta+\theta'+1, \theta'+l+2\}} (\|\mathbf{r}\|_{[\mathcal{K}_{\mathbf{a}'+1}^{l+2}(\Omega)]^2} + \|s\|_{\mathcal{K}_{\mathbf{a}'}^{l+1}(\Omega)}), \end{aligned}$$

where $j = 1, 2, 3$.

Note that

$$T_4 = T_{41} + T_{42} = \langle \mathbf{F} - \mathbf{F}_n, \mathbf{r}_n - \mathbf{r} \rangle + \langle \mathbf{F} - \mathbf{F}_n, \mathbf{r} \rangle.$$

By (4.50) and (4.54), we have

$$\begin{aligned} |T_{41}| &\leq \|\mathbf{F} - \mathbf{F}_n\|_{[H^{-1}(\Omega)]^2} \|\mathbf{r} - \mathbf{r}_n\|_{[H^1(\Omega)]^2} \leq Ch^{\min\{\theta'+1, 2\theta'\} + \min\{\theta, l+1\}} \|\mathbf{r}\|_{[\mathcal{K}_{\mathbf{a}'+1}^{l+2}(\Omega)]^2} \\ &= Ch^{\min\{\theta+\theta'+1, \theta'+l+2, 2\theta'+l+1, \theta+2\theta'\}} \|\mathbf{r}\|_{[\mathcal{K}_{\mathbf{a}'+1}^{l+2}(\Omega)]^2}. \end{aligned}$$

By Theorem 4.14 for $\psi \in \mathcal{K}_{\mathbf{a}'+2}^{l+3}(\Omega)$ satisfying (3.26) with $\kappa_{Q_i} = 2^{-\frac{\theta}{a_i}} = 2^{-\frac{\theta_1}{1+a_i}}$, we have

$$\|\psi - \psi_I\|_{H^1(\Omega)} \leq Ch^{\min\{k, \theta_1, l+2\}} \|\mathbf{r}\|_{[\mathcal{K}_{\mathbf{a}'+1}^{l+2}(\Omega)]^2}, \quad (4.55)$$

where $\theta_1 = (1 + \frac{1}{a_i})\theta \geq (1 + \frac{1}{a_i})\theta \geq \theta + 1$ and ψ_I is the nodal interpolation of ψ .

By (4.50) and (4.55), we have

$$\begin{aligned} |T_{42}| &\leq \|\mathbf{F} - \mathbf{F}_n\|_{[L^2(\Omega)]^2} \|\psi - \psi_I\|_{H^1(\Omega)} \leq Ch^{\theta' + \min\{k, \theta + \theta'_1, l+2\}} \|\mathbf{r}\|_{[\mathcal{K}_{\mathbf{a}'+1}^{l+2}(\Omega)]^2} \\ &\leq Ch^{\min\{k+\theta', \theta'+l+2, \theta+\theta'+\theta'_1\}} \|\mathbf{r}\|_{[\mathcal{K}_{\mathbf{a}'+1}^{l+2}(\Omega)]^2}, \end{aligned}$$

where $\theta'_1 = \min_i \{\frac{1}{a_i}\theta\} \geq 1$. It can be verified that

$$|T_4| \leq |T_{41}| + |T_{42}| \leq Ch^{\min\{k+\theta', \theta+\theta'+1, \theta'+l+2, 2\theta'+l+1, \theta+2\theta'\}} \|\mathbf{r}\|_{[\mathcal{K}_{\mathbf{a}'+1}^{l+2}(\Omega)]^2}.$$

By the regularity (4.52) and the summation of estimates $|T_i|$, $i = 1, \dots, 4$, and $\theta < 2\theta'$,

we have the error estimate

$$\|\mathbf{u} - \mathbf{u}_n\|_{[(\mathcal{K}_b^1(\Omega))^*]^2} \leq Ch^{\min\{2\theta, \theta+l+1, k+\theta', \theta+\theta'+1, \theta'+l+2\}}. \quad (4.56)$$

Recall that $k \geq 1$, $\theta \leq k$, and when $\omega > \pi$, we have $\theta < \theta'$, then it follows

$$\theta + 1 \leq k + \theta', \quad (4.57)$$

and when $\omega < \pi$, we have $\theta' > 1$, so the inequality (4.57) still holds. The estimates in Equation (4.53) follows from Equation (4.56) with the fact (4.57). \square

Remark 4.24. *By Theorem 4.22 and Theorem 4.23, we can find that if we take*

$$\theta = k \quad (4.58)$$

in the grading parameter κ_{Q_i} , then we can obtain the optimal convergence rate for the Stokes approximations in Algorithm 2.18 [68],

$$\|\mathbf{u} - \mathbf{u}_n\|_{[H^1(\Omega)]^2} + \|p - p_n\| \leq Ch^{\min\left\{\frac{\beta_0}{\alpha_0} \max\{k, \alpha_0\} + 1, k\right\}}, \quad (4.59a)$$

$$\|\mathbf{u} - \mathbf{u}_n\|_{[L^2(\Omega)]^2} \leq Ch^{\min\left\{k+1, \frac{\beta_0}{\alpha_0} \max\{k, \alpha_0\} + 2\right\}}. \quad (4.59b)$$

Recall that, to obtain the optimal convergence rate for the biharmonic approximation, the convergence rates of Mini element or Taylor-Hood element approximations don't have to be optimal. Therefore, we shall figure out the admissible parameters θ such that the convergence rate of the biharmonic approximation is optimal.

Theorem 4.25. [68] Set the grading parameters $\kappa_{Q_i} = 2^{-\frac{\theta}{a_i}}$ with $0 < a_i < \alpha_0^i$ and

$$\theta = \max\{k - 1, a'_i\}, \quad (4.60)$$

where $a'_i = \min\{\alpha_0, a_i\} \leq \alpha_0$ for α_0 given by (2.19). Let $\phi_n \in V_n^k$ be the solution of finite element solution of (2.74), and ϕ is the solution of the biharmonic problem (2.1). If ϕ_n is the solution in Algorithm 2.18, then it follows

$$\|\phi - \phi_n\|_{H^1(\Omega)} \leq Ch^{\min\{k, \max\{\frac{\beta_0}{\alpha_0}(k-1)+2, \beta_0+2\}\}}. \quad (4.61)$$

Proof. Denote by $\phi_I \in V_n^k$ the nodal interpolation of ϕ . Similar to Theorem 3.5, we have

$$\|\phi - \phi_n\|_{H^1(\Omega)} \leq C (\|\phi - \phi_I\|_{H^1(\Omega)} + \|\mathbf{u} - \mathbf{u}_n\|_{[L^2(\Omega)]^2}) \quad (4.62)$$

Recall that $\phi \in \mathcal{K}_{\mathbf{a}+2}^{m+2}(\Omega) = \mathcal{K}_{(\mathbf{a}+1)+1}^{(m+1)+1}(\Omega)$ with $m \geq k$, so by Lemma 4.14 with grading parameter $\kappa_{Q_i} = 2^{-\frac{\theta_1}{1+a_i}} (= 2^{-\frac{\theta}{a_i}})$ with θ given in (4.60) and $\theta_1 = \frac{1+a_i}{a_i}\theta = \theta + \frac{1}{a_i}\theta \geq \theta + 1 \geq k$, we have

$$\|\phi - \phi_I\|_{H^1(\Omega)} \leq Ch^{\min\{k, \theta_1\}} = Ch^k. \quad (4.63)$$

For θ given in (4.60), Theorem 4.23 indicates for Algorithm 2.18, we have

$$\|\mathbf{u} - \mathbf{u}_n\|_{[L^2(\Omega)]^2} \leq Ch^{\min\{\max\{2\alpha_0, 2(k-1)\}, \max\{\alpha_0+1, k\}, \frac{\beta_0}{\alpha_0} \max\{k-1, \alpha_0\}+2\}}. \quad (4.64)$$

By plugging (4.63) and (4.64) into (4.62), it follows the estimate (4.61). \square

Theorem 4.26. [68] Set the grading parameters $\kappa_{Q_i} = 2^{-\frac{\theta}{a_i}}$ with $0 < a_i < \alpha_0^i$ and θ given by

$$\theta = \max \left\{ k - 1, \frac{k + 1}{2}, a'_i \right\}, \quad (4.65)$$

where $a'_i = \min\{\alpha_0, a_i\} \leq \alpha_0$ for α_0 given by Equation (2.19). Let ϕ_n be the solution of finite element solution of Equation (2.74), and ϕ be the solution of the biharmonic problem (2.1).

If ϕ_n is the solution in Algorithm 2.18, then it follows

$$\|\phi - \phi_n\| \leq Ch^{\min\{k+1, \max\{\frac{\beta_0}{\alpha_0}(k-1)+2, \beta_0+2\}+1\}}. \quad (4.66)$$

Proof. Set $\psi = v_I \in V_n^k$ the nodal interpolation of v of the Poisson problem (3.42). Similar to Theorem 3.6, we have

$$\begin{aligned} \|\phi - \phi_n\|^2 &\leq \|\phi - \phi_n\|_{H^1(\Omega)} \|v - v_I\|_{H^1(\Omega)} + \|\mathbf{u} - \mathbf{u}_n\|_{[L^2(\Omega)]^2} \|v - v_I\|_{H^1(\Omega)} \\ &\quad + \|\mathbf{u} - \mathbf{u}_n\|_{[(\mathcal{K}_b^1(\Omega))^*]^2} \|\mathbf{curl} v\|_{[\mathcal{K}_b^1(\Omega)]^2} := T_1 + T_2 + T_3. \end{aligned} \quad (4.67)$$

Based on the results in [13], the solution $v \in \mathcal{K}_{\mathbf{b}'_{+1}}^2(\Omega)$ satisfies the regularity estimate

$$\|v\|_{\mathcal{K}_{\mathbf{b}'_{+1}}^2(\Omega)} \leq C \|\phi - \phi_n\|, \quad (4.68)$$

where the i th entry of \mathbf{b}' is given by $b'_i = \min\{b_i, 1\}$ with $b_i < \frac{\pi}{\omega_i}$. If $\omega > \pi$, we have

$$\theta' \geq \theta \geq \frac{k+1}{2} \geq 1,$$

so it follows the interpolation error

$$\|v - v_I\|_{H^1(\Omega)} \leq Ch^{\min\{\theta', 1\}} \|v\|_{K_{\mathbf{b}'_{+1}}^2(\Omega)} = Ch \|v\|_{K_{\mathbf{b}'_{+1}}^2(\Omega)}. \quad (4.69)$$

If $\omega < \pi$, the interpolation error (4.69) is obvious since $v \in H^2(\Omega)$.

For Algorithm 2.18, we have the following estimate for T_i . By Theorem 4.19 and Equation (4.69), it follows

$$T_1 \leq Ch^{\min\{k+1, \max\{\frac{\beta_0}{\alpha_0}(k-1)+2, \beta_0+2\}+1\}} \|v\|_{K_{\mathbf{b}'_{+1}}^2(\Omega)}.$$

By Theorem 4.23 and Equation (4.69), it follows

$$T_2 \leq Ch^{\min\{k+2, \max\{\frac{\beta_0}{\alpha_0}(k-1)+2, \beta_0+2\}+2\}} \|v\|_{K_{\mathbf{b}'_{+1}}^2(\Omega)}.$$

Again, it follows by Theorem 4.23,

$$T_3 \leq Ch^{\min\{k+1, \max\{\frac{\beta_0}{\alpha_0}(k-1)+2, \beta_0+2\}+1\}} \|v\|_{K_{\mathbf{b}'_{+1}}^2(\Omega)}.$$

Thus, the regularity estimate (4.68) and the summation of T_i , $i = 1, 2, 3$ again give the estimate (4.66). □

Remark 4.27. For the results in Theorems 4.19, 4.20, 4.25 and 4.26, we have the following facts.

- If $k = 1$ in (4.60), then $\theta = a_i$, $i = 1, \dots, N$ gives $\kappa_{Q_i} = \frac{1}{2}$, which indicates the mesh is

exactly the uniform mesh.

- With the given grading parameters, the finite element approximation ϕ_n from Algorithm 2.18 achieves the optimal convergence rates for $k = 1, 2, 3$ in both H^1 and L^2 norm. Moreover, the optimal convergence rates can be obtained for any $k \geq 1$ when $\omega > \pi$ by (2.23).
- With the given grading parameters, the finite element approximation ϕ_n from Algorithm 2.17 can achieve optimal convergence rate for any $k \geq 1$.
- Based on the regularity (4.41) for the involved Stokes problem in Algorithm 2.18, if we take the grading parameter $\kappa_{Q_i} = 2^{-\frac{\theta}{c_i}} \left(\leq 2^{-\frac{\theta}{a_i}} \right)$, then the corresponding error estimates (4.43), (4.51), (4.53) and (4.61) still hold.
- By (2.52) and $\phi \in H_0^2(\Omega)$, we have that

$$\|\phi\|_{H^2(\Omega)} \leq C \|\mathbf{u}\|_{[H^1(\Omega)]^2},$$

so $\|\mathbf{u} - \mathbf{u}_n\|_{[H^1(\Omega)]^2}$ is an estimate of the solution error to ϕ in H^2 norm.

CHAPTER 5 NUMERICAL ILLUSTRATIONS

In this section, we present numerical tests to validate our theoretical predictions for the proposed finite element algorithm solving the biharmonic problem (2.1). If an exact solution (or vector) v is unknown, we use the following numerical convergence rate

$$\mathcal{R} = \log_2 \frac{|v_j - v_{j-1}|_{[H^l(\Omega)]^{l'}}}{|v_{j+1} - v_j|_{[H^l(\Omega)]^{l'}}}, \quad (5.1)$$

$l = 0, 1$ as an indicator of the actual convergence rate [65]. Here v_j denotes the finite element solution on the mesh \mathcal{T}_j obtained after j refinements of the initial triangulation \mathcal{T}_0 . For scalar functions, we take $l' = 1$, otherwise, $l' = 2$. So if $v_j = w_j, \phi_j, p_j$, we take $l' = 1$; if $v_j = \mathbf{u}_j$, we take $l' = 2$.

In addition to the numerical tests in this section, we also provided some other tests in the published version of this research [68].

5.1 Numerical Results For Algorithm 2.17

5.1.1 A Comparison with a Reference Solution

In order to test the performance of Algorithm 2.17 for solving the biharmonic problem (2.1), we shall use the H^2 -conforming Argyris finite element approximation [6] as a reference solution ϕ_R , which is computed on exactly the same mesh as that for Algorithm 2.17. Since the solution of H^2 -conforming finite element method converges to the exact solution ϕ regardless of the convexity of the domain as the mesh is refined, so we can use ϕ_R as a good approximation of the exact solution ϕ . In this example, we mainly solve the biharmonic problem (2.1) in following two methods:

- **M1**: Poisson equation is solved using linear finite elements and the Stokes equation is solve using Mini finite elements.
- **M2**: Poisson equation is solved using quadratic finite elements and the Stokes equation is solve using Hood-Taylor finite elements.

Example 5.1. We consider the biharmonic problem (2.1) with $f = 1$ in the square domain Ω , we solve this problem using Algorithm 2.17 with the methods **M1** and **M2** on uniform meshes obtained by the midpoint refinements with initial meshes given in Figure 8(a). The Stokes problem (2.24) with source term $\mathbf{F} = (0, x)^T$ which satisfies (2.25) is solved in Algorithm 2.17.

Convex domain: We solve this problem in a square domain $\Omega = (-1, 1)^2$ with the initial mesh in Figure 8a. The errors in L^∞ norm between the finite element solution ϕ_j and the reference solution ϕ_R are given in Table 2 for both methods **M1** and **M2**. The finite element solution based on **M2** and its difference with the reference solution ϕ_R are shown in 8b and 8c, respectively. These results indicate that the solutions of Algorithm 2.17 converge to the exact solution. We further report the convergence rates in Table 3, from which we can find that optimal convergence rates are obtained for solutions based on both methods **M1** and **M2**. This result is consistent with our expectation in Theorem 3.5, and Theorem 3.6 for the biharmonic problem (2.1) in a convex domain.

Table 2: The L^∞ error $\|\phi_R - \phi_j\|_{L^\infty(\Omega)}$ in the square domain on quasi-uniform meshes.

	$j = 3$	$j = 4$	$j = 5$	$j = 6$	$j = 7$	$j = 8$
M1	0.00261	6.63931e-04	1.65096e-04	4.10355e-05	1.02225e-05	2.55318e-06
M2	6.66250e-05	9.10404e-06	1.17798e-06	1.49996e-07	1.89341e-08	2.37885e-09

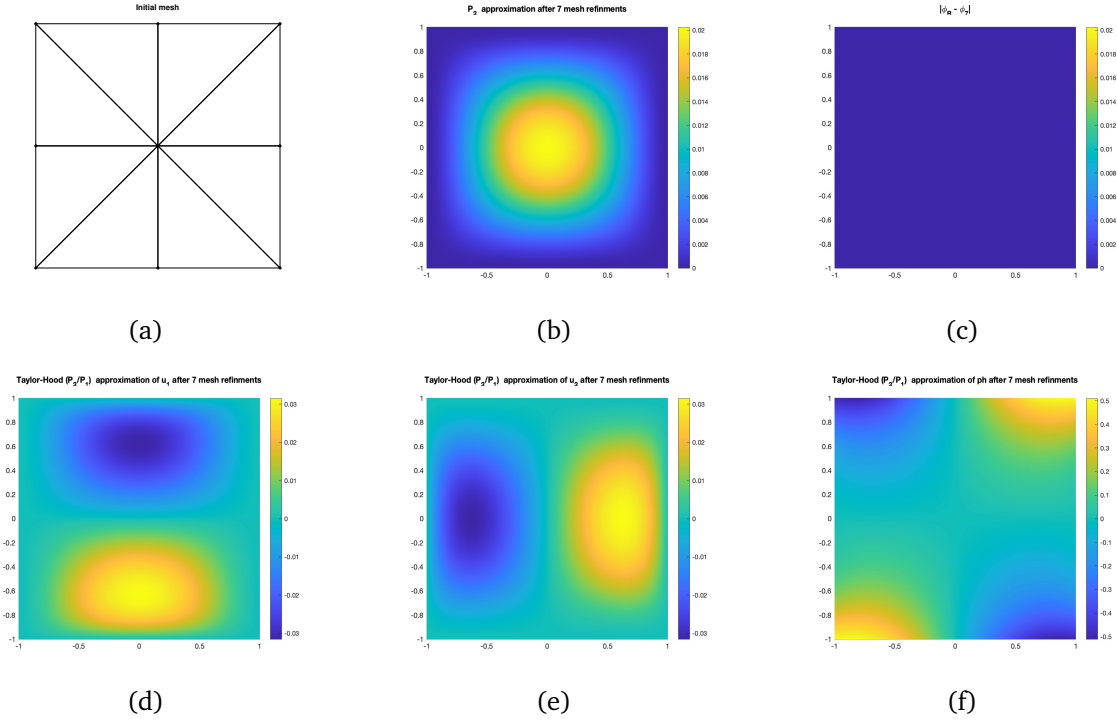


Figure 8: The Square domain: (a) the initial mesh; (b) the solution ϕ_7 ; (c) the difference $|\phi_R - \phi_7|$; (d) the Stokes solution u_1 ; (e) the Stokes solution u_2 ; (f) the pressure.

Table 3: Numerical convergence rates in the square domain with uniform meshes.

	M1		M2	
	H^1 rate of ϕ_j	L^2 rate of ϕ_j	H^1 rate of ϕ_j	L^2 rate of ϕ_j
$j = 4$	0.9763	1.9588	1.9751	2.9964
$j = 5$	0.9935	1.9889	1.9903	2.9960
$j = 6$	0.9935	1.9972	1.9959	2.9969
$j = 7$	0.9995	1.9993	1.9982	2.9981
$j = 8$	0.9995	1.9998	1.9991	2.9986

Non convex domain. We solve this problem in an L-shaped domain $\Omega = \Omega_0 \setminus \Omega_1$ with $\Omega_0 = (-1, 1)^2$ and $\Omega_1 = (0, 1) \times (-1, 0)$ and use the initial mesh in Figure 9a. The errors $\|\phi_R - \phi_j\|_{L^\infty(\Omega)}$ based on methods **M1** and **M2** are given in Table 4. The finite element solution based on **M2** and its difference with the reference solution are shown in 9b and

9c, respectively. These results indicate that the solutions of Algorithm 2.17 converge to the exact solution in a nonconvex domain.

Table 4: The L^∞ error $\|u_R - \phi_j^h\|_{L^\infty(\Omega)}$ in the L-shaped domain on quasi-uniform meshes.

	$j = 3$	$j = 4$	$j = 5$	$j = 6$	$j = 7$	$j = 8$
M1	6.85397e-04	1.91224e-04	4.36547e-05	1.00564e-05	3.16496e-06	5.81197e-07
M2	8.74987e-04	3.94122e-04	1.77980e-04	8.26205e-05	3.86434e-05	1.81330e-05

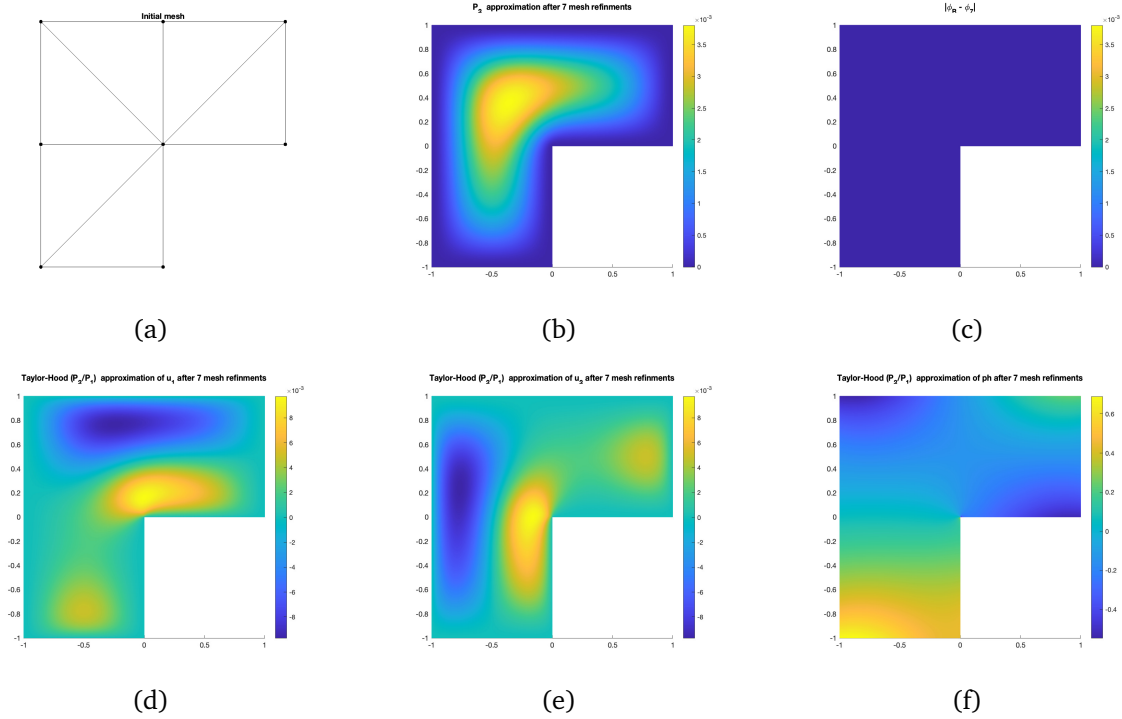


Figure 9: The L-shaped domain: (a) the initial mesh; (b) the solution ϕ_7 ; (c) the difference $|u_R - \phi_7|$; (d) the Stokes solution u_1 ; (e) the Stokes solution u_2 ; (f) the pressure.

5.1.2 Convergent Rates on Graded Meshes

Example 5.2. In this example we continue with the non convex domain in Example 5.1 on a sequence of graded meshes (including uniform mesh). To resolve the singularity due to re-entrant corner, we also use the graded mesh generated by iFEM [34]. The initial mesh and the graded mesh after 2 and 4 mesh refinements are shown in Figure 10a, Figure 10b,

and Figure 10c respectively. In Table 5, we show the numerical convergence rates of finite element approximations of the biharmonic problem for the methods **M1** and **M2**.

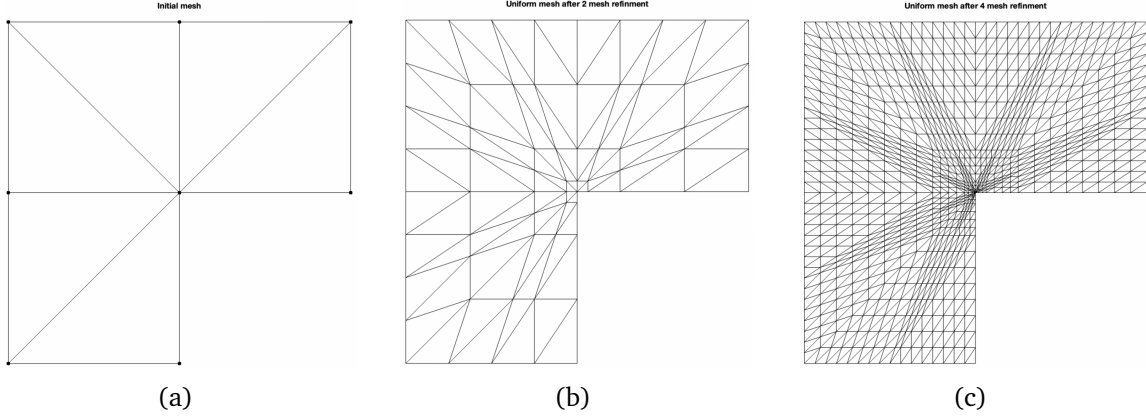


Figure 10: The L-shaped domain (Example 5.2): (a) the initial mesh; (b), (c) the graded mesh after two and four mesh refinements respectively with $\kappa = 0.2$.

We find on uniform meshes ($\kappa = 0.5$) that the H^1 convergence rate for the method **M1** is optimal with $\mathcal{R} = 1$, and that of the method **M2** is suboptimal with $\mathcal{R} \approx 1.1540$. Both of them are consistent the theoretical result in Theorem 3.5 in an L-shaped domain, that is $\mathcal{R} = \min\{k, \alpha + 1, 2\alpha\} \approx \min\{k, 1.54448, 1.0890\}$, where α is given in Table 1 with $\omega = \frac{3\pi}{2}$. We also find that the convergence rates for the method **M1** are optimal on graded meshes with $\kappa < 0.5$, and that of the method **M2** are optimal on graded meshes with $\kappa \leq 0.3$, which are consistent with the theoretical result in Theorem 4.19, namely, the optimal convergence rate can be obtained when $\kappa < 2^{-\frac{\alpha_0}{\alpha_0}} = 0.5$ for method **M1**, and $\kappa < 2^{-\frac{1}{\alpha_0}} \approx 0.28$ for the method **M2**.

The L^2 convergence rates of both methods **M1** and **M2** on uniform meshes are suboptimal with $\mathcal{R} \approx 1.0616$ and $\mathcal{R} \approx 1.0805$ respectively, which are consistent with the theoretical result in Theorem 3.6 with $\mathcal{R} = \min\{k+1, \alpha+2, 2\alpha\} \approx \min\{k+1, 2.54448, 1.0890\} = 1.0890$. On graded meshes, the convergence rates of the method **M1** are optimal with $\kappa \leq 0.3$, and

that of the method **M2** are optimal with $\kappa \leq 0.1$, which are consistent with the theoretical result in Theorem 4.20, namely, the optimal convergence rate can be obtained when $\kappa < 2^{-\frac{1}{\alpha_0}} \approx 0.28$ for the method **M1**, and $\kappa < 2^{-\frac{1.5}{\alpha_0}} \approx 0.15$ for the method **M2**.

Table 5: Convergence history of finite element approximation of the biharmonic problem in the L-shaped domain.

	κ	H_1 rate of ϕ_j						L_2 rate of ϕ_j					
		0.05	0.1	0.2	0.3	0.4	0.5	0.05	0.1	0.2	0.3	0.4	0.5
M1	$j = 4$	0.8324	0.8549	0.8902	0.9178	0.9430	0.9427	1.7882	1.8026	1.8387	1.8796	1.9381	1.8915
	$j = 5$	0.9530	0.9606	0.9707	0.9781	0.9854	0.9830	1.9369	1.9422	1.9541	1.9689	2.0061	1.6962
	$j = 6$	0.9871	0.9896	0.9925	0.9944	0.9963	0.9947	1.9840	1.9848	1.9876	1.9938	2.0123	1.3203
	$j = 7$	0.9965	0.9973	0.9981	0.9986	0.9991	0.9982	1.9963	1.9962	1.9966	1.9938	1.9670	1.1064
	$j = 8$	0.9990	0.9993	0.9995	0.9996	0.9998	0.9994	1.9991	1.9991	1.9990	2.0022	1.8482	1.0616
M2	$j = 4$	1.8894	1.9056	1.9282	1.9455	1.9280	1.7161	3.0413	3.0513	3.0289	2.5176	1.5439	1.2040
	$j = 5$	1.9578	1.9686	1.9777	1.9825	1.9281	1.5562	3.0551	3.0392	3.0111	2.1078	1.4309	1.1106
	$j = 6$	1.9822	1.9883	1.9923	1.9935	1.8868	1.3666	3.0485	3.0179	2.9904	1.9412	1.4273	1.0836
	$j = 7$	1.9920	1.9953	1.9972	1.9971	1.8108	1.2280	3.0321	3.0077	2.9753	1.9014	1.4324	1.0787
	$j = 8$	1.9963	1.9980	1.9989	1.9983	1.7107	1.1540	3.0155	3.0034	2.9554	1.8934	1.4360	1.0805

In Table 6, we display numerical convergence rates of the Taylor-Hood approximations for the involved Stokes problem in Algorithm 2.17. The H^1 convergence rates of \mathbf{u}_j and the L^2 convergence rates of p_j are suboptimal on uniform meshes with convergence rate $\mathcal{R} \approx 0.54$, which is consistent with the theoretical result $\mathcal{R} = \alpha \approx 0.5445$ in Lemma 3.4 in an L-shaped domain. On graded meshes, the convergence rates are optimal with $\mathcal{R} = k = 2$ for $\kappa \leq 0.05$, which is consistent with the result in Theorem 4.16 and Remark 4.18, namely, the optimal convergence rate can be achieved for $\kappa < 2^{-\frac{2}{\alpha_0}} \approx 0.08$ for $k = 2$.

The L^2 convergence rates of \mathbf{u}_n are suboptimal on uniform meshes with convergence rate $\mathcal{R} \approx 1.1854$, which is consistent with the theoretical result $\mathcal{R} = 2\alpha \approx 1.0890$ in Lemma 3.4 in an L-shaped domain. On graded meshes, the convergence rates are optimal with $\mathcal{R} = k+1 = 3$ for $\kappa \leq 0.1$, which is consistent with the results in Theorem 4.17 and Remark

4.18, namely, the optimal convergence rate can be achieved for $\kappa < 2^{-\frac{2}{\alpha_0}} \approx 0.08$ for $k = 2$.

Table 6: Convergence history of the Taylor-Hood element approximations of Stokes problem in the L-shaped domain.

		H_1 rate						L_2 rate						
		κ	0.05	0.1	0.2	0.3	0.4	0.5	0.05	0.1	0.2	0.3	0.4	0.5
\mathbf{u}_j	$j = 4$		1.7060	1.8267	1.6426	1.1491	0.8049	0.6227	2.8364	2.9669	2.9978	2.6388	1.8795	1.4997
	$j = 5$		1.7359	1.8263	1.4873	1.0041	0.7337	0.5628	2.8748	2.9766	2.9807	2.2905	1.6907	1.3982
	$j = 6$		1.8229	1.8343	1.3719	0.9601	0.7205	0.5474	2.9662	3.0000	2.9876	2.0379	1.5732	1.3152
	$j = 7$		1.9011	1.8371	1.3087	0.9490	0.7189	0.5437	3.0288	3.0113	2.9893	1.9344	1.5049	1.2426
	$j = 8$		1.9474	1.8337	1.2811	0.9465	0.7191	0.5432	3.0295	3.0078	2.9751	1.9035	1.4697	1.1854
p_j	$j = 4$								1.7582	1.8854	1.5888	1.0760	0.7652	0.6459
	$j = 5$								1.7120	1.8289	1.4151	0.9752	0.7205	0.5752
	$j = 6$								1.8104	1.8191	1.3259	0.9522	0.7165	0.5522
	$j = 7$								1.9122	1.8192	1.2876	0.9472	0.7177	0.5451
	$j = 8$								1.9685	1.8181	1.2728	0.9461	0.7188	0.5434

5.1.3 Re-entrant Corners on the Domain Other Than $3\pi/2$

Example 5.3. In this example we report the numerical convergence rates on a sequence of graded meshes including quasi-uniform meshes for different re-entrant corners. We particularly use a domain with one re-entrant corner $7\pi/4$ and a domain with two re-entrant corners $4\pi/3$. As in example 5.1, we consider the biharmonic problem (2.1) with $f = 1$. We solve this problem using Algorithm 2.17 with the methods **M1** and **M2**. The Stokes problem (2.24) with source term $\mathbf{F} = (0, x)^T$ which satisfies (2.25) is used in Algorithm 2.17.

One Re-entrant Corner. The re-entrant corner of the domain under consideration is $7\pi/4$ as shown in the Figure 11a. Table 7 we show the numerical convergence rates of finite element approximations of the biharmonic problem for the methods **M1** and **M2**.

In Table 8 we show the numerical convergence rates of finite element approximations of

the Stokes equation using Hood-Taylor elements.

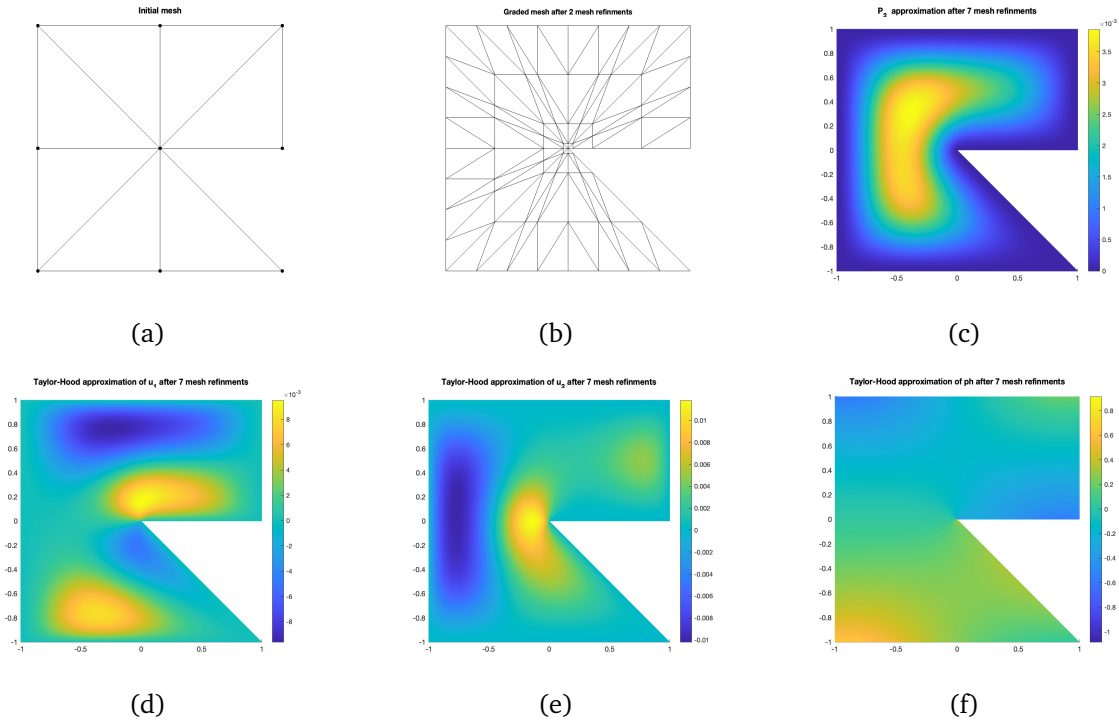


Figure 11: The domain with re-entrant corner $7\pi/4$: (a) the initial mesh; (b) the mesh after two refinements; (c) the solution ϕ_7 ; (d) the Stokes solution u_1 ; (e) the Stokes solution u_2 ; (f) the pressure .

Table 7: Convergence history of finite element approximation of the biharmonic problem on a domain with re-entrant corner $7\pi/4$.

	κ	H_1 rate						L_2 rate					
		0.05	0.1	0.2	0.3	0.4	0.5	0.05	0.1	0.2	0.3	0.4	0.5
M1	$j = 4$	0.3191	0.4464	0.6193	0.7277	0.7970	0.8304	1.3128	1.3746	1.5045	1.6253	1.7494	1.7402
	$j = 5$	0.8357	0.8586	0.8947	0.9232	0.9495	0.9494	1.8048	1.8120	1.8419	1.8946	1.9239	1.4110
	$j = 6$	0.9540	0.9617	0.9720	0.9796	0.9876	0.9840	1.9455	1.9464	1.9539	1.9823	1.8609	1.0593
	$j = 7$	0.9872	0.9898	0.9928	0.9948	0.9972	0.9945	1.9875	1.9863	1.9863	2.0074	1.6286	0.9668
	$j = 8$	0.9964	0.9973	0.9982	0.9987	0.9995	0.9979	1.9976	1.9967	1.9951	2.0145	1.4064	0.9705
M2	$j = 4$	1.8921	1.9088	1.9324	1.9426	1.7996	1.4043	3.0187	3.0426	2.8991	1.8391	1.3548	1.1034
	$j = 5$	1.9559	1.9684	1.9785	1.9719	1.6927	1.2181	3.0371	3.0318	2.7710	1.7516	1.3269	1.0426
	$j = 6$	1.9800	1.9876	1.9924	1.9774	1.5557	1.1009	3.0580	3.0167	2.6238	1.7473	1.3243	1.0144
	$j = 7$	1.9905	1.9949	1.9972	1.9747	1.4475	1.0467	3.0578	3.0098	2.5003	1.7506	1.3269	1.0046
	$j = 8$	1.9955	1.9978	1.9989	1.9679	1.3855	1.0244	3.0370	3.0062	2.4204	1.7527	1.3299	1.0027

We find on uniform meshes ($\kappa = 0.5$) that the H^1 convergence rate for the method **M1** is optimal with $\mathcal{R} = 1$, and that of the method **M2** is suboptimal with $\mathcal{R} \approx 1.0244$. Both of them are consistent the theoretical result in Theorem 3.5 in a domain with re-entrant corner $7\pi/4$, that is $\mathcal{R} = \min\{k, \alpha + 1, 2\alpha\} \approx \min\{k, 1.50501, 1.01002\}$, where α is given in Table 1 with $\omega = \frac{7\pi}{4}$. We also find that the convergence rates for the method **M1** are optimal on graded meshes with $\kappa < 0.5$, and that of the method **M2** are optimal on graded meshes with $\kappa \leq 0.3$, which are consistent with the theoretical result in Theorem 4.19, namely, the optimal convergence rate can be obtained when $\kappa < 2^{-\frac{\alpha_0}{\alpha_0}} = 0.5$ for method **M1**, and $\kappa < 2^{-\frac{1}{\alpha_0}} \approx 0.25$ for the method **M2**.

The L^2 convergence rates of both methods **M1** and **M2** on uniform meshes are suboptimal with $\mathcal{R} \approx 0.9705$ and $\mathcal{R} \approx 1.0027$ respectively, which are consistent with the theoretical result in Theorem 3.6 with $\mathcal{R} = \min\{k+1, \alpha+2, 2\alpha\} \approx \min\{k+1, 2.5050, 1.0100\} = 1.0100$. On graded meshes, the convergence rates of the method **M1** are optimal with $\kappa \leq 0.3$, and that of the method **M2** are optimal with $\kappa \leq 0.1$, which are consistent with the theoretical result in Theorem 4.20, namely, the optimal convergence rate can be obtained when $\kappa < 2^{-\frac{1}{\alpha_0}} \approx 0.25$ for the method **M1**, and $\kappa < 2^{-\frac{1.5}{\alpha_0}} \approx 0.13$ for the method **M2**.

Table 8: Numerical convergence rates of the Stokes equation with Taylor-Hood elements on a domain with two re-entrant corner $7\pi/4$.

		H_1 rate						L_2 rate					
κ		0.05	0.1	0.2	0.3	0.4	0.5	0.05	0.1	0.2	0.3	0.4	0.5
\mathbf{u}_n	$j = 4$	1.6837	1.7993	1.5243	1.0391	0.7479	0.5960	2.7828	2.9510	2.9322	2.0926	1.6303	1.3675
	$j = 5$	1.6883	1.7672	1.3388	0.9136	0.6800	0.5330	2.8360	2.9691	2.8400	1.8554	1.4783	1.2505
	$j = 6$	1.7704	1.7494	1.2364	0.8831	0.6665	0.5120	2.9519	3.0047	2.7247	1.7802	1.3977	1.1587
	$j = 7$	1.8522	1.7322	1.1942	0.8774	0.6649	0.5049	3.0342	3.0177	2.5840	1.7607	1.3604	1.0943
	$j = 8$	1.9051	1.7159	1.1795	0.8767	0.6655	0.5030	3.0420	3.0121	2.4681	1.7559	1.3449	1.0547
p_n	$j = 4$							1.8815	1.9110	1.6329	1.2072	0.9351	0.8371
	$j = 5$							1.6409	1.7726	1.3757	0.9548	0.7323	0.6449
	$j = 6$							1.6169	1.7056	1.2440	0.8902	0.6799	0.5618
	$j = 7$							1.7372	1.6897	1.1958	0.8784	0.6681	0.5265
	$j = 8$							1.8468	1.6860	1.1800	0.8768	0.6660	0.5119

In Table 8, we display numerical convergence rates of the Taylor-Hood approximations for the involved Stokes problem in Algorithm 2.17. The H^1 convergence rates of \mathbf{u}_j and the L^2 convergence rates of p_j are suboptimal on uniform meshes with convergence rate $\mathcal{R} \approx 0.50$, which is consistent with the theoretical result $\mathcal{R} = \alpha \approx 0.5050$ in Lemma 3.4 in a domain with re-entrant corner $7\pi/4$. On graded meshes, the convergence rates are optimal with $\mathcal{R} = k = 2$ for $\kappa \leq 0.05$, which is consistent with the result in Theorem 4.16 and Remark 4.18, namely, the optimal convergence rate can be achieved for $\kappa < 2^{-\frac{2}{\alpha_0}} \approx 0.06$ for $k = 2$.

The L^2 convergence rates of \mathbf{u}_n are suboptimal on uniform meshes with convergence rate $\mathcal{R} \approx 1.0547$, which is consistent with the theoretical result $\mathcal{R} = 2\alpha \approx 1.0100$ in Lemma 3.4 in a domain with re-entrant corner $7\pi/4$. On graded meshes, the convergence rates are optimal with $\mathcal{R} = k + 1 = 3$ for $\kappa \leq 0.05$, which is consistent with the results in Theorem 4.17 and Remark 4.18, namely, the optimal convergence rate can be achieved for

$$\kappa < 2^{-\frac{2}{\alpha_0}} \approx 0.06 \text{ for } k = 2.$$

Two Re-entrant Corners. The re-entrant corners of the domain under consideration is $4\pi/3$ as shown in the Figure 12a. In table 9 we show the numerical convergence rates of finite element approximations of the biharmonic problem for the methods methods **M1** and **M2**. In Table 8 we show the numerical convergence rates of finite element approximations of the Stokes equation using Hood-Taylor elements.

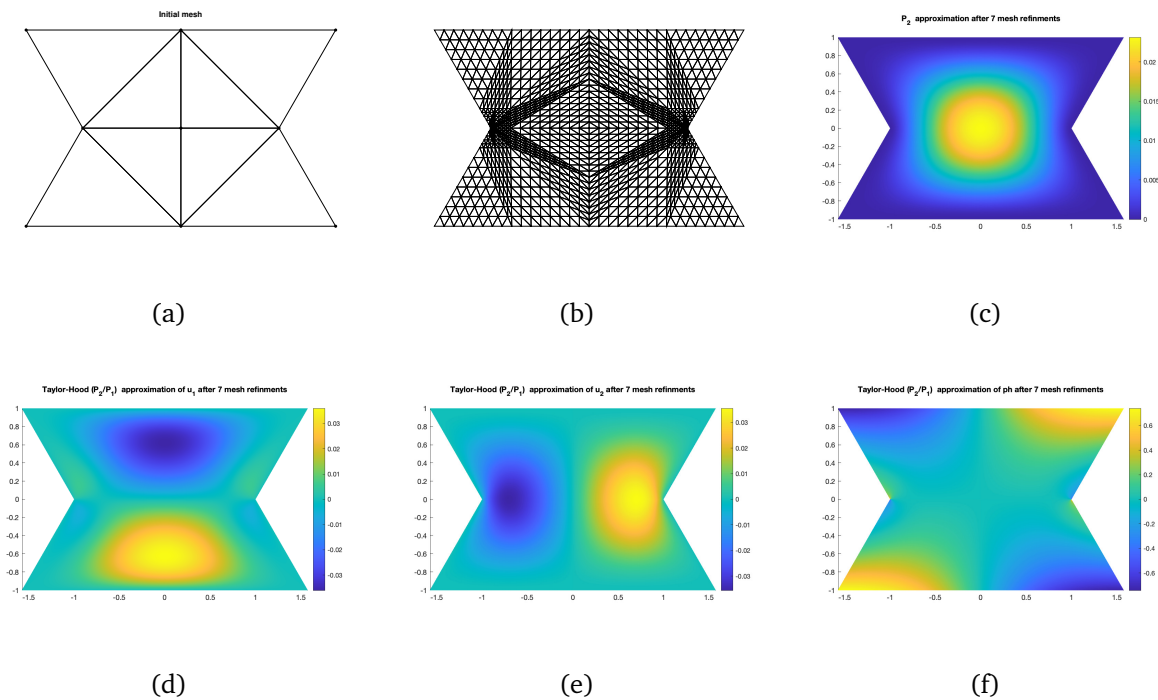


Figure 12: Domain with two re-entrant corner $4\pi/3$: (a) the initial mesh; (b) the mesh after four refinements; (c) the solution ϕ_7 (d) the Stokes solution u_1 ; (e) the Stokes solution u_2 ; (f) the pressure.

Table 9: Convergence history of finite element approximation of the biharmonic problem in the domain with two re-entrant corners $4\pi/3$.

	κ	H_1 rate of ϕ_j						L_2 rate of ϕ_j					
		0.05	0.1	0.2	0.3	0.4	0.5	0.05	0.1	0.2	0.3	0.4	0.5
M1	$j = 5$	0.5920	0.6429	0.7369	0.8194	0.8866	0.8695	1.5687	1.5706	1.6304	1.7213	1.8391	1.8665
	$j = 6$	0.8680	0.8871	0.9190	0.9450	0.9688	0.9615	1.8266	1.8404	1.8769	1.9133	1.9661	2.0075
	$j = 7$	0.9609	0.9675	0.9775	0.9850	0.9914	0.9883	1.9488	1.9528	1.9652	1.9752	2.0086	2.0416
	$j = 8$	0.9891	0.9912	0.9941	0.9961	0.9977	0.9962	1.9875	1.9876	1.9909	1.9926	2.0247	1.9282
	$j = 9$	0.9971	0.9977	0.9985	0.9990	0.9994	0.9987	1.9972	1.9969	1.9978	1.9972	2.0336	1.5764
M2	$j = 5$	1.8100	1.8276	1.8620	1.8948	1.9149	1.7926	3.0626	3.0691	3.0245	2.9415	2.1881	1.6630
	$j = 6$	1.9249	1.9412	1.9560	1.9654	1.9606	1.7814	3.0429	3.0607	3.0239	2.7869	1.7272	1.3274
	$j = 7$	1.9675	1.9779	1.9842	1.9872	1.9735	1.7195	3.0574	3.0361	3.0086	2.5517	1.6344	1.2511
	$j = 8$	1.9858	1.9910	1.9937	1.9948	1.9752	1.6396	3.0680	3.0193	3.0024	2.3341	1.6248	1.2321
	$j = 9$	1.9936	1.9960	1.9973	1.9977	1.9709	1.5562	3.0438	3.0087	3.0002	2.2117	1.6256	1.2278

We find on uniform meshes ($\kappa = 0.5$) that the H^1 convergence rate for the method **M1** is optimal with $\mathcal{R} = 1$, and that of the method **M2** is suboptimal with $\mathcal{R} \approx 1.5562$ which is little bit higher than the expected. We can reach to the expected convergent rate of the method **M2** by doing at least two more mesh refinements. However, doing more than 9 mesh refinements for two re-entrant corners by using quadratic finite elements consumes more memory space in a computer and thus unable to perform this action in a MacBook Air (2020) with 8GB memory. Both of above results are consistent the theoretical result in Theorem 3.5 in a domain with re-entrant corner $4\pi/3$, that is $\mathcal{R} = \min\{k, \alpha + 1, 2\alpha\} \approx \min\{k, 1.6157, 1.2315\}$, where α is given in Table 1 for $\omega = \frac{4\pi}{3}$. We also find that the convergence rates for the method **M1** are optimal on graded meshes with $\kappa < 0.5$, and that of the method **M2** are optimal on graded meshes with $\kappa \leq 0.3$, which are consistent with the theoretical result in Theorem 4.19, namely, the optimal convergence rate can be obtained when $\kappa < 2^{-\frac{\alpha_0}{\alpha_0}} = 0.5$ for method **M1**, and $\kappa < 2^{-\frac{1}{\alpha_0}} \approx 0.32$ for the method **M2**.

The L^2 convergence rate $\mathcal{R} \approx 1.5764$, after 9 mesh refinements, of the method **M1** on a uniform mesh which is higher than expected due to the same reason mentioned above. Thus more mesh refinements are needed to achieve the expected convergent rate. The L^2 convergence rates of the method **M2** on uniform meshes is suboptimal with $\mathcal{R} \approx 1.2278$ which is consistent with the theoretical result in Theorem 3.6 with $\mathcal{R} = \min\{k + 1, \alpha + 2, 2\alpha\} \approx \min\{k + 1, 2.6157, 1.2315\} = 1.2315$. On graded meshes, the convergence rates of the method **M1** are optimal with $\kappa \leq 0.4$, and that of the method **M2** are optimal with $\kappa \leq 0.2$, which are consistent with the theoretical result in Theorem 4.20, namely, the optimal convergence rate can be obtained when $\kappa < 2^{-\frac{1}{\alpha_0}} \approx 0.32$ for the method **M1**, and $\kappa < 2^{-\frac{1.5}{\alpha_0}} \approx 0.18$ for the method **M2**.

Table 10: Numerical convergence rates of the Stokes equation with Taylor-Hood elements on a domain with re-entrant corner $4\pi/3$.

		H_1 rate						L_2 rate						
		κ	0.05	0.1	0.2	0.3	0.4	0.5	0.05	0.1	0.2	0.3	0.4	0.5
\mathbf{u}_n	$j = 5$		1.9005	1.9629	1.9302	1.6723	1.2685	0.9488	2.8300	2.9720	3.0377	2.9510	2.2666	1.7101
	$j = 6$		1.8047	1.9341	1.8307	1.3633	0.9404	0.7049	2.7989	3.0099	3.0810	2.9030	2.0833	1.6073
	$j = 7$		1.8000	1.9201	1.6991	1.1692	0.8393	0.6370	2.8519	3.0277	3.0573	2.7393	1.9614	1.5509
	$j = 8$		1.8848	1.9256	1.5860	1.0981	0.8183	0.6211	2.9701	3.0352	3.0342	2.5295	1.8614	1.5034
	$j = 9$		1.9558	1.9350	1.5109	1.0773	0.8145	0.6171	3.0250	3.0237	3.0187	2.3414	1.7765	1.4532
p_n	$j = 5$								1.8958	1.9829	1.8716	2.0212	1.1019	0.8510
	$j = 6$								1.6962	1.8863	1.7041	1.4738	0.8800	0.6919
	$j = 7$								1.7238	1.8772	1.5774	1.2053	0.8253	0.6400
	$j = 8$								1.8861	1.9057	1.5028	1.1068	0.8152	0.6232
	$j = 9$								1.9968	1.9280	1.4642	1.0794	0.8138	0.6178

In Table 10, we display numerical convergence rates of the Taylor-Hood approximations for the involved Stokes problem in Algorithm 2.17. The H^1 convergence rates of \mathbf{u}_j and the L^2 convergence rates of p_j are suboptimal on uniform meshes with convergence rate $\mathcal{R} \approx 0.61$, which is consistent with the theoretical result $\mathcal{R} = \alpha \approx 0.6157$ in Lemma

3.4 in a domain with two re-entrant corner $4\pi/3$. On graded meshes, the convergence rates are optimal with $\mathcal{R} = k = 2$ for $\kappa \leq 0.1$, which is consistent with the result in Theorem 4.16 and Remark 4.18, namely, the optimal convergence rate can be achieved for $\kappa < 2^{-\frac{2}{\alpha_0}} \approx 0.11$ for $k = 2$.

The L^2 convergence rate $\mathcal{R} \approx 1.4532$, after 9 mesh refinements, of the method **M1** on uniform meshes which is higher than expected due to the same reason mentioned above. Thus, with more mesh refinements the expected rate, which $\mathcal{R} = 2\alpha = 1.2315$, can be achieved. On graded meshes, the convergence rates are optimal with $\mathcal{R} = k + 1 = 3$ for $\kappa \leq 0.2$, which is consistent with the results in Theorem 4.17 and Remark 4.18, namely, the optimal convergence rate can be achieved for $\kappa < 2^{-\frac{1.5}{\alpha_0}} \approx 1.18$ for $k = 2$.

5.1.4 Different Source Terms \mathbf{F} for the Stokes Problem

Example 5.4. This example is presented to highlight the fact that the source term of the Stokes equation in Algorithm 2.17 is not unique. In this example we continue with the non convex domain in Example 5.1 on a quasi uniform meshes with different source terms \mathbf{F} for the involved Stokes problem in Algorithm 2.17. More specifically, we consider both $\mathbf{F} = \mathbf{F}_1 = (-1/2y, 1/2x)^T$ and $\mathbf{F} = \mathbf{F}_2 = (-y, 0)^T$, and they both satisfy (2.25), namely, $\text{curl } \mathbf{F}_1 = \text{curl } \mathbf{F}_2 = f = 1$. We show the convergence rates of the finite element approximations ϕ_j of the biharmonic problem obtained from method **M2** in Table 11, from which we can find that both H^1 and L^2 convergence rates of the numerical solutions are the same that obtained in Example 5.2 on uniform meshes. Moreover, we take the solution obtained in Example 5.2 on uniform meshes as a reference solution, and compare their differences with the solutions obtain based on \mathbf{F}_l , $l = 1, 2$, the H^1 and L^2 errors as well as the convergence rates are reported in Table 12, from which we find that the errors are small

and decay fast (convergence rates are larger than the solution convergence rates), thus the errors are neglectable compared with the those of the finite element approximations with the exact solution. All these results indicate that the finite element approximations \mathbf{u}_j and ϕ_j are independent of the choice of the source term \mathbf{F} as long as it satisfies (2.25), which is consistent with the theoretical results in Lemma 2.8 and Lemma 2.16.

Table 11: Convergence history of the biharmonic approximations ϕ_j in the L-shaped domain.

\mathbf{F}		H_1 rate	L_2 rate	\mathbf{F}		H_1 rate	L_2 rate
\mathbf{F}_1	j=4	1.6642	1.2053	\mathbf{F}_2	j=4	1.6642	1.2053
	j=5	1.5234	1.1107		j=5	1.5234	1.1107
	j=6	1.3510	1.0836		j=6	1.3510	1.0836
	j=7	1.2213	1.0787		j=7	1.2213	1.0787
	j=8	1.1509	1.0805		j=8	1.1509	1.0805

Table 12: Errors with the reference solution and convergence rates in the L-shaped domain.

\mathbf{F}		H_1 error	H_1 rate	L_2 error	L_2 rate	\mathbf{F}		H_1 error	H_1 rate	L_2 error	L_2 rate
\mathbf{F}_1	j=3	7.5946e-07	--	6.8863e-08	--	\mathbf{F}_2	j=3	1.5189e-06	--	1.3773e-07	--
	j=4	5.2615e-08	3.8514	3.4838e-09	4.3050		j=4	1.0523e-07	3.8514	6.9675e-09	4.3050
	j=5	3.7524e-09	3.8096	1.8641e-10	4.2241		j=5	7.5048e-09	3.8096	3.7282e-10	4.2241
	j=6	2.7967e-10	3.7460	1.0549e-11	4.1433		j=6	5.5934e-10	3.7460	2.1098e-11	4.1433
	j=7	2.1857e-11	3.6776	6.2232e-13	4.0833		j=7	4.3714e-11	3.6776	1.2446e-12	4.0833
	j=8	1.7829e-12	3.6157	3.7714e-14	4.0445		j=8	3.5659e-12	3.6157	7.5428e-14	4.0445
	j=9	1.5023e-13	3.5690	2.3836e-15	3.9839		j=9	3.0041e-13	3.5693	4.7259e-15	3.9964

5.1.5 A Complex Source Term in the Biharmonic Problem

Example 5.5. This example is presented as an additional example to example 5.1 to show the accuracy of our algorithm with a complex source term other than $f = 1$.

Test case 1. First, we set the source term of the bi-harmonic equation $f = \frac{x}{2}(x^2 + y^2)^{-3/4} +$

$\cos(\pi x) + 1$ as our complex source term. Then we solve this problem using Algorithm 2.17 and using the Argyris finite element method by setting the source term of the Stokes problem $\mathbf{F} = (0, (x^2 + y^2)^{1/4} + \frac{\sin(\pi x)}{\pi} + x)$. Alternatively, we can set \mathbf{F} in several other ways since it is not unique. For examples $\mathbf{F} = (-(y\cos(\pi x) + y), (x^2 + y^2)^{1/4})$ and $\mathbf{F} = (-\frac{y\cos(\pi x)+y}{2}, (x^2 + y^2)^{1/4} + \frac{\sin(\pi x)}{2\pi} + \frac{x}{2})$ are two other possibilities for the choice of f above. In table 13 and table 14 we report the error $\|u_R - \phi_j^h\|_{L^\infty(\Omega)}$ for uniformly refined square and L shaped domains used in example 5.1 respectively, where ϕ_j^h, u_R are the numerical solutions to biharmonic equation in Algorithm 2.17 and the Argyris finite element solution respectively. In table 15 we record the H_1 and L_2 convergent rates on a sequence of graded meshes including quasi-uniform meshes for L shaped domain.

Table 13: The L^∞ error $\|u_R - \phi_j^h\|_{L^\infty(\Omega)}$ in the square domain on quasi-uniform meshes for $f = \frac{x}{2}(x^2 + y^2)^{-3/4} + \cos(\pi x) + 1$.

	$j = 3$	$j = 4$	$j = 5$	$j = 6$	$j = 7$	$j = 8$
M1	2.84053e-04	1.05492e-04	3.47262e-05	1.07467e-05	3.19748e-06	8.74116e-07
M2	1.49839e-05	1.97924e-06	2.54877e-07	3.23668e-08	4.67500e-09	5.48447e-08

Table 14: The L^∞ error $\|u_R - \phi_j^h\|_{L^\infty(\Omega)}$ in the L-shaped domain on quasi-uniform meshes for $f = \frac{x}{2}(x^2 + y^2)^{-3/4} + \cos(\pi x) + 1$.

	$j = 3$	$j = 4$	$j = 5$	$j = 6$	$j = 7$	$j = 8$
M1	4.15461e-04	1.90923e-04	8.84911e-05	4.12234e-05	1.92680e-05	9.02750e-06
M2	4.19756e-04	1.87990e-04	8.71583e-05	4.07645e-05	1.91318e-05	8.98925e-06

Table 15: Convergence history of finite element approximation of the biharmonic problem in the L-shaped domain for $f = \frac{x}{2}(x^2 + y^2)^{-3/4} + \cos(\pi x) + 1$.

		H_1 rate						L_2 rate					
κ		0.05	0.1	0.2	0.3	0.4	0.5	0.05	0.1	0.2	0.3	0.4	0.5
M1	$j = 4$	0.8353	0.8570	0.8925	0.9200	0.9439	0.9412	1.7815	1.7962	1.8354	1.8784	1.9328	1.8863
	$j = 5$	0.9535	0.9608	0.9709	0.9784	0.9854	0.9828	1.9345	1.9405	1.9533	1.9683	1.9998	1.7293
	$j = 6$	0.9872	0.9896	0.9925	0.9944	0.9963	0.9947	1.9832	1.9844	1.9875	1.9934	2.0053	1.3718
	$j = 7$	0.9965	0.9973	0.9981	0.9986	0.9991	0.9983	1.9960	1.9961	1.9966	2.0000	1.9631	1.1331
	$j = 8$	0.9991	0.9993	0.9995	0.9996	0.9998	0.9994	1.9991	1.9991	1.9990	2.0018	1.8554	1.0704
M2	$j = 4$	1.8927	1.9086	1.9283	1.9431	1.9271	1.7471	3.0675	3.0763	3.0498	2.5354	1.5559	1.2652
	$j = 5$	1.9567	1.9677	1.9765	1.9811	1.9310	1.5924	3.0643	3.0488	3.0184	2.1087	1.4276	1.1207
	$j = 6$	1.9817	1.9878	1.9919	1.9930	1.8934	1.3917	3.0500	3.0206	2.9923	1.9402	1.4245	1.0819
	$j = 7$	1.9918	1.9951	1.9970	1.9969	1.8208	1.2387	3.0319	3.0085	2.9760	1.9010	1.4311	1.0759
	$j = 8$	1.9962	1.9979	1.9988	1.9982	1.7221	1.1570	3.0152	3.0036	2.9560	1.8933	1.4355	1.0785

Table 16: Numerical convergence rates of the Stokes equation with Taylor-Hood elements on the L-shaped domain for $f = \frac{x}{2}(x^2 + y^2)^{-3/4} + \cos(\pi x) + 1$.

		H_1 rate						L_2 rate					
κ		0.05	0.1	0.2	0.3	0.4	0.5	0.05	0.1	0.2	0.3	0.4	0.5
\mathbf{u}_n	$j = 4$	1.7701	1.8725	1.7365	1.2460	0.8497	0.6600	2.8350	2.9471	2.9853	2.6823	1.8998	1.5330
	$j = 5$	1.7936	1.8790	1.5775	1.0418	0.7449	0.5700	2.8959	2.9928	3.0044	2.3337	1.6918	1.4039
	$j = 6$	1.8573	1.8788	1.4269	0.9715	0.7248	0.5506	2.9808	3.0158	3.0053	2.0524	1.5715	1.3143
	$j = 7$	1.9176	1.8718	1.3345	0.9529	0.7216	0.5464	3.0303	3.0141	2.9944	1.9377	1.5038	1.2407
	$j = 8$	1.9554	1.8628	1.2919	0.9482	0.7211	0.5457	3.0277	3.0070	2.9789	1.9042	1.4691	1.1839
p_n	$j = 4$							1.8457	1.9408	1.7019	1.1603	0.8042	0.6929
	$j = 5$							1.7941	1.8941	1.4993	0.9995	0.7248	0.5820
	$j = 6$							1.8526	1.8725	1.3678	0.9581	0.7163	0.5515
	$j = 7$							1.9290	1.8608	1.3048	0.9487	0.7174	0.5438
	$j = 8$							1.9744	1.8515	1.2793	0.9465	0.7187	0.5425

Tables 13, 14, 15, and 16 follow the same conclusions as in the example 5.1. Thus we show that our method works for complex source terms.

5.2 Numerical Tests for Algorithm 2.18

In this section we present numerical simulations for Algorithm 2.18 to validate our theoretical findings. Recall that $\mathcal{R} = \log_2 \frac{|v_j - v_{j-1}|_{[H^1(\Omega)]^{l' }}}{|v_{j+1} - v_j|_{[H^1(\Omega)]^{l' }}}}$. In this section we do not present solution plots as they look similar to the solution plots in sub section 5.1. We also do not present mesh plots in this sub section since we use the same domains to solve the problems using Algorithm 2.18 as a comparison to Algorithm 2.17. Instead we present table values to validate our theoretical findings.

Since the convergence rate of the finite element approximation w_j of the Poisson equation in Algorithm 2.18 has been well investigated in many papers (see e.g., [70, 67]), so we will not report the convergence rates of w_j in the following numerical tests.

5.2.1 A Comparison with a Reference Solution

In this example, we mainly solve the biharmonic problem (2.1) in following two methods:

- **M1**: Both Poisson equations are solved using linear finite elements and the Stokes equation is solve using Mini finite elements.
- **M2**: Both Poisson equations are solved using quadratic finite elements and the Stokes equation is solve using Hood-Taylor finite elements.

Example 5.6. We consider the biharmonic problem (2.1) with $f = 1$ in the square domain Ω , we solve this problem using Algorithm 2.18 with the methods **M1** and **M2** on uniform meshes obtained by the midpoint refinements with initial meshes given in Figure 8(a).

Convex Domain. We solve this problem in a square domain $\Omega = (-1, 1)^2$ with the initial mesh in Figure 8a. The errors in L^∞ norm between the finite element solution ϕ_j and the

reference solution ϕ_R are given in Table 17. These results indicate that the solutions of Algorithm 2.18 converge to the exact solution in a convex domain.

Table 17: The L^∞ error $\|\phi_R - \phi_j\|_{L^\infty(\Omega)}$ in the square domain on quasi-uniform meshes.

	$j = 3$	$j = 4$	$j = 5$	$j = 6$	$j = 7$	$j = 8$
M1	0.0021	5.4337e-04	1.3555e-04	3.3704e-05	8.3951e-06	2.0946e-06
M2	6.6907e-05	9.1130e-06	1.1783e-06	1.5000e-07	1.8934e-08	2.3789e-09

Non Convex Domain. We solve this problem in an L-shaped domain $\Omega = \Omega_0 \setminus \Omega_1$ with $\Omega_0 = (-1, 1)^2$ and $\Omega_1 = (0, 1) \times (-1, 0)$ and use the initial mesh in Figure 9a. The errors $\|\phi_R - \phi_j\|_{L^\infty(\Omega)}$ based on methods **M1** and **M2** are given in Table 18. These results indicate that the solutions of Algorithm 2.18 converge to the exact solution in a nonconvex domain.

Table 18: The L^∞ error $\|u_R - \phi_j^h\|_{L^\infty(\Omega)}$ in the L-shaped domain on quasi-uniform meshes.

	$j = 3$	$j = 4$	$j = 5$	$j = 6$	$j = 7$	$j = 8$
M1	6.0562e-04	2.9050e-04	1.5251e-04	7.6796e-05	3.8681e-05	1.8817e-05
M2	0.0017	7.6795e-04	3.2917e-04	1.5283e-04	7.1483e-05	3.3533e-05

5.2.2 Convergent Rates on Graded Meshes

Example 5.7. In this example we follow the Example 5.2 similarly for the Algorithm 2.18. we continue with the non convex domain in Example 5.1 on a sequence of graded meshes (including uniform mesh). The initial mesh and the graded mesh after 2 and 4 mesh refinements are shown in Figure 10a, Figure 10b, and Figure 10c respectively. In Table 19, we show the numerical convergence rates of finite element approximations of the biharmonic problem for the methods methods **M1** and **M2**.

We find on uniform meshes ($\kappa = 0.5$) that the H^1 convergence rate for the method **M1** is optimal with $\mathcal{R} = 1$, and that of the method **M2** is suboptimal with $\mathcal{R} \approx 1.1463$. Both of them are consistent the theoretical result in Theorem 3.12 in an L-shaped domain, that is $\mathcal{R} = \min\{k, \beta + 2, \alpha + 1, 2\alpha\} \approx \min\{k, 2.6667, 1.54448, 1.0890\}$, where α is given in Table 1 with $\omega = \frac{3\pi}{2}$ and $\beta = \frac{\pi}{\omega}$. We also find that the convergence rates for the method **M1** are optimal on graded meshes with $\kappa < 0.5$, and that of the method **M2** are optimal on graded meshes with $\kappa \leq 0.3$, which are consistent with the theoretical result in Theorem 4.25, namely, the optimal convergence rate can be obtained when $\kappa < 2^{-\frac{\alpha_0}{\alpha_0}} = 0.5$ for method **M1**, and $\kappa < 2^{-\frac{1}{\alpha_0}} \approx 0.28$ for the method **M2**.

Table 19: Convergence history of finite element approximation of the biharmonic problem in the L-shaped domain.

	κ	H_1 rate of ϕ_j					L_2 rate of ϕ_j				
		0.1	0.2	0.3	0.4	0.5	0.1	0.2	0.3	0.4	0.5
M1	$j = 4$	0.9503	0.9601	0.9729	0.9867	0.9892	1.7592	1.8224	1.8604	1.8577	1.7675
	$j = 5$	0.9908	0.9908	0.9934	0.9978	0.9989	1.9500	1.9587	1.9488	1.8834	1.6836
	$j = 6$	0.9973	0.9975	0.9983	0.9999	1.0010	1.9936	1.9900	1.9639	1.8492	1.5343
	$j = 7$	0.9992	0.9993	0.9996	1.0002	1.0012	2.0025	1.9969	1.9634	1.7943	1.3811
	$j = 8$	0.9998	0.9998	0.9999	1.0002	1.0010	2.0034	1.9984	1.9602	1.7306	1.2619
M2	$j = 4$	1.9061	1.9284	1.9453	1.9259	1.7193	3.0225	3.0100	2.6079	1.5236	1.0230
	$j = 5$	1.9686	1.9777	1.9824	1.9267	1.5493	3.0199	3.0029	2.1834	1.3979	1.0082
	$j = 6$	1.9883	1.9923	1.9935	1.8858	1.3523	3.0093	2.9914	1.9663	1.4135	1.0357
	$j = 7$	1.9953	1.9972	1.9971	1.8100	1.2154	3.0040	2.9820	1.9073	1.4274	1.0568
	$j = 8$	1.9980	1.9989	1.9983	1.7101	1.1463	3.0018	2.9683	1.8946	1.4342	1.0705

The L^2 convergence rates of both methods **M1** and **M2** on uniform meshes are suboptimal with $\mathcal{R} \approx 1.2619$ or $\mathcal{R} \approx 1.0705$, which are consistent with the theoretical result in Theorem 3.13 with $\mathcal{R} = \min\{k+1, \alpha+2, \beta+3, \alpha+\beta+1, 2\alpha\} \approx \min\{k+1, 1.0890\} = 1.0890$.

On graded meshes, the convergence rates of the method **M1** are optimal with $\kappa \leq 0.3$, and that of the method **M2** are optimal with $\kappa \leq 0.1$, which are consistent with the theoretical result in Theorem 4.26, namely, the optimal convergence rate can be obtained when $\kappa < 2^{-\frac{1}{\alpha_0}} \approx 0.28$ for the method **M1**, and $\kappa < 2^{-\frac{1.5}{\alpha_0}} \approx 0.15$ for the method **M2**.

5.2.3 Re-entrant Corners on the Domain Other Than $3\pi/2$

Example 5.8. Similar to the example 5.3, in this example we report the numerical convergence rates on a sequence of graded meshes including quasi-uniform meshes for different re-entrant corners. We particularly use a domain with one re-entrant corner $7\pi/4$ and a domain with two re-entrant corners $4\pi/3$. As in example 5.1, we consider the biharmonic problem (2.1) with $f = 1$. We solve this problem using Algorithm 2.18 with the methods **M1** and **M2**.

One Re-entrant Corner. The re-entrant corner of the domain under consideration is $7\pi/4$ as shown in the Figure 11a. In table 20 we show the numerical convergence rates of finite element approximations of the biharmonic problem for the methods **M1** and **M2**.

Table 20: Numerical Convergence rates of finite element approximation of the biharmonic problem on a domain with re-entrant corner $7\pi/4$.

	κ	H_1 rate					L_2 rate				
		0.1	0.2	0.3	0.4	0.5	0.1	0.2	0.3	0.4	0.5
M1	$j = 4$	0.9490	0.9598	0.9732	0.9869	0.9865	1.7435	1.8107	1.8485	1.8404	1.7424
	$j = 5$	0.9913	0.9911	0.9937	0.9980	0.9974	1.9394	1.9472	1.9285	1.8483	1.6378
	$j = 6$	0.9976	0.9977	0.9985	1.0000	1.0001	1.9877	1.9800	1.9360	1.7894	1.4633
	$j = 7$	0.9992	0.9994	0.9997	1.0003	1.0006	1.9995	1.9884	1.9274	1.7053	1.2932
	$j = 8$	0.9998	0.9998	1.0000	1.0003	1.0005	2.0021	1.9912	1.9154	1.6148	1.1692
M2	$j = 4$	1.7565	1.7913	1.8330	1.7931	1.5778	3.0707	2.9742	2.3553	1.4123	0.8719
	$j = 5$	1.9093	1.9325	1.9410	1.7894	1.3734	3.0120	2.9126	1.8590	1.2377	0.8845
	$j = 6$	1.9684	1.9785	1.9713	1.6829	1.1649	3.0126	2.8199	1.7492	1.2795	0.9316
	$j = 7$	1.9876	1.9924	1.9772	1.5480	1.0604	3.0076	2.6878	1.7453	1.3065	0.9604
	$j = 8$	1.9949	1.9972	1.9747	1.4430	1.0238	3.0050	2.5526	1.7498	1.3203	0.9787

We find on uniform meshes ($\kappa = 0.5$) that the H^1 convergence rate for the method **M1** is optimal with $\mathcal{R} = 1$, and that of the method **M2** is suboptimal with $\mathcal{R} \approx 1.0238$. Both of them are consistent the theoretical result in Theorem 3.12 in a domain with re-entrant corner $7\pi/4$, that is $\mathcal{R} = \min\{k, \beta + 2, \alpha + 1, 2\alpha\} \approx \min\{k, 2.5714, 1.5050, 1.0100\}$, where α is given in Table 1 for $\omega = \frac{7\pi}{4}$. We also find that the convergence rates for the method **M1** are optimal on graded meshes with $\kappa < 0.5$, and that of the method **M2** are optimal on graded meshes with $\kappa \leq 0.3$, which are consistent with the theoretical result in Theorem 4.25, namely, the optimal convergence rate can be obtained when $\kappa < 2^{-\frac{\alpha_0}{\alpha_0}} = 0.5$ for method **M1**, and $\kappa < 2^{-\frac{1}{\alpha_0}} \approx 0.25$ for the method **M2**.

The L^2 convergence rates of both methods **M1** and **M2** on uniform meshes are suboptimal with $\mathcal{R} \approx 1.1692$ and $\mathcal{R} \approx 0.9787$ respectively, which are consistent with the theoretical result in Theorem 3.13 with $\mathcal{R} = \min\{k + 1, \alpha + 2, \beta + 3, \alpha + \beta + 1, 2\alpha\} =$

$\min\{k + 1, 2.5050, 3.5714, 2.0764, 1.0100\}$. On graded meshes, the convergence rates of the method **M1** are optimal with $\kappa \leq 0.3$, and that of the method **M2** are optimal with $\kappa \leq 0.1$, which are consistent with the theoretical result in Theorem 4.26, namely, the optimal convergence rate can be obtained when $\kappa < 2^{-\frac{1}{\alpha_0}} \approx 0.25$ for the method **M1**, and $\kappa < 2^{-\frac{1.5}{\alpha_0}} \approx 0.13$ for the method **M2**.

Two Re-Entrant Corners. The re-entrant corners of the domain under consideration is $4\pi/3$ as shown in the Figure 12a. In table 21 we show the numerical convergence rates of finite element approximations of the biharmonic problem for the methods **M1** and **M2**.

Table 21: Numerical convergence rates of the second the Poisson equation for the methods **M1** and **M2** with two re-entrant corner $4\pi/3$.

		H_1 rate					L_2 rate					
		κ	0.1	0.2	0.3	0.4	0.5	0.1	0.2	0.3	0.4	0.5
M1	$j = 4$		0.8517	0.9021	0.9436	0.9773	0.9575	1.4034	1.5625	1.6811	1.7424	1.6902
	$j = 5$		0.9908	0.9859	0.9896	0.9991	0.9903	1.8596	1.8951	1.9074	1.8743	1.7312
	$j = 6$		0.9963	0.9953	0.9970	1.0005	0.9977	1.9720	1.9747	1.9600	1.8852	1.6624
	$j = 7$		0.9984	0.9985	0.9992	1.0005	0.9998	1.9988	1.9945	1.9735	1.8672	1.5593
	$j = 8$		0.9995	0.9996	0.9998	1.0003	1.0004	2.0035	1.9993	1.9780	1.8426	1.4590
M2	$j = 4$		1.8316	1.8640	1.8955	1.9140	1.7916	3.0679	3.0285	2.9741	2.3759	1.8035
	$j = 5$		1.9415	1.9561	1.9654	1.9600	1.7804	3.0453	3.0175	2.8393	1.7311	1.2239
	$j = 6$		1.9779	1.9842	1.9872	1.9731	1.7181	3.0248	3.0055	2.6299	1.6149	1.1806
	$j = 7$		1.9910	1.9937	1.9948	1.9750	1.6378	3.0126	3.0013	2.3965	1.6156	1.1988
	$j = 8$		1.9960	1.9973	1.9977	1.9708	1.5543	3.0055	2.9999	2.2415	1.6221	1.2127

We find on uniform meshes ($\kappa = 0.5$) that the H^1 convergence rate for the method **M1** is optimal with $\mathcal{R} = 1$, and that of the method **M2** is suboptimal with $\mathcal{R} \approx 1.5543$ which is little bit higher than the expected due to the reason explained in example 5.3. Both of above results are consistent the theoretical result in Theorem 3.12 in a domain with

re-entrant corner $4\pi/3$, that is $\mathcal{R} = \min\{k, \beta + 2, \alpha + 1, 2\alpha\} = \min\{k, 2.75, 1.6157, 1.2315\}$, where α is given in Table 1 for $\omega = \frac{4\pi}{3}$. We also find that the convergence rates for the method **M1** are optimal on graded meshes with $\kappa < 0.5$, and that of the method **M2** are optimal on graded meshes with $\kappa \leq 0.3$, which are consistent with the theoretical result in Theorem 4.25, namely, the optimal convergence rate can be obtained when $\kappa < 2^{-\frac{\alpha_0}{\alpha_0}} = 0.5$ for method **M1**, and $\kappa < 2^{-\frac{1}{\alpha_0}} \approx 0.32$ for the method **M2**.

The L^2 convergence rate $\mathcal{R} \approx 1.4590$, after 8 mesh refinements, of the method **M1** on a uniform mesh which is higher than expected due to the same reason mentioned above. Thus more mesh refinements are needed to achieve the expected convergent rate. The L^2 convergence rates of the method **M2** on uniform meshes is suboptimal with $\mathcal{R} \approx 1.2127$ which is consistent with the theoretical result in Theorem 3.13 with $\mathcal{R} = \min\{k + 1, \alpha + 2, \beta + 3, \alpha + \beta + 1, 2\alpha\} = \min\{k + 1, 2.6157, 3.75, 2.3657, 1.2315\} = 1.2315$. On graded meshes, the convergence rates of the method **M1** are optimal with $\kappa \leq 0.3$, and that of the method **M2** are optimal with $\kappa \leq 0.2$, which are consistent with the theoretical result in Theorem 4.26, namely, the optimal convergence rate can be obtained when $\kappa < 2^{-\frac{1}{\alpha_0}} \approx 0.32$ for the method **M1**, and $\kappa < 2^{-\frac{1.5}{\alpha_0}} \approx 0.18$ for the method **M2**.

5.2.4 CPU Time

Example 5.9. In this example, we compare the CPU time of the proposed finite element algorithms (Algorithm 2.17 and Algorithm 2.18) with those of H^2 -conforming Argyris finite element method by solving the biharmonic problem (2.1) with $f = 1$ in the same square domain Ω . The Stokes problem (2.24) with source term $\mathbf{F} = (0, x)^T$ which satisfies (2.25) is solved in Algorithm 2.17. The results of the CPU time comparison (in seconds) are shown in Table 22. All results are tested on MATLAB R2021a in MacBook Air (M1,

2020) with 8 GB memory.

From Table 22, we find that Algorithm 2.17 and Algorithm 2.18 are much faster than the Argyris finite element method due to the availability of fast Stokes solvers and Poisson solvers. Moreover, Algorithm 2.17 is faster than Algorithm 2.18, since Algorithm 2.18 has one extra Poisson problem to compute.

Table 22: The CPU time (in seconds) of Algorithm 2.17, Algorithm 2.18, and the Argyris finite element method.

method\j	Convex domain as in Figure 8a						Non convex domain as in Figure 9a					
	j = 3	j = 4	j = 5	j = 6	j = 7	j = 8	j = 3	j = 4	j = 5	j = 6	j = 7	j = 8
Argyris FEM	3.19	10.88	27.22	113.28	461.15	1883.50	3.62	13.49	53.58	220.43	915.98	3793.90
Algorithm 2.17(M1)	0.07	0.29	0.51	1.49	5.12	15.72	0.08	0.11	0.29	1.29	4.02	12.74
Algorithm 2.18(M1)	0.07	0.07	0.19	0.82	4.42	24.05	0.08	0.09	0.11	0.71	2.40	15.91
Algorithm 2.17(M2)	0.05	0.18	0.62	2.02	6.46	22.29	0.09	0.27	0.58	1.70	4.99	18.62
Algorithm 2.18(M2)	0.07	0.19	0.67	2.96	12.06	60.08	0.06	0.22	0.24	1.60	7.79	41.65

CHAPTER 6 SUMMARY AND DISCUSSION

6.1 General Conclusion

In this dissertation, we studied the biharmonic equation $\Delta^2\phi = f$ in Ω , with Dirichlet boundary conditions in a polygonal domain. We briefly summarize our work below:

- We introduced two methods to decouple the biharmonic equation 2.1. First we decoupled the biharmonic equation into a Steady state Stokes equation and a Poisson equation. As a generalization to the first decoupled system we introduced the second formulation by decoupling the biharmonic equation 2.1 into a steady state Stokes equation and two Poisson equations. Based on the general regularity theory for second-order elliptic equations and Stokes equation, we reviewed the weak solutions of all involved equations, and show the equivalence of solution of the proposed systems to that of original problem 2.1.
- Based on the first decoupled formulation in section 2.3.1 we proposed finite element Algorithm 2.17 to solve the biharmonic equation 2.1. Based on the second decoupled formulation in section 2.3.2 we proposed finite element Algorithm 2.18 to solve the biharmonic equation 2.1. The involved Stokes equations in both algorithms are solved using the Mini finite elements and the Taylor-Hood finite elements while the Poisson equations are solved using linear finite elements and quadratic finite elements.
- We presented error analysis of Algorithm 2.17 and Algorithm 2.18 on quasi-uniform meshes. The error estimate Theorem 3.5, Theorem 3.6, Theorem 3.12, and Theorem 3.13 show that Algorithm 2.17 produces numerical solutions that converge to the

solution of the biharmonic problem (2.1) no matter the polygonal domain is convex or non-convex. We note that if the domain is non-convex, the convergence rate on quasi-uniform meshes is suboptimal.

- To improve the convergence rate, we presented the construction of graded meshes and the regularity in weighted Sobolev space. As an intermediate step we presented interpolation error estimate on graded mesh and then we showed the error estimate results of both Algorithms 2.17 and Algorithm 2.18.
- We presented several numerical simulations to validate our theoretical results. First, we compared our numerical solution with the finite element solution obtained using Argyris finite element under convex and non convex domains. Those results indicated that the solutions of Algorithm 2.17 and Algorithm 2.18 converge to the exact solution in both convex and nonconvex domains. We further showed convergent rates on graded meshes for different re-entrant corners. All those numerical convergent rates followed our theoretical finding. Finally, we calculated the CPU time to run our algorithms and the algorithm based on Argyris finite elements. We found that our Algorithms are much faster than the Argyris finite element method due to the availability of fast Stokes solvers and Poisson solvers. Moreover, Algorithm 2.17 is faster than Algorithm 2.18, since Algorithm 2.18 has one extra Poisson problem to compute.

6.2 Future Work

This dissertation inspires some new research directions:

- Some special source terms could be considered, such as the Dirac delta function at a point in a domain [88], or line Dirac measures [67, 32].
- It would be interesting to explore the possibility to extend proposed method to time-dependent fourth order problems and nonlinear fourth order partial differential equations, such as Swift-Hohenberg equation [93], and the Cahn-Hilliard equation [31]. It has been explored that the fully discrete numerical schemes for these types of equations are elliptic fourth order equations with lower order terms [71, 72, 73, 74, 75, 98]. The extensions could involve new challenges, we will leave it to our future work.
- The proposed method has potential to extend to sixth order or even higher order problems.

REFERENCES

- [1] A. Adini and R. Clough. Analysis of plate bending by the finite element method, nsf report g. 7337. *University of California, Berkeley, CA*, 1961.
- [2] S. Agmon, A. Douglis, and L. Nirenberg. Estimates near the boundary for solutions of elliptic partial differential equations satisfying general boundary conditions. I. *Communications on Pure and Applied Mathematics*, 12(4):623–727, 1959.
- [3] R. Aitbayev. A quadrature finite element galerkin scheme for a biharmonic problem on a rectangular polygon. *Numerical Methods for Partial Differential Equations: An International Journal*, 24(2):518–534, 2008.
- [4] M. Amara, D. Capatina-Papaghiuc, and A. Chatti. Bending moment mixed method for the kirchhoff–love plate model. *SIAM Journal on Numerical Analysis*, 40(5):1632–1649, 2002.
- [5] T. Apel, A.-M. Sändig, and J. Whiteman. Graded mesh refinement and error estimates for finite element solutions of elliptic boundary value problems in non-smooth domains. *Math. Methods Appl. Sci.*, 19(1):63–85, 1996.
- [6] J. H. Argyris, I. Fried, and D. W. Scharpf. The TUBA family of plate elements for the matrix displacement method. *The Aeronautical Journal*, 72(692):701–709, 1968.
- [7] J. H. Argyris and S. Kelsey. *Energy theorems and structural analysis*, volume 60. Springer, 1960.
- [8] D. N. Arnold, F. Brezzi, and M. Fortin. A stable finite element for the stokes equations. *Calcolo*, 21(4):337–344, 1984.
- [9] I. Babuška. Finite element method for domains with corners. *Computing*, 6(3):264–

273, 1970.

- [10] I. Babuška, R. B. Kellogg, and J. Pitkäranta. Direct and inverse error estimates for finite elements with mesh refinements. *Numerische Mathematik*, 33(4):447–471, 1979.
- [11] I. Babuška, J. Osborn, and J. Pitkäranta. Analysis of mixed methods using mesh dependent norms. *Mathematics of Computation*, 35(152):1039–1062, 1980.
- [12] C. Bacuta, J. H. Bramble, and J. E. Pasciak. Shift theorems for the biharmonic Dirichlet problem. In *Recent Progress in Computational and Applied PDEs*, pages 1–26. Springer, 2002.
- [13] C. Băcuță, V. Nistor, and L. T. Zikatanov. Improving the rate of convergence of ‘high order finite elements’ on polygons and domains with cusps. *Numer. Math.*, 100(2):165–184, 2005.
- [14] G. A. Baker. Finite element methods for elliptic equations using nonconforming elements. *Mathematics of Computation*, 31(137):45–59, 1977.
- [15] L. Banz, B. P. Lamichhane, and E. P. Stephan. A new three-field formulation of the biharmonic problem and its finite element discretization. *Numerical Methods for Partial Differential Equations*, 33(1):199–217, 2017.
- [16] G. Batchelor. Fluid mechanics. by ld landau and em lifshitz.(translated from the russian by jb sykes and wh reid.) london: Pergamon press, 1959. 536 pp.£ 5 5s. *Journal of Fluid Mechanics*, 8(2):315–318, 1960.
- [17] K.-J. Bathe and E. N. Dvorkin. A four-node plate bending element based on mindlin/reissner plate theory and a mixed interpolation. *International Journal for Numerical Methods in Engineering*, 21(2):367–383, 1985.

- [18] E. M. Behrens and J. Guzmán. A mixed method for the biharmonic problem based on a system of first-order equations. *SIAM Journal on Numerical Analysis*, 49(2):789–817, 2011.
- [19] C. Bernardi and G. Raugel. Méthodes d’éléments finis mixtes pour les équations de Stokes et de Navier-Stokes dans un polygone non convexe. *Calcolo*, 18(3):255–291, 1981.
- [20] P. Binev, W. Dahmen, and R. DeVore. Adaptive finite element methods with convergence rates. *Numerische Mathematik*, 97(2):219–268, 2004.
- [21] H. Blum, R. Rannacher, and R. Leis. On the boundary value problem of the biharmonic operator on domains with angular corners. *Mathematical Methods in the Applied Sciences*, 2(4):556–581, 1980.
- [22] J. Boland and R. A. Nicolaides. Stability of finite elements under divergence constraints. *SIAM Journal on Numerical Analysis*, 20(4):722–731, 1983.
- [23] M. Bourlard, M. Dauge, M.-S. Lubuma, and S. Nicaise. Coefficients of the singularities for elliptic boundary value problems on domains with conical points. III: Finite element methods on polygonal domains. *SIAM Journal on Numerical Analysis*, 29(1):136–155, 1992.
- [24] S. C. Brenner and L. R. Scott. *The Mathematical Theory of Finite Element Methods*, volume 15 of *Texts in Applied Mathematics*. Springer-Verlag, New York, second edition, 2002.
- [25] S. C. Brenner, L. R. Scott, and L. R. Scott. *The mathematical theory of finite element methods*, volume 3. Springer, 2008.

- [26] F. Brezzi. On the existence, uniqueness and approximation of saddle-point problems arising from lagrangian multipliers. *RAIRO. Anal. numér.*, 8(R2):129–151, 1974.
- [27] F. Brezzi, K.-J. Bathe, and M. Fortin. Mixed-interpolated elements for reissner–mindlin plates. *International Journal for Numerical Methods in Engineering*, 28(8):1787–1801, 1989.
- [28] F. Brezzi and R. S. Falk. Stability of higher-order hood–taylor methods. *SIAM Journal on Numerical Analysis*, 28(3):581–590, 1991.
- [29] F. Brezzi and M. Fortin. Numerical approximation of mindlin-reissner plates. *Mathematics of computation*, 47(175):151–158, 1986.
- [30] F. Brezzi, M. Fortin, and R. Stenberg. Error analysis of mixed-interpolated elements for reissner-mindlin plates. *Mathematical Models and Methods in Applied Sciences*, 1(02):125–151, 1991.
- [31] J. W. Cahn and J. E. Hilliard. Free energy of a nonuniform system. i. interfacial free energy. *The Journal of chemical physics*, 28(2):258–267, 1958.
- [32] H. Cao, H. Li, N. Yi, and P. Yin. An adaptive finite element method for two-dimensional elliptic equations with line Dirac sources. *arXiv preprint arXiv:2112.08565*, 2021.
- [33] J. M. Cascon, C. Kreuzer, R. H. Nochetto, and K. G. Siebert. Quasi-optimal convergence rate for an adaptive finite element method. *SIAM Journal on Numerical Analysis*, 46(5):2524–2550, 2008.
- [34] L. Chen. ifem: an innovative finite element methods package in matlab. *Preprint, University of Maryland*, 2008.

- [35] L. Chen and H. Li. Superconvergence of gradient recovery schemes on graded meshes for corner singularities. *Journal of Computational Mathematics*, pages 11–31, 2010.
- [36] X.-l. Cheng, W. Han, and H.-c. Huang. Some mixed finite element methods for biharmonic equation. *Journal of computational and applied mathematics*, 126(1-2):91–109, 2000.
- [37] P. Ciarlet. *The Finite Element Method for Elliptic Problems*, volume 4 of *Studies in Mathematics and Its Applications*. North-Holland, Amsterdam, 1978.
- [38] P. G. Ciarlet. Basic error estimates for elliptic problems. 1991.
- [39] P. G. Ciarlet. *The finite element method for elliptic problems*. SIAM, 2002.
- [40] P. G. Ciarlet and P.-A. Raviart. A mixed finite element method for the biharmonic equation. In *Mathematical aspects of finite elements in partial differential equations (Proc. Sympos., Math. Res. Center, Univ. Wisconsin, Madison, Wis., 1974)*, pages 125–145. Publication No. 33, 1974.
- [41] R. Courant. Variational methods for the solution of problems of equilibrium and vibrations. *Bulletin of the American Mathematical Society*, 49:1–23, 1943.
- [42] M. Dauge. *Elliptic Boundary Value Problems on Corner Domains*, volume 1341 of *Lecture Notes in Mathematics*. Springer-Verlag, Berlin, 1988.
- [43] P. Destuynder and M. Salaun. *Mathematical analysis of thin plate models*, volume 24. Springer Science & Business Media, 2013.
- [44] R. S. Falk. Approximation of the biharmonic equation by a mixed finite element method. *SIAM Journal on Numerical Analysis*, 15(3):556–567, 1978.
- [45] M. Fortin and F. Brezzi. *Mixed and hybrid finite element methods*, volume 3. New York: Springer-Verlag, 1991.

- [46] D. Gallistl. Stable splitting of polyharmonic operators by generalized stokes systems. *Mathematics of Computation*, 86(308):2555–2577, 2017.
- [47] V. Girault and P.-A. Raviart. *Finite Element Approximation of the Navier-Stokes Equations*, volume 749. Springer Berlin, 1979.
- [48] V. Girault and P.-A. Raviart. *Finite element methods for Navier-Stokes equations: theory and algorithms*, volume 5. Springer Science & Business Media, 2012.
- [49] R. Glowinski and O. Pironneau. Numerical methods for the first biharmonic equation and for the two-dimensional stokes problem. *SIAM review*, 21(2):167–212, 1979.
- [50] P. Grisvard. *Elliptic Problems in Nonsmooth Domains*. Pitman, Boston, 1985.
- [51] P. Grisvard. *Singularities in Boundary Value Problems*, volume 22 of *Research Notes in Applied Mathematics*. Springer-Verlag, New York, 1992.
- [52] H. Guo, Z. Zhang, and Q. Zou. A C^0 linear finite element method for biharmonic problems. *Journal of Scientific Computing*, 74(3):1397–1422, 2018.
- [53] G. Hay. Is sokolnikoff, mathematical theory of elasticity. *Bulletin of the American Mathematical Society*, 62(4):416–417, 1956.
- [54] Y.-Q. HUANG and Q. LIN. Elliptic boundary value problems on polygonal domains and finite element approximations. *Journal of Systems Science and Mathematical Sciences*, 12(3):263, 1992.
- [55] Y. Q. Huang and Q. Lin. Some estimates of green functions and their finite element approximations on angular domains. *J. Systems Sci. Math. Sci*, 14(1):1–8, 1994.
- [56] C. Johnson. On the convergence of a mixed finite-element method for plate bending problems. *Numerische Mathematik*, 21(1):43–62, 1973.

- [57] C. Johnson and J. Pitkäranta. Analysis of some mixed finite element methods related to reduced integration. *Mathematics of Computation*, 38(158):375–400, 1982.
- [58] V. Kondrat'ev. Boundary value problems for elliptic equations in domains with conical or angular points. *Trudy Moskov. Mat. Obšč.*, 16:209–292, 1967.
- [59] V. Kozlov, V. V. Kozlov, V. Mazia, V. G. Maza, and J. Rossmann. *Spectral problems associated with corner singularities of solutions to elliptic equations*. Number 85. American Mathematical Soc., 2001.
- [60] M. Krizek, P. Neittaanmaki, and R. Stenberg. *Finite element methods: fifty years of the Courant element*. CRC Press, 2016.
- [61] V. Kupradze. Potential methods in the theory of elasticity, israel program sc. *Transl., Jerusalem*, 1965.
- [62] O. A. Ladyzhenskaya. *The Mathematical Theory of Viscous Incompressible Flow*, volume 2. Gordon and Breach New York, 1969.
- [63] P. Lascaux and P. Lesaint. Some nonconforming finite elements for the plate bending problem. *Revue française d'automatique, informatique, recherche opérationnelle. Analyse numérique*, 9(R1):9–53, 1975.
- [64] H. Li, A. Mazzucato, and V. Nistor. Analysis of the finite element method for transmission/mixed boundary value problems on general polygonal domains. *Electron. Trans. Numer. Anal*, 37:41–69, 2010.
- [65] H. Li and S. Nicaise. Regularity and a priori error analysis on anisotropic meshes of a Dirichlet problem in polyhedral domains. *Numer. Math.*, 139(1):47–92, 2018.
- [66] H. Li and V. Nistor. Analysis of a modified Schrödinger operator in 2D: regularity, index, and FEM. *J. Comput. Appl. Math.*, 224(1):320–338, 2009.

- [67] H. Li, X. Wan, P. Yin, and L. Zhao. Regularity and finite element approximation for two-dimensional elliptic equations with line dirac sources. *Journal of Computational and Applied Mathematics*, 393:113518, 2021.
- [68] H. Li, C. D. Wickramasinghe, and P. Yin. A C^0 finite element method for the biharmonic problem with Dirichlet boundary conditions in a polygonal domain. *arXiv preprint arXiv:2207.03838*, 2022.
- [69] H. Li, P. Yin, and Z. Zhang. A C^0 finite element method for the biharmonic problem with navier boundary conditions in a polygonal domain. *arXiv preprint arXiv:2012.12374*, 2020.
- [70] H. Li, P. Yin, and Z. Zhang. A C^0 finite element method for the biharmonic problem with Navier boundary conditions in a polygonal domain. *IMA Journal of Numerical Analysis*, drac026, <https://doi.org/10.1093/imanum/drac026>, 2022.
- [71] H. Liu and P. Yin. A mixed discontinuous Galerkin method without interior penalty for time-dependent fourth order problems. *Journal of Scientific Computing*, 77(1):467–501, 2018.
- [72] H. Liu and P. Yin. Unconditionally energy stable DG schemes for the Swift–Hohenberg equation. *Journal of Scientific Computing*, 81(2):789–819, 2019.
- [73] H. Liu and P. Yin. On the SAV-DG method for a class of fourth order gradient flows. *arXiv preprint arXiv:2008.11877*, 2020.
- [74] H. Liu and P. Yin. Unconditionally energy stable discontinuous Galerkin schemes for the Cahn–Hilliard equation. *Journal of Computational and Applied Mathematics*, 390:113375, 2021.

- [75] H. Liu and P. Yin. High order unconditionally energy stable RKDG schemes for the Swift–Hohenberg equation. *Journal of Computational and Applied Mathematics*, 407:114015, 2022.
- [76] M. Lyly, R. Stenberg, and T. Vihinen. A stable bilinear element for the reissner-mindlin plate model. *Computer Methods in Applied Mechanics and Engineering*, 110(3-4):343–357, 1993.
- [77] D. S. Malkus and T. J. Hughes. Mixed finite element methods—reduced and selective integration techniques: a unification of concepts. *Computer Methods in Applied Mechanics and Engineering*, 15(1):63–81, 1978.
- [78] S. G. Mikhailin and L. Chambers. *Variational methods in mathematical physics*, volume 1. Pergamon Press Oxford, 1964.
- [79] W. Ming and J. Xu. The morley element for fourth order elliptic equations in any dimensions. *Numerische Mathematik*, 103(1):155–169, 2006.
- [80] P. Monk. A mixed finite element method for the biharmonic equation. *SIAM Journal on Numerical Analysis*, 24(4):737–749, 1987.
- [81] L. S. D. Morley. The triangular equilibrium element in the solution of plate bending problems. *Aeronautical Quarterly*, 19(2):149–169, 1968.
- [82] N. Muskhelishvili. Some basic problems of the mathematical theory of elasticity. *Noordhoff, Groningen*, 17404(6.2):1, 1963.
- [83] J.-H. Pyo. A finite element dual singular function method to solve the stokes equations including corner singularities. *International Journal of Numerical Analysis & Modeling*, 12(3), 2015.

- [84] G. Raugel et al. Resolution numerique par une methode d'elements finis du probleme de dirichlet pour le laplacien dans un polygone. 1978.
- [85] J. Roberts and J. Thomas. Mixed and hybrid methods in handbook of numerical analysis ii: Finite element methods (part 1), pg ciarlet and jl lions eds, 1991.
- [86] R. Scholz. Interior error estimates for a mixed finite element method. *Numerical Functional Analysis and Optimization*, 1(4):415–429, 1979.
- [87] R. Scholz. A mixed method for 4th order problems using linear finite elements. *RAIRO. Analyse numérique*, 12(1):85–90, 1978.
- [88] R. Scott. Finite element convergence for singular data. *Numerische Mathematik*, 21(4):317–327, 1973.
- [89] R. Stenberg. Analysis of mixed finite elements methods for the Stokes problem: a unified approach. *Math. Comp.*, 42(165):9–23, 1984.
- [90] R. Stenberg. Error analysis of some finite element methods for the Stokes problem. *Mathematics of Computation*, 54(190):495–508, 1990.
- [91] R. Stevenson. Optimality of a standard adaptive finite element method. *Foundations of Computational Mathematics*, 7(2):245–269, 2007.
- [92] G. Sweers. A survey on boundary conditions for the biharmonic. *Complex variables and elliptic equations*, 54(2):79–93, 2009.
- [93] J. Swift and P. C. Hohenberg. Hydrodynamic fluctuations at the convective instability. *Physical Review A*, 15(1):319, 1977.
- [94] R. Temam. Navier-stokes equations: Theory and numerical analysis(book). *Amsterdam, North-Holland Publishing Co.(Studies in Mathematics and Its Applications*, 2:510, 1977.

- [95] R. Temam. Navier-Stokes Equations: Amsterdam-New York. North-Holland Publishing Company. 1977. (Studies in Mathematics and its Applications 2). *ZAMM - Journal of Applied Mathematics and Mechanics*, 59(9):489–489, 1979.
- [96] M. J. Turner, R. W. Clough, H. C. Martin, and L. Topp. Stiffness and deflection analysis of complex structures. *journal of the Aeronautical Sciences*, 23(9):805–823, 1956.
- [97] R. Verfürth. Error estimates for a mixed finite element approximation of the stokes equations. *RAIRO. Analyse numérique*, 18(2):175–182, 1984.
- [98] P. Yin. *Efficient discontinuous Galerkin (DG) methods for time-dependent fourth order problems*. PhD thesis, Iowa State University, 2019.
- [99] M. Zlámal. On the finite element method. *Numerische Mathematik*, 12(5):394–409, 1968.

ABSTRACT**A C^0 FINITE ELEMENT METHOD FOR THE BIHARMONIC PROBLEM
IN A POLYGONAL DOMAIN**

by

CHARUKA DILHARA WICKRAMASINGHE**August 2022****Advisor:** Dr. Hengguang Li**Major:** Mathematics**Degree:** Doctor of Philosophy

This dissertation studies the biharmonic equation with Dirichlet boundary conditions in a polygonal domain. The biharmonic problem appears in various real-world applications, for example in plate problems, human face recognition, radar imaging, and hydrodynamics problems. There are three classical approaches to discretizing the biharmonic equation in the literature: conforming finite element methods, nonconforming finite element methods, and mixed finite element methods. We propose a mixed finite element method that effectively decouples the fourth-order problem into a system of one steady-state Stokes equation and one Poisson equation. As a generalization to the above-decoupled formulation, we propose another decoupled formulation using a system of two Poisson equations and one steady-state Stokes equation. We solve Poisson equations using linear and quadratic Lagrange's elements and the Stokes equation using Hood-Taylor elements and Mini finite elements.

It is shown that the solution of each system is equivalent to that of the original fourth-order problem on both convex and non-convex polygonal domains. Two finite element

algorithms are, in turn, proposed to solve the decoupled systems. Solving this problem in a non-convex domain is challenging due to the singularity occurring near re-entrant corners. We introduce a weighted Sobolev space and a graded mesh refine Algorithm to attack the singularity near re-entrant corners. We show the regularity results of each decoupled system in both Sobolev space and weighted Sobolev space. We derive the H^1 and L^2 error estimates for the numerical solutions on quasi-uniform and graded meshes. We present various numerical test results to justify the theoretical findings. Given the availability of fast Poisson solvers and Stokes solvers, our Algorithm is a relatively easy and cost-effective alternative to existing algorithms for solving the biharmonic equation.

AUTOBIOGRAPHICAL STATEMENT

Charuka Wickramasinghe

Education

- Ph.D. in Mathematics, Wayne State University, Detroit, Michigan, USA, 2022.
- M.A. in Applied Mathematics, Wayne State University, Detroit, Michigan, USA, 2022.
- M.A. in Mathematics, Bowling Green State University, Ohio, USA, 2017.
- Diploma in Industrial Mathematics, University of Peradeniya, Sri Lanka, 2015.
- B.S.(Hons) in Mathematics, University of Peradeniya, Sri Lanka, 2013.

Selected List of Awards and Scholarships

- (a) Thomas C. Rumble University Graduate Fellowship, Wayne State University, 2021-2022.
- (b) Nominated for the Garrett T. Heberlein Excellence in Teaching Awards, Wayne State University, 2022.
- (c) Paul Catlin, Ph.D. Endowed Memorial Scholarship Award, Wayne State University, 2021.
- (d) Excellence in Teaching Award, TRIO Upward Bound Program, Bowling Green State University, 2021.
- (e) Mahapola Higher Education Scholarship Award, Sri Lanka, 2008-2013.

Publications

- [1] H. Li, **C. D. Wickramasinghe**, and P. Yin. A C^0 finite element method for the biharmonic problem with Dirichlet boundary conditions in a polygonal domain. arXiv preprint arXiv:2207.03838, 2022.